UiO : University of Oslo

Britt Paulsen

Total Synthesis of Agelasine F and Synthesis Directed towards *ent*-Ageloxime D: Two Natural Products with Interesting Biological Activities

Thesis submitted for the degree of Philosophiae Doctor

Department of Chemistry
The Faculty of Mathematics and Natural Sciences

2020

Series of dissertations submitted to the
Faculty of Mathematics and Natural Sciences, University of Oslo
No. 2262

ISSN 1501-7710

Cover: Hanne Baadsgaard Utigard.
Print production: Reprosentralen, University of Oslo.

Acknowledgements

First and foremost, I would like to thank my supervisor professor Lise-Lotte Gundersen. Thank you for giving me the opportunity to do my PhD under your supervision and for all your valuable feedback during these years. Your attention to detail is unprecedented.

I have been blessed with excellent colleagues with vast knowledge in their fields. Dirk Peterson, you are truly a NMR wizard and I am so grateful for all our discussions and your help. Also, thank you for the extensive amount of work you put into Table 4 in the thesis. Frode Rise, thank you for in depth knowledge and enthusiasm for the field of NMR, and for making sure we always have superb equipment. Osamu Sekiguchi, thank you for running the MS service. Line Altern Halvorsen Valbø, the institute is lucky to have a rockstar like you working in the administration. You are awesome.

I would also like to extend a big thank you to Charlotte Miller, Lars Jacob Stovner and Peter Molesworth for providing invaluable feedback on the final versions of the thesis.

To all my friends and former colleagues at KI – Peter, Charlotte, Martin, Matthew, Håkon, Kim and Jakob – thank you for all scientific (and nonscientific (except a few)) discussions and support. I have truly learned a lot from you. Charlotte, you are a great inspiration and friend. Kim, you helped me in a time of need, and I am truly grateful. Håkon, thank you for moving into my office and being my sparring partner for the last period of this thesis; it prevented my brain from short-circuiting. To you all: this journey would have been way too bland without you.

Thanks to my huge family, mamma og pappa, Marianne, Sven-Are, Liza, Hanne-Kristin, Sissel-Marie, tante Hanne, onkel Arve and Kristina and the gang. Thank you for always supporting me and being game for randonnée, running in the mountains, or skiing and for inspiring me to do my best even on the days I just want to sit inside and eat popcorn. Marianne, I am extremely lucky to have a sister with whom I can discuss the challenges of this field. Hanne-Kristin, your word-excel-knowledge knows no bounds, thank you for always helping me over the phone when I was stuck. To Marit, thank you for keeping me sane all these years of the PhD and for looking after me when I needed it the most. I always look forward to our next mountain adventure. Roar, thank you for celebrating my birthday for the last 100 days. Thank you for reminding me that the PhD is not my entire life. Thank you for signing me up for a 100 miles run through the Norwegian mountains as a celebration of finishing this degree. Thank you for being you. **To all of you, I could not have done this without you.**

Table of contents

Abstract

The work described in this thesis has focused on total synthesis directed towards two different classes of secondary metabolites isolated from the Agelas sponge, ageloxime D and analogs, and agelasine F. Ageloximes were reported to be 7,9-dialkylpurinium salts carrying a diterpenoid side chain in the 7-position and a hydroxylamine substituent in the 6-position. The enantiomer of the reported structure of ageloxime D was the target compound, along with two different analogs carrying either a geranyl or geranylgeranyl side chain. The enantiomer of the naturally occurring ageloxime D was chosen as the target compound because the enantiomer of the side chain of ageloxime D can be bought. Starting from (+)-manool, the sidechain was converted into (+)-copalol in four steps. There are no reported syntheses of ageloximes, and therefore a synthetic strategy was established. Starting from 9-methylated 6-chloropurine, a method for introducing a hydroxylamine in high yields had to be developed. As the selectivity of the alkylation of the sidechain at *N*7 was rather poor, it was necessary to introduce a removable directing group on the hydroxylamine. *Tert*-butyldimethylsilyl was the preferred choice, as it is sterically demanding and possible to remove under mild conditions. The selectivity of the alkylation at *N*7 was improved dramatically with the directing group. The removal of the directing group was eventually performed with ammonium fluoride, yielding *ent*-ageloxime D and analogs. The compounds were tested for biological activity and *ent*-ageloxime D and geranylgeranyl-ageloxime displayed high activity against the protozoa causing leishmaniasis and Chagas disease in addition to *Mycobacterium tuberculosis.*

Agelasines are also 7,9-dialkylpurinium salts carrying a diterpenoid side chain in the adenine 7-position. Agelasine F was synthesized starting from (*S*)-carvone, and the synthesis of the side chain focused on avoiding and improving some key steps was the main goal. The key steps were the introduction of the chloromethyl phenyl sulfide with the right stereochemistry, including the formation of the silyl enol ether and the avoidance of the expensive alternative starting material, (*S*)-pulegone. This compound has shown interesting activity against some drug resistant strains of *M. tuberculosis in vitro* and also inhibition of Na,K-ATPase.

Graphical abstract for the synthesis of ageloxime D and analogs

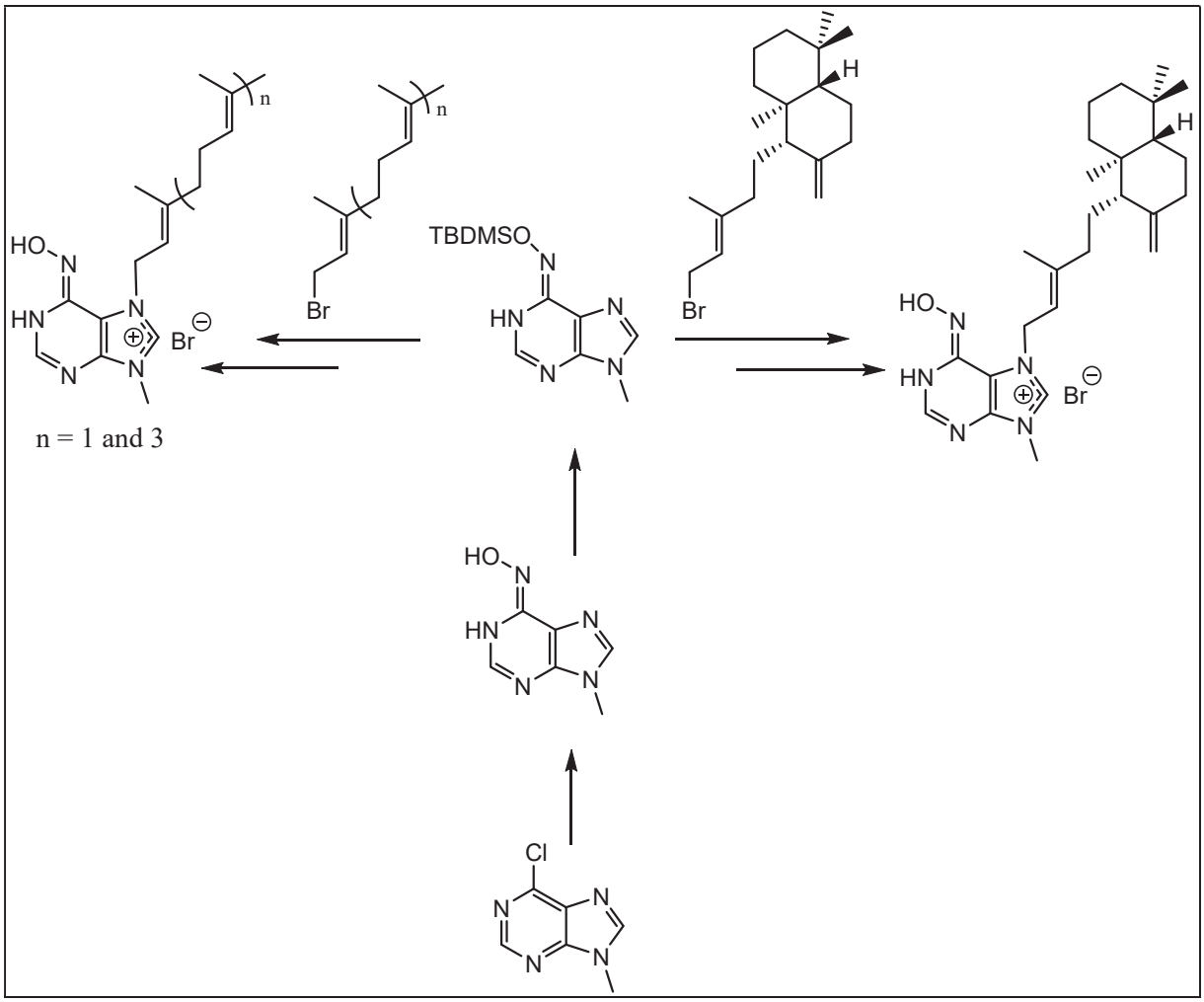

Graphical abstract for the synthesis of agelasine F

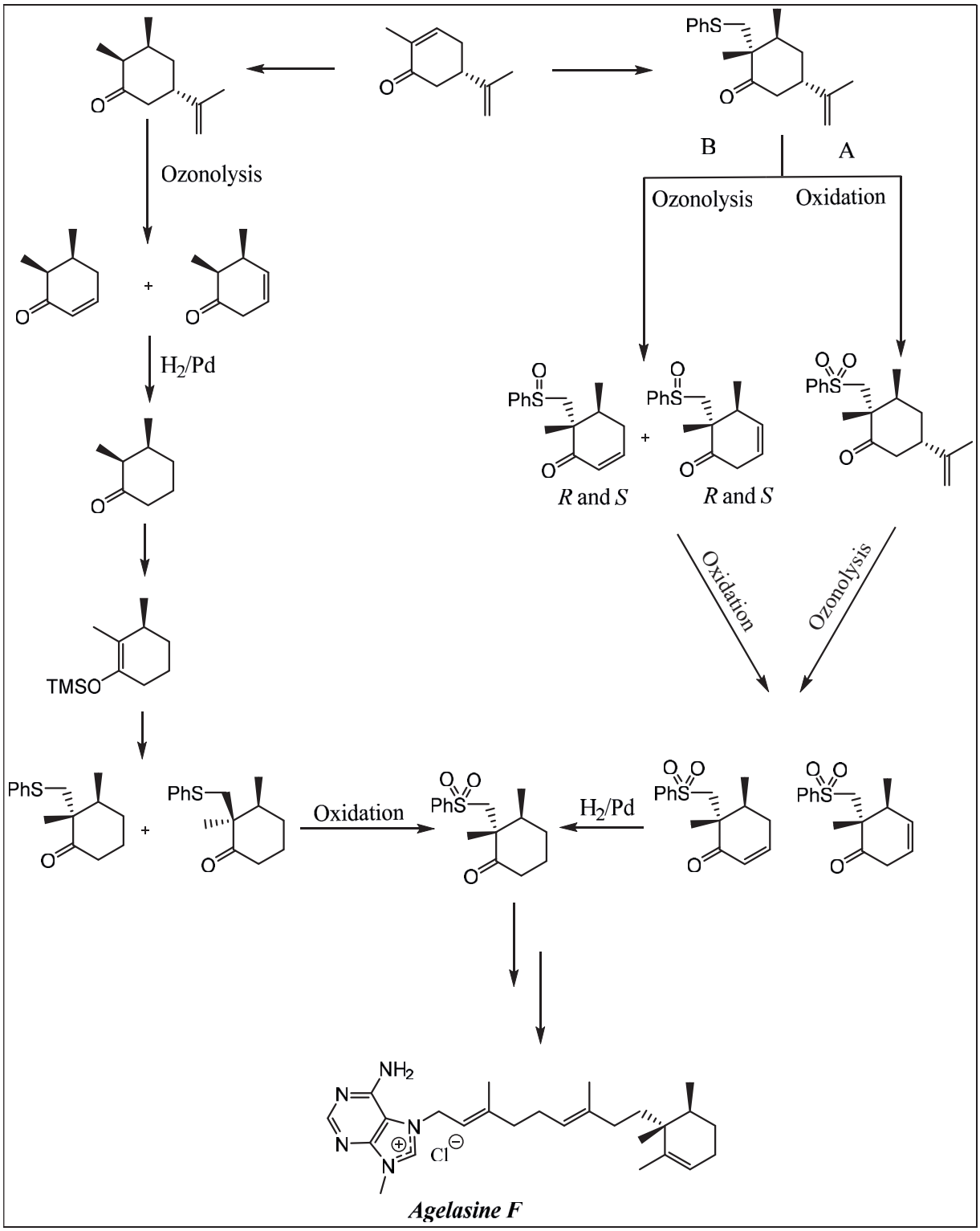

List of publications

I. Paulsen, B.; Fredriksen, K. A.; Petersen, D.; Maes, L.; Matheeussen, A.; Naemi, A. O.; Scheie, A. A.; Simm, R.; Ma, R.; Wan, B.; Franzblau, S.; Gundersen, L. L., Synthesis and antimicrobial activities of N(6)-hydroxyagelasine analogs and revision of the structure of ageloximes. *Bioorg. Med. Chem.* **2019,** *27* (4), 620-629.

II. Paulsen, B. Gundersen, L-L. (In press)
The first synthesis of (–)-agelasine F; an antimycobacterial natural product found in marine sponges in the Agelas genus.

Author contributions

In the following list, all minor and major contributions to the work presented in this thesis and related articles are presented:

Chapter 2

Kim Alex Fredriksen: Synthesized starting materials and contributed to the solution of the deprotection reaction of the benzyl ageloxime in section 2.2.

Dirk Peterson: Structure elucidation, NMR reported in section 2.6: author of Table 4, Figure 18 and Figure 19 (edited by BP).

Louis Maes, An Matheeussen, Ali-Oddin Naemi, Anne Aamdal Scheie, Roger Simm, Rui Ma, Baojie Wan and Scott Franzblau: All biological testing in section 2.7.

Chapter 3

Agnes Proszenyàk: Synthesis, Scheme 15.

Abbreviations

^{1}H	Proton
Ac	Acetyl
AMR	Antimicrobial resistance
Bu	Butyl
C. albicans	*Candida albicans*
DHP	3,4-Dihydro-2*H*-pyran
DMA	Dimethylacetamide
DMF	Dimethylformamide
DMSO	Dimethylsulfoxide
DNA	Deoxyribonucleic acid
E. coli	*Escherichia coli*
Ent	Enantiomer
ESI-MS	Electrospray ionization mass spectrometry
Et	Ethyl
HIV	Human immunodeficiency virus
HMBC	Heteronuclear Multiple Bond Correlation (2D)
HRMS	High resolution mass spectrometry
L.infantum	*Leishmania infantum*
LORA	Low-oxygen recovery assay
M. tuberculosis	*Mycobacterium tuberculosis*
MABA	Micro plate alamar blue assay
MDR-TB	Multidrug-resistant tuberculosis
Me	Methyl
MHz	Mega Hertz
MIC	Minimum inhibitory concentration
ml	Millilitre
Mmol	Millimol
MS	Mass spectrometry
NGO	Nongovernmental organizations
NMR	Nuclear magnetic resonance
NOESY	Nuclear Overhauser Effect Spectroscopy (2D)
P. aeruginosa	*Pseudomonas aeruginosa*

Pd/C	Palladium on charcoal
PPTS	Pyridinium *p*-toluenesulfonate
RR-TB	Rifampicin-resistant tuberculosis
RT	Room temperature
S. aureus	*Staphylococcus aureus*
SELNOE	Selective Nuclear Overhauser Effect (1D)
T. brucei	*Trypanosoma brucei*
T. cruzi	*Trypanosoma cruzi*
T. rhodesiense	*Trypanosoma rhodesiense*
TB	Tuberculosis
TBAF	Tetra-butyl ammonium fluoride
TBDMS	*Tert*-butyldimethylsilyl
THF	Tetrahydrofuran
THP	Tetrahydropyran
TMS	Trimethylsilyl
US	United States
WHO	World Health Organization
XDR-TB	Extensively drug-resistant tuberculosis

1 Introduction

1.1 Antimicrobials and antimicrobial resistance

The world today faces an enormous threat from multidrug-resistant bacteria and microorganisms, and the World Health Organization (WHO) has deemed resistance to antibacterial medicines to be one of the biggest threats towards global health, food security, and development. The extensive use of antibiotics as growth mediating compounds in agriculture, and its overuse in humans are two of the main causes for the current accelerated development of antibiotic resistance. Because many people around the world travel more, the spread of resistant superbugs is accelerating and is now becoming a global problem. Worldwide, it has been forecasted that by 2050 multirestistant bacteria could cause 10 million deaths each year and that the economy could suffer equal damage as during the 2008-2009 global financial crisis.[1]

The term antimicrobial resistance, AMR, is defined as resistance against drugs that treat and prevent infections caused by bacteria, viruses, fungi and parasites. AMR will increase the cost of health care for patients, owing to prolonged duration of illness, disability, and need for additional tests and more expensive drugs. Owing to widespread AMR, treatment and prevention of infections will become difficult, and it will make medical procedures such as major surgery, organ transplantation, and cancer chemotherapy high-risk procedures. To avoid a situation similar to the one in the pre-antibiotic era, when small injuries could become lethal, development of new antimicrobial drugs is of paramount importance.

After the discovery of Penicillin G (Figure 1) in 1928 by Sir Alexander Fleming,[2] a dozen different classes of antibiotic were released the following two decades.

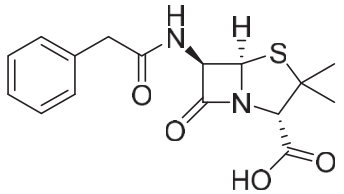

Penicillin G

Figure 1. The structure of Penicillin G.

Then, there was a halt in the development of new antibiotics, and no new classes were discovered and released between 1968 and 2000. Since then, a few new classes have been

launched and a total of 22 new drugs. There are currently 42 compounds in development for clinical use (as per March 2019), but very few of these belong to a novel drug class.[3, 4] Historically, only one of five drugs that enter clinical phase testing will be approved for use on humans. The WHO has published a list of twelve priority pathogens that pose the greatest threat towards the health of humans, including *Pseudomonas aeruginosa, Staphylococcus aureus,* and *Escherichia coli.*[5] Looking into the pipeline of new antibiotics, it should be noted that most of the new antibiotics have a narrow antimicrobial spectrum, and many target acute bacterial skin and skin structure infections, pneumonia, and urinary tract infections. There is a critical lack of antibiotics treating severe bloodstream infections caused by bacteria such as gram-negative *E. coli*. Unfortunately, development of new drugs is a time consuming and costly affair. Given that the new drugs will only be used in cases where the old drugs do not work, development of new drugs is not profitable for pharmaceutical companies. Ninety percent of the companies developing new antibiotics are small companies, and 60% do not have any drugs on sale in the market.

The main goal of this project has been to synthesize agelasine F, *ent*-ageloxime D and ageloxime analogs. The structures of ageloximes and agelasines will be presented in detail in section 1.6.3 and 1.6.2, respectively. These target compounds will be tested for biological activity towards the microorganisms causing leishmaniasis, Chagas disease, African sleeping sickness and biofilm formation. The microorganisms causing these diseases that have developed AMR are listed in Table 1, and these were used as a testing panel in our work. *S. epidermidis, P. aeruginosa* and *E. coli* were subject to biofilm testing, and the results will be presented in section 2.7. A few examples of diseases caused by these microorganisms are given in the last column. These particular microorganisms were of interest as they have been used as a test panel for previously synthesized agelsines, and it was desirable to compare the biological activities of the agelasines against the ageloximes synthesized.

Table 1. Examples of microorganisms causing disease in humans that have developed resistance, and also being the test panel for testing for biological activity.

Microorganism	Type of microorganism	Diseases
Mycobacterium tuberculosis	Mycobacterium	Tuberculosis
Escherichia coli	Gram-negative bacteria	Food poisoning, urinary tract infections
Pseudomonas aeruginosa	Gram-negative bacteria	Inflammation and sepsis
Staphylococcus aureus	Gram-positive bacteria	Pneumonia and meningitis, MRSA
Staphylococcus epidermidis	Gram-positive bacteria	Biofilm formation on surgical implants
Leishmania infantum	Protozoa	Leishmania disease
Trypanosoma cruzi	Protozoa	Chagas disease
Trypanosoma brucei	Protozoa	West African sleeping sickness
Trypanosoma rhodesiense	Protozoa	East African sleeping sickness
Candida albicans	Fungi	Skin and mucous membrane infections

As it will need a profound effort to deal with AMR, some of the diseases caused by the different microorganisms and the challenges these diseases pose will be presented in further detail below.

1.2 Antibacterial drugs and resistance

1.2.1 Tuberculosis – *M. tuberculosis*

Mycobacterium tuberculosis is the cause of tuberculosis (TB), one of the ten major causes of death worldwide, and the top cause of death amongst people with HIV. The disease is found all over the world, up to one-third of the world's population has latent TB, and there is a 5-15% chance that it develops into TB over their lifetime.[6] According to WHO, important risk factors for acquiring the disease are malnutrition, HIV, diabetes, and the use of tobacco. After developing the disease, there is a 45% chance of dying if left untreated. If combined with HIV, chances of survival are very low. However, the disease is curable with proper treatment, and also preventable, as the bacteria spreads through air, typically after an infected person coughs or sneezes without covering their mouth and nose.[7] Ninety-five percent of the cases and deaths occur in developing countries, and two thirds of all TB cases are found in eight high-burden countries: India, China, Indonesia, the Philippines, Pakistan, Nigeria, Bangladesh and South Africa.[7]

Rifampicin (Figure 2) is the most effective first-line drug used in treatment regimens. According to the WHO Global Tuberculosis Report 2019, approximately 484 000 cases of a

total of 10 million had developed rifampicin-resistant tuberculosis (RR-TB).[7] Of these, 78% were multidrug-resistant TB (MDR-TB), and among these, 6.2% of the cases worldwide were estimated to have extensively drug-resistant TB (XDR-TB). According to WHO, resistance is due to improper use of the antibiotics in treatment regimens.

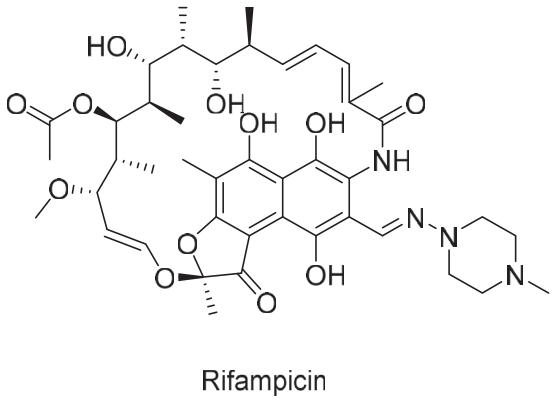

Rifampicin

Figure 2. The structure of rifampicin.

1.2.2 Biofilm – when an infection goes from bad to worse

Biofilm is a polysaccharide-containing slime that some microorganisms produce in order to irreversibly attach to and grow on surfaces. *P. aeruginosa, E. coli, S. epidermidis* and *C. albicans* are common sources of biofilm formation, and are often found on medical devices such as urinary catheters, central venous catheters and artificial hip prostheses.[8] The National Institutes of Health (US) have estimated that 60% of all microbial infections, and 80% of all chronic infections, are associated with biofilm formation.[9] This poses a serious threat to medical health care, because once the biofilm has formed, the microorganisms are much less susceptible to antibiotics, and thus very hard to get rid of. Administering high doses of antibiotics will in most cases not dissolve the biofilm, but it may keep the chronic infection under control. In order to eliminate the biofilm, the infected medical device or implant must be removed, and this solution is troublesome for the patient and expensive for the society.[10] This underlines the need for better treatment options for infections caused by biofilm-producing microorganisms.

1.2.3 Biofilm – problems in underwater establishments

Biofilm is not only a problem in health care. On underwater appliances, biofilm formed by bacteria is an important contribution to the accumulation of microorganisms, algae, animals and plants on wetted surfaces.[11] Vessels at sea may suffer a 40% increase in fuel consumption and up to 10% reduction in speed because of biofilm on their hulls. The US Army has reported extra

costs of approximately 1 billon US dollars annually for the extra fuel costs and maintenance to keep their vessels free of barnacles, oysters and algae.[12] Previously employed antifouling paint has caused irreversible damage to aquatic life, and today 70% of all vessels are using copper-based paints to keep their hulls free of biofouling. This type of paint causes copper to build up in high concentration in harbors, waterways and the ocean. This is a danger to aquatic life, but also humans who work there or eat the fish caught in the contaminated waters. New antifouling agents with low toxicity are therefore needed.

1.3 Antiparasitic drugs and resistance

1.3.1 Leishmaniasis – *L. infantum*

Leishmaniasis is the second largest tropical disease after malaria and is caused by a protozoan parasite. WHO estimate that 12 million people are infected with the Leishmaniasis disease. The disease may affect the skin or internal organs, the latter being potentially deadly, killing approximately 70 000 people per year.[13] In cases where only the skin is affected, the patient may suffer from extensive scarring.

Resistance towards the most used drugs against leishmaniasis, pentavalent antimonial (the structure shown in Figure 3, antimony shown in blue) has been reported.[14] Again, WHO reports that global misuse of the medicines is the reason for this development, and effective monitoring of drug use and response is important to limit further spread and development of resistance.

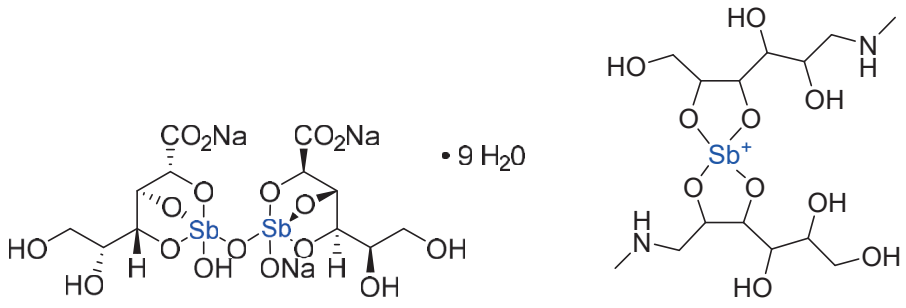

Figure 3. The two most used pentavalent antimonial drugs in the treatment of leishmaniasis. Antimony shown in blue to highlight the position of the metal.

1.3.2 Chagas disease/American trypanosomiasis – *T. cruzi*

According to the WHO, 6-7 million people are infected with the parasite causing Chagas disease, and 100 million people live in the endemic areas.[15] Most cases are found in the rural

areas of Latin America, where the bug (known as the kissing bug or vampire bug) that carries the parasite exists. In the acute phase of the disease, often only mild and unspecific symptoms occur, which can make it hard to realize that one has been infected. In the second and chronic phase, the parasites hide in the heart and digestive muscles. Thirty percent of the infected people develop cardiac disorders, and ten percent suffers from digestive or neurological disease or a combination of the two. If left untreated, the infection can cause sudden death due to destruction of the heart muscle and its surrounding nervous system.

The commonly employed drugs are benznidazole and nifurtimox (Figure 4), which are almost 100% effective on certain strains of the parasite if administered early after infection. Some strains have a naturally occurring resistance, and this causes a big challenge in the treatment of such infections.

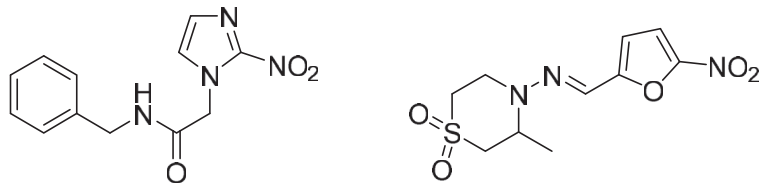

Figure 4. The structure of the two most used drugs against Chagas disease.

1.3.3 African sleeping sickness – *T. brucei* and *T. rhodesiense*

There have been several human epidemics of the African sleeping sickness in Africa, but luckily the combined efforts of WHO, national control programs, and nongovernmental organizations (NGOs) have managed to turn the tide in a positive direction during the 1990's and later. The disease threatens 65 million people in 36 countries in sub-Saharan Africa, but with the latest effort the estimated number of undiagnosed and untreated cases has been reduced from 300 000 in 1998 to under 10 000 cases today. The disease is caused by two different parasites, *T. gambiense* and *T. rhodesiense*. *T. gambiense* is responsible for 98% of the cases, and causes a chronic infection that does not have major symptoms before the disease is in an advanced stage.[16] The other parasite, *T. rhodesiense* is responsible for the remaining 2% of the infections, and causes a more acute disease by invading the central nervous system. Both parasites are carried by the tsetse fly, which infects humans with the parasites with a bite. In the later stages of the disease, the patient shows a marked change of behavior, sensory disturbances, confusion and poor coordination. Another important feature is the disturbance of the sleep cycle, which

gives the disease its name. Early treatment increases the chance of being cured, and relatively safe medications can be used in the early onset of the disease.

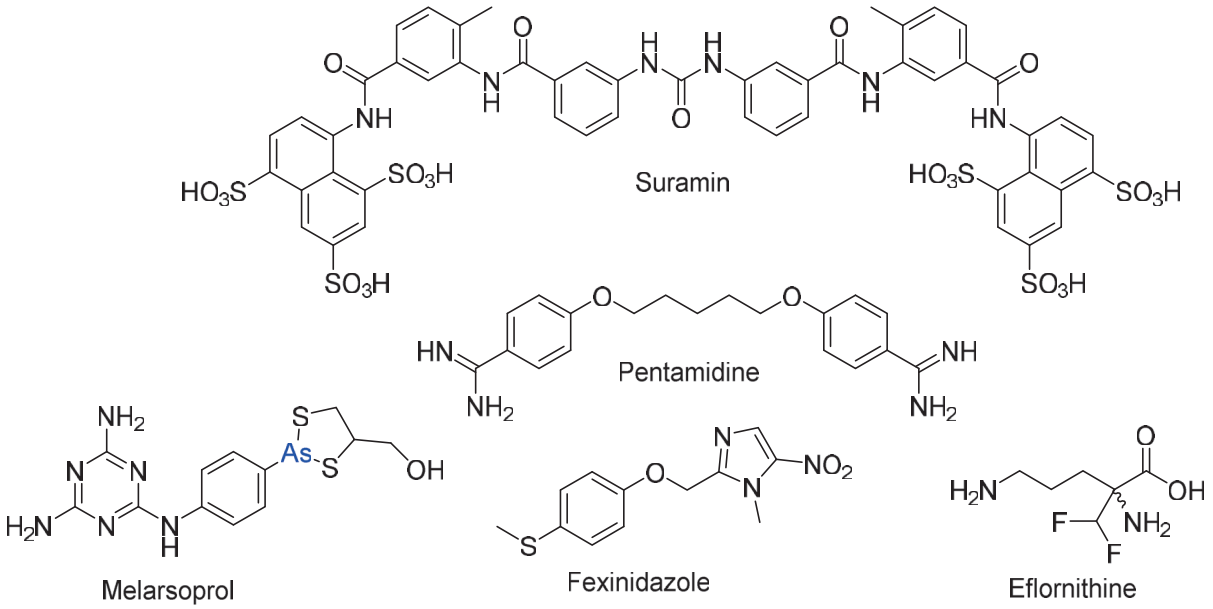

Figure 5. The six most used drugs towards battling the African sleeping sickness. Arsenic shown in blue.

There are two main classes of drugs against the sickness; the arsenicals and diamidines (Figure 5).[17] However, antiparasitic resistance to several of the six drugs used against both parasites has increased. If the infection is left untreated for longer periods, medicines that are complicated to administer and have serious side effects are necessary to combat the disease, as it is fatal if left untreated.

1.4 Combat resistance – what is the strategy?

This world-spanning problem requires global action.[18] The WHO has outlined a five-point strategy to combat the increasing drug-resistance in microorganisms: (1) improve awareness and understanding of antimicrobial resistance, (2) strengthen surveillance and research, (3) reduce the incidence of infection, (4) optimize the use of antimicrobial medicines, (5) and ensure sustainable investment in efforts to counter antimicrobial resistance. This degree is part of the research targeting new potential antimicrobial medicines, even though at a very early stage.

1.5 New antimicrobials – where can we find them?

Nature itself has a wide variety of antimicrobial substances. A large number of commercial drugs today have been isolated either from plants and terrestrial organisms or from derivatives

of these isolated compounds.[19, 20] Secondary metabolites are an excellent starting place to look for new bioactive compounds, as the metabolites reveal an enormous chemical and biological diversity in both terrestrial and marine species, including fungi and bacteria. The very famous Penicillin G was isolated from a fungi.[2] These secondary metabolites are organic compounds not involved with normal growth, development, or reproduction of the species and thus often harbor interesting bioactive properties. For instance, artemisinin and its derivatives are powerful drugs for treating malaria in combination with other drugs,[21] and it was isolated from the plant *Artemisia annua.*[22] Another example of a secondary metabolite with interesting medicinal properties, is quinine, an alkaloid used to treat malaria (Figure 6). This natural product was isolated from the bark of the Cinchona tree. Given its bitter taste, British colonials in India mixed it with gin, creating the popular cocktail gin and tonic. Quinine is on the WHO list of core medicines that are considered vital for a basic health care system (2019). Of these medicines, 11% originate from flowering plants.[23]

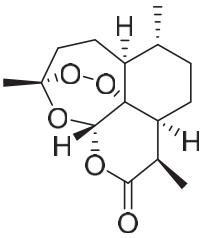

Artemisinin

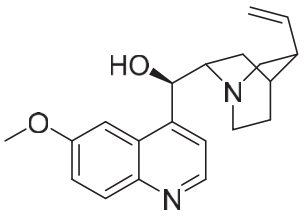

Quinine

Figure 6. The structure of artemisinin and quinine.

Natural products harvested from marine environments have become increasingly popular as a source of lead compounds for new drugs the last fifty years, because marine species reveal an enormous chemical and biological diversity of metabolites.[24, 25] Marine organisms also produce interesting secondary metabolites, but the marine environment has not been explored to the same extent as plants and terrestrial organisms. Over the last fifty years the isolation of natural products from the marine environment has increased.[26,27] Sponges are promising targets when looking for bioactive compounds, owing to the fact that they lack an immune system. This makes it necessary for them, and microorganisms living together in symbiosis, to produce a chemical defense of toxic substances. In addition, sponges often stay free of biofouling organisms, and it is therefore interesting to look for antifouling agents among these species.[28]

1.6 Purine-containing natural products – from addictive to deadly properties

This thesis presents work to synthesize compounds found in a sponge, and these compounds are believed to be secondary metabolite built on a purine scaffold. The purine scaffold is a very common structure in nature, and can be found in many natural products.[29] Caffeine is one example of a purine-containing natural product, and this compound is a very popular (and addictive) stimulant found in coffee beans and tea leaves (Figure 7).[30] Even though one may believe that caffeine is the most important purine to humankind, most people would agree that the DNA bases adenine and guanine are even more important.[31] The purine moiety is also present in many marine natural products. A purine-containing marine natural product that is definitely not beneficial for human health, is saxitoxin (Figure 7).[32] This compound has been classified as a Schedule I Chemical Warfare Agent per the Chemical Weapons Convention of 1993, being 1000-fold more toxic than the chemical weapon Sarin.[33] The lethal dose for an average human is 0.2 mg.[33] Its toxicity arises from its ability to bind to voltage-gated sodium channels, resulting in blockage of the passage of nerve impulses.[34] This leads to death via respiratory paralysis. The normal ingestion pathway is through contaminated shellfish.[35] In sea water, it is produced by dinoflagellates, a type of algae, and in fresh by cyanobacteria.[36] Other purine-containing marine natural products have more positive biological effects, such as the 1,3-dimethylisoguanine (Figure 7). This compound was isolated from the sponge *Amphimedon viridis*, and shows high cytotoxity on an ovarian cancer cell line.[37]

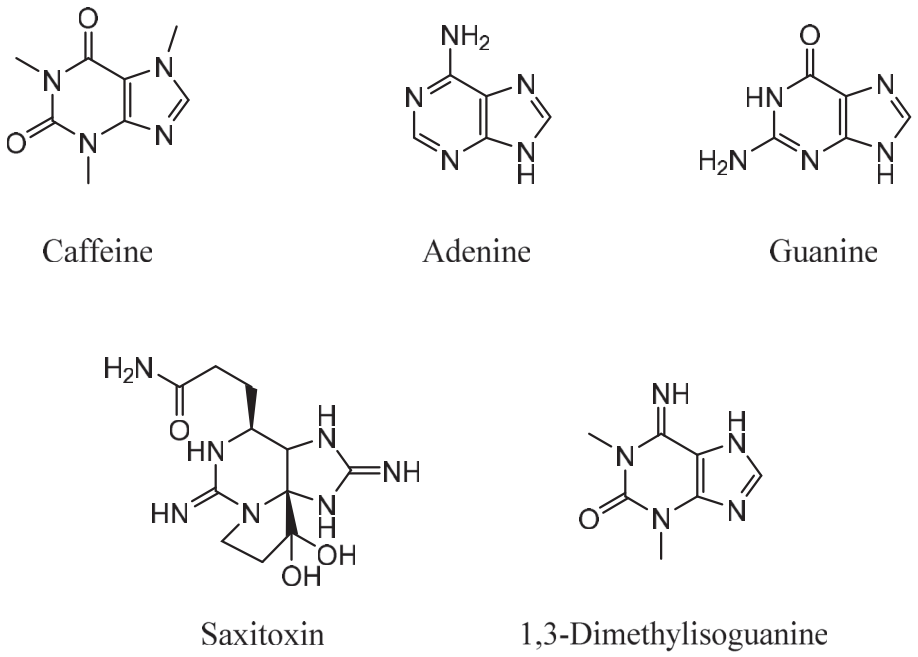

Figure 7. The chemical structure of purine containing natural products.

Agelas sponges, found in shallow tropical and subtropical waters,[38] are rich sources for the discovery and isolation of novel marine natural products.[39] Alkaloids are nitrogen-containing secondary metabolites that constitute of a major class of compounds that has been isolated from these sponges. Amongst these alkaloids there are reported several different classes of complex purine-terpene hybrids, for example agelasines and ageloximes.[39] One example of a compound that belongs to each of these different classes can be seen in Figure 8. The agelasines and ageloximes will be discussed further as they are relevant for this thesis.

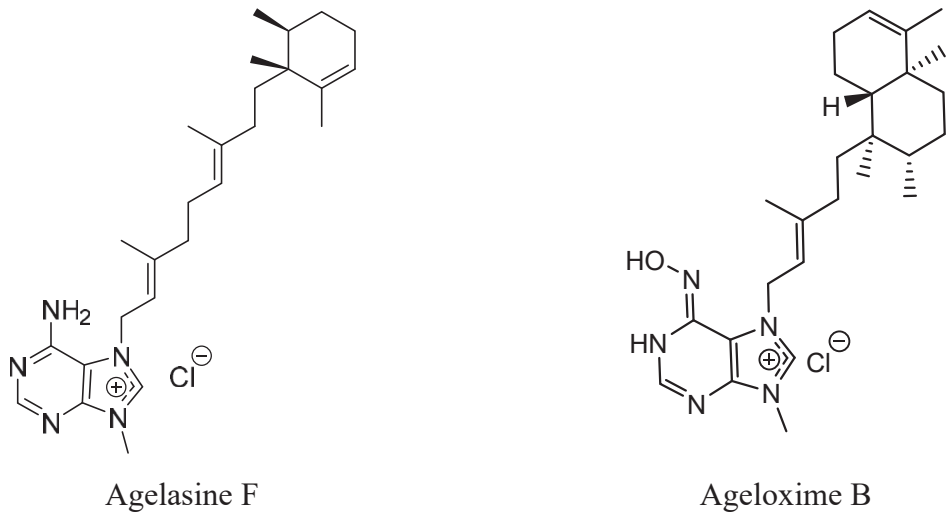

Figure 8. Examples of compounds from two different classes of purine containing marine natural products isolated from the *Agelas* sponge.

1.6.1 The structure of purine – a privileged scaffold

Purine itself is an imidazole ring fused to a pyrimidine ring, and can be seen in Figure 9, along with its numbering system. It can exist as a 1*H*, 3*H*, 7*H* or 9*H* tautomer, the difference being the position of the hydrogen. This structure is a privileged scaffold, meaning that it can bind to different receptors depending on its sidechains.[40]

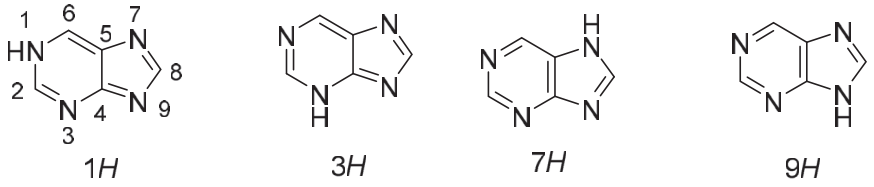

Figure 9. The chemical structure of purine. The hydrogen can be located at four different nitrogens, causing the existence of four different tautomers.

1.6.2 Agelasines – can the *Agelas* sponge defense system aid ours?

One major class of compounds isolated from the *Agelas* sponge is the agelasines.[41, 42] The agelasines A to V (Figure 10) have been isolated to date.[43-56] These compounds are 7,9-dialkylpurinium salts, that are endowed with several biological activities such as antimicrobial activity,[45, 49, 50, 57] cytotoxic activity,[58] antifouling activity,[49] anti-tuberculosis activity,[52] antifungal activity,[49, 57] antileukemic activity,[48] and they can induce contraction of smooth muscles[48] and inhibit Na/K-ATPase.[44, 47, 59] The difference between the agelasines are found in the sidechains, which are the diterpene part of the molecule. These diterpene sidechains are divided into four different types: Clerodane, halimane, labdane and monocyclic diterpenoid. Their key features are marked in red in Figure 10. For instance, the distinguishing features of the clerodane type agelasines are its stereochemistry and that they have different groups substituted on the diterpene ring.

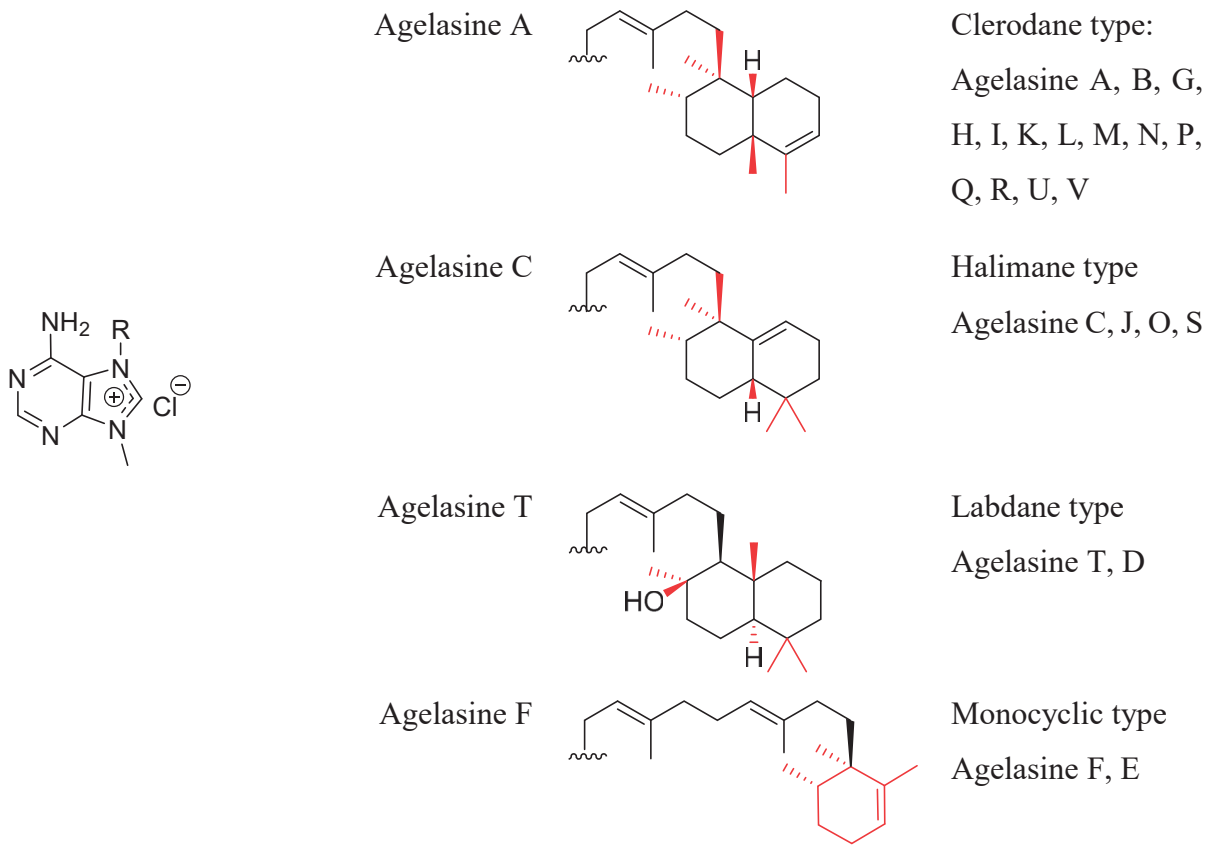

Figure 10. An overview of the different types of agelasines divided in to four types: clerodane, halimane, labdane and monocyclic. The bonds and atoms marked in red are the key features for the different types, and variations within the types between the different agelasines occur at these places. In addition, other substituents can be substituted on the bicyclic rings.

The agelasines have shown interesting antimicrobial activityand, several of them have been synthesized (Figure 11). Previous work in our group has involved the total synthesis of (+)-agelasine D[58, 60], *ent*-agelasine F[61] and (-)-agelasine E[62, 63]. In addition, (-)-agelasine A[64], (-)-agelasine B[65], (+)-agelasine C[66] and racemic (±)-agelasine F[67] (also called ageline A) has been synthesized by other groups.

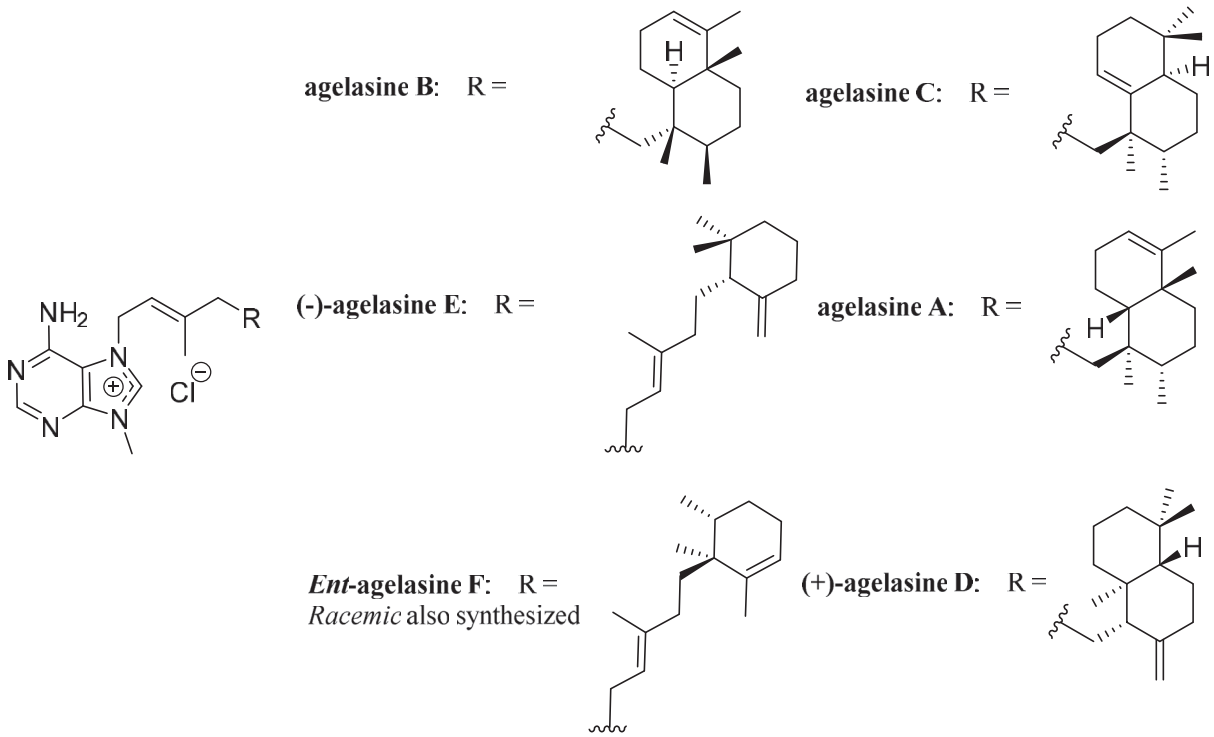

Figure 11. An overview of the structures of the agelasines that have been synthesized by our group and others.

The synthesis of the agelasines is divided in two parts, the synthesis of the purine moiety, and the more complex synthesis of the diterpene side chain. As an example synthesis of an agelasine, the total synthesis of (*ent*)-Agelasine D by Vik *et al*.[58] and Utenova *et al*.[60] is shown in Scheme 1. The replacement of the chlorine in compound **1** was performed with an alkylated hydroxylamine salt (Scheme 1). Until 2009, a methyl substituent on the hydroxyl group was utilized, and the synthesis involved reacting a N^6-methoxy-purine (**2a** or **2b**) with the alkyl bromide (**3**) of the desired side chain. Utilizing N^6-methoxy-purin, lead to substantial alkylation on N^6 in addition to *N*7. Vik *et al.* tested other alkoxy derivatives on the N^6 and discovered that the sterically demanding *tert*-BuO-group resulted in less formation of the N^6-alkylated isomer.[58] To ensure a good stereoselectivity of the attachment of the sidechain to the *N*7 in the purine

moiety, the bulky *tert*-butylhydroxy-group was used as a directing group as can be seen in Scheme 1.

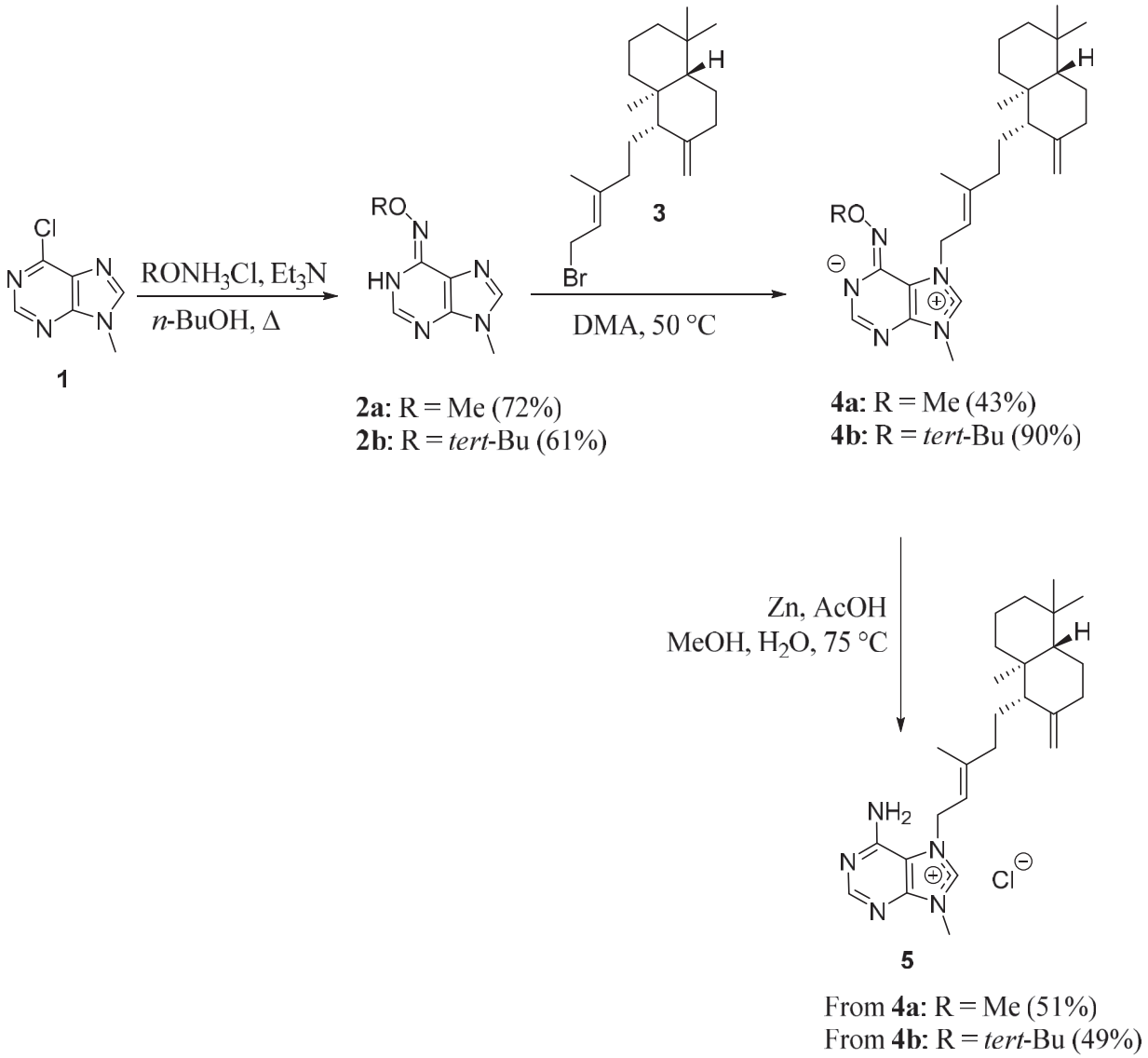

Scheme 1. Total synthesis of *ent*-agelasine D from anticopalol bromide and 9-methylated 6-chloropurine, with both methoxy and *tert*-butoxy substituted on N^6, yielding different selectivity in the alkylation step. The *tert*-butoxy substituent being superior in directing the bromide 3 to *N*7.

Synthetically prepared analogs have also displayed equally high antimicrobial activity as the naturally occurring compounds. Analogs of agelasine D carrying a MeO-group on N^6 and a geranylgeranyl sidechain at *N*7 were potent inhibitors against a wide variety of microbials (Figure 12).[58, 68, 69] The substituent on N^6 (or the lack of) is important for the specific biological activity. Compounds having similar side chain on *N*7, but a different N^6 substituent, vary in biological activity for some organisms.[68] The features believed to be important for biological activity are marked with orange in Figure 12. For instance, compound **6a** and **6b** in Figure 12

have the same side chain on *N*7, but the MeO-geranylgeranyl-agelasine **6a** had one third of the IC_{50} value towards *L. infantum* as *tert*-BuO-geranylgeranyl-agelasine **6b**.[68] Studying the effect on MRC-5 (human fibroblast cells) the effect of the MeO-group seemed to lower the toxicity: IC_{50} for MeO-geranylgeranyl-agelasine **6a** was lower than for *tert*-BuO-geranylgeranyl-agelasine **6b**. Comparing the activity against *M. tuberculosis* of four different compounds showed that all except MeO-agelasine **4a** had equal effect against the bacteria. Compound **4a** and **4b** was isolated as betaines, which mean they are deprotoned from the use of a basic eluent system in the purification method. Betaines are a type of zwitterion, but without the presence of a hydrogen at the charged locations.

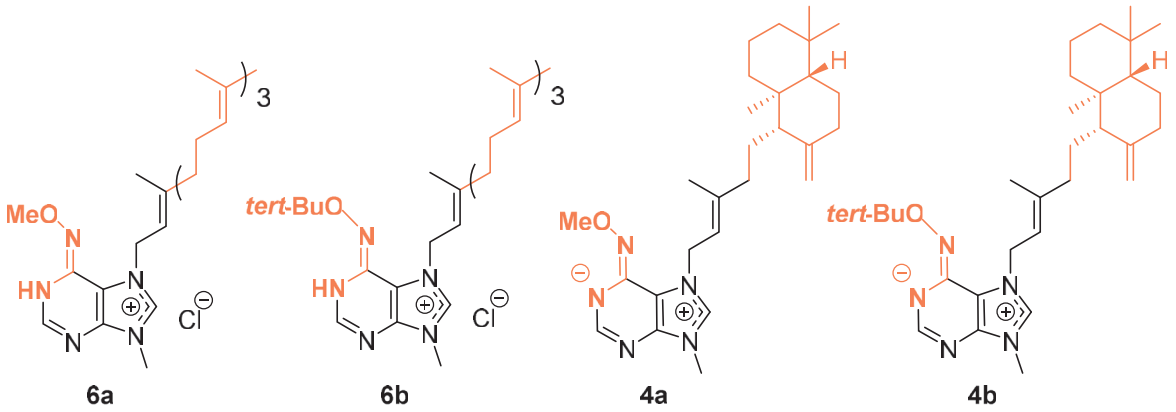

Figure 12. Compounds displaying high antimicrobial activity. The two structures on the right are betaines, which in this case are deprotoned agelasine with both a positive and negative charge.

Table 2. Overview of the biological activities compounds 6a, 6b, 4a and 4b exhibits on *M. tuberculosis* and *L. infantum*.

	6a	**6b**	**4a**	**4b**
	MIC (µg/mL)			
M. tuberculosis	3.13	3.13	>6.25	3.13
	IC_{50} (µg/mL)			
L. infantum	0.097	0.27	0.63	4.0
MRC-5	2.0	0.26	4.5	0.45

If the length of the side chain was shortened compared to the side chain in the structure shown in Figure 12

, the antimicrobial activity was significantly reduced (Figure 13). Thus, it seemed that the length of the sidechain was more important than its exact structure for the biological activity.

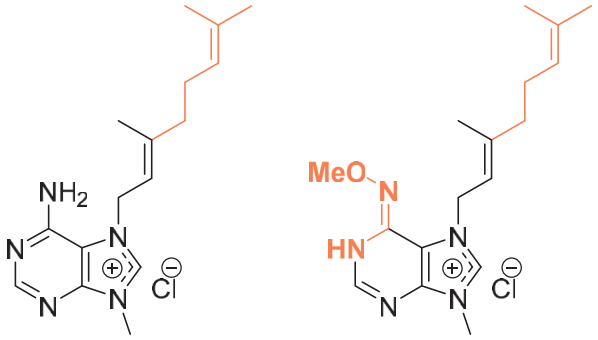

Figure 13. Agelasine analogs displaying poor antimicrobial activity.

The second part of the thesis will present attempts to improve the synthesis of agelasine F previously published by our group. As this synthesis resulted in the *ent*-agelasine F, the focus in this project was to make the stereochemically correct (-)-agelasine F.

1.6.3 Ageloximes – no more biofilm?

The proposed structure of the ageloximes are oxime derivates of the agelasines, hence the name ageloxime. Their structure is similar to the agelasines, the only difference in the proposed structure being the hydroxyl group in the N^6-position. The assigned letter comes from the agelasine that carries an identical sidechain. They are reported to be 7,9-dialkylpurinium salts carrying a diterpenoid side chain in the 7-position and an oxime substituent in the 6-position.[59, 70] Two ageloximes, ageloxime B (compound **7** in Figure 14) and ageloxime D (compound *ent*-**8d** in Figure 14), have been isolated from an *Agelas* sponge by Hertiani *et al.*[70]

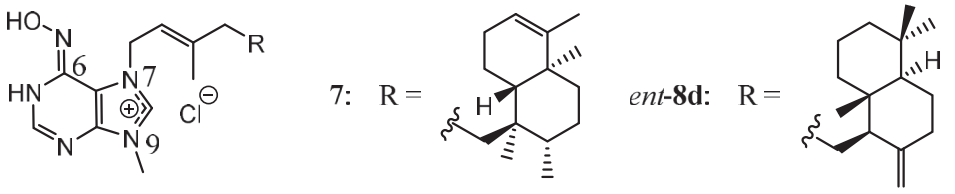

Figure 14. The purine moiety of the proposed structure of ageloximes contains a methyl group in position 9, a hydroxylamine group in position 6 and a copalool alkyl chain in position 7 resulting in a purinium salt.

These two ageloximes have shown interesting biological activity against several species.[59, 70] Both display activity towards the opportunistic pathogen *C. neoformans* which is an exceptionally dangerous fungus that can cause encephalitis or menigitis, often in humans with an already weakened immune system.[71] Antileishmanial activity against the parasite *L.*

donovani has also been reported.[59] In addition, Ageloxime B exhibited antibacterial activity against *S. aureus* and methicillin-resistant *S. aureus.* Ageloxime D is reported to inhibit biofilm formation of *Staphylococcus epidermidis*, which is very interesting considering the problems biofilm cause in both healthcare and underwater establishments.[59] The aim of the work described in this thesis was to synthesize *ent*-ageloxime D, in order to perform more biological activity tests, and also to verify the structure of this natural product, as it has never been synthesized before. It has on many occasions proved important to verify structure elucidations of natural products by synthesizing them, but it is still underused.[72] Seeing as biofilm formation is an increasing problem in health care and on underwater establishments, it is of high interest to synthesize compounds that can help defeat this problem. As the structure of the side chain in ageloxime D is rather complex (the enantiomer can be seen in Scheme 2, compound **8d**), a synthetic route involving the synthesis of this part of the molecule from scratch would be too comprehensive. Instead the enantiomer (which is readily available) served as the starting point for the total synthesis. As mentioned in section 1.6.2, analogs of agelasines with simpler side chains (as the geranylgeranyl) bearing a MeO-group in the N^6 position have proven to have a high biological activity towards *M. tuberculosis.* Therefore, it was of interest to explore if the unsubstituted hydroxylamine at C6 would influence the activity towards this bacteria.

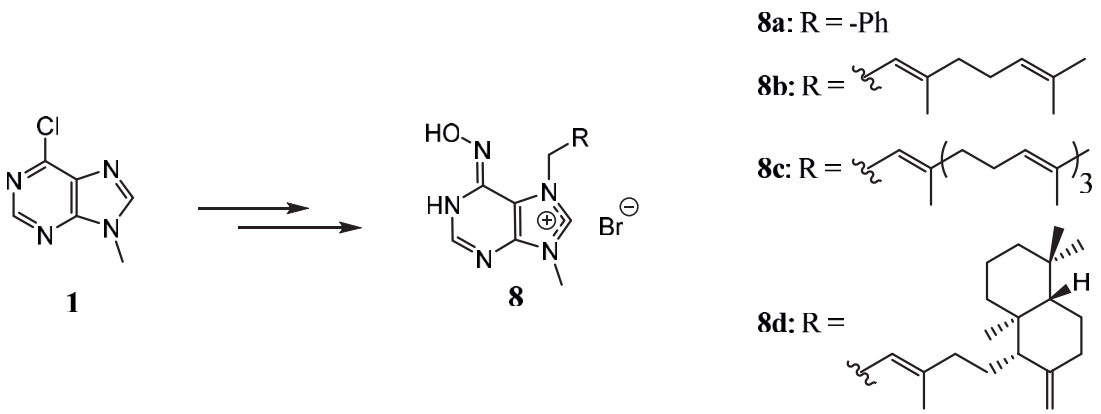

Scheme 2. Target compounds (8a, 8b, 8c and 8d) starting from 9-methylated 6-chloropurine.

2 Synthesis of *ent*-ageloxime D and analogs

2.1 Introduction

The following chapter describes the synthesis of the proposed structure of *ent*-ageloxime D and analogs. As mentioned in the introduction, prior work in our group has identified the geranylgeraniol side chain at *N*7 as an important feature of the structure in order for the structure to be a potent inhibitor against bacterial growth of the TB bacteria. Synthesizing the ageloxime carrying this side chain was therefore of interest. The agelasine analog carrying a geranyl side chain has previously shown poor antimicrobial activity, but it was decided to synthesize the geranyl-ageloxime to see if the same trend of reduced biological activity existed for the ageloxime as well. The synthesis of the target compounds involves methylation at *N*9, before introducing the hydroxylamine group at C6, an alkylation reaction between the altered purine and an alkyl bromide, see Figure 15. As the methylation of 6-chloropurine is a known reaction, it was therefore decided to be the first reaction in the sequence.[73] The selectivity in this methylation reaction favors methylation at *N*9. The hydroxylamination has been done on similar compounds, and was the second step.[74-76] As the starting material (manool, Scheme 3) for the side chain of the ageloxime D is very expensive, it was desirable to introduce this sidechain as late as possible in the synthesis. The alkylation step was therefore the last in the sequence.

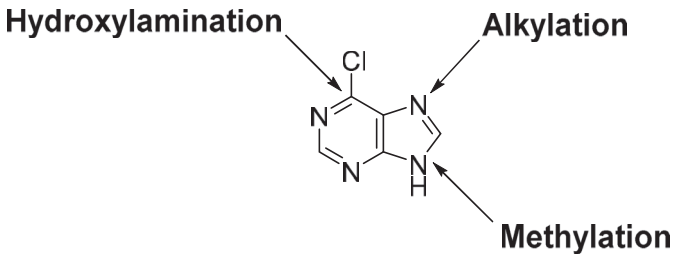

Figure 15. Key reactions for the synthesis for the target compounds (8a, 8b, 8c and 8d) from 6-chloropurine.

As described in section 1.6.2 (Scheme 1), the alkylation on *N*7 requires an alkyl bromide as alkylating agent. Benzyl bromide is easily available and was used as a model alkylating agent to give an idea of the reactivity of the purine moiety when alkylating the *N*7. An overview of the four target compounds is found in Figure 16.

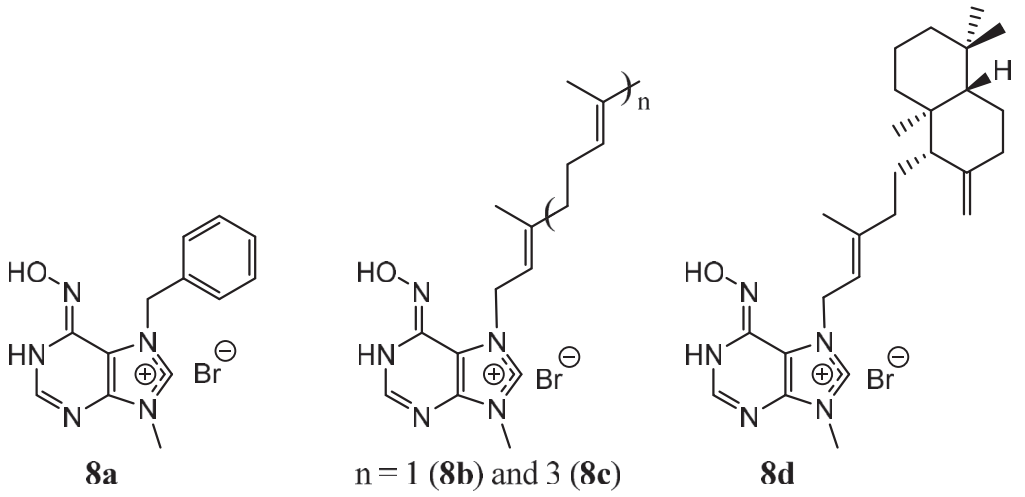

Figure 16. Target compounds benzyl-ageloxime 8a, geranyl-ageloxime 8b, geranylgeranyl-ageloxime 8c and ageloxime D 8d.

The reason for synthesizing *ent*-ageloxime D **8d** was that it is not possible to buy or easily synthesize the complex sidechain with the right stereochemistry. Therefore, the side chain was synthesized in four steps from (+)-manool[58] (Scheme 3) to anticopalol bromide, and after alkylation of the purine moiety it resulted in *ent*-ageloxime D.[58, 60]

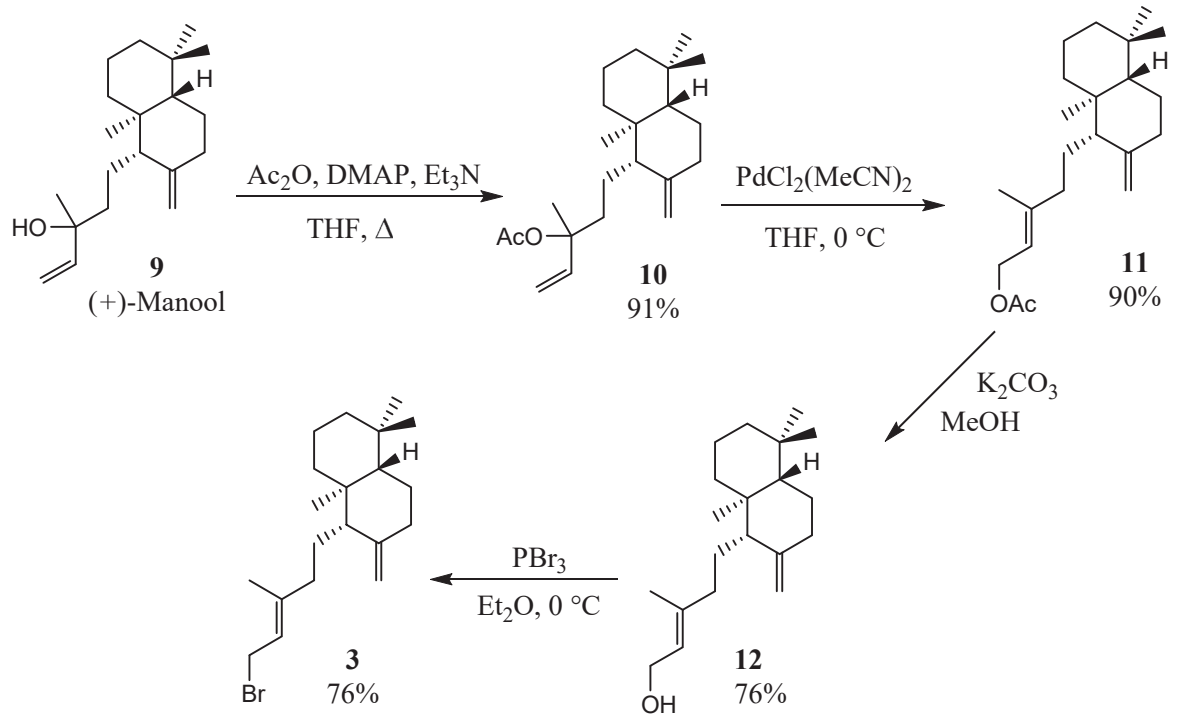

Scheme 3. The synthesis of anticopalol bromide (3) from (+)-manool (9) following a published synthesis by Vik *et al.*[58]

2.2 Model reaction: Synthesis of benzyl-ageloxime

The first step in the synthesis of the benzyl-ageloxime (**8a**) was to synthesize 9-methylated 6-chloropurine **1**. This was a known procedure, and was followed without modifications (step one in Scheme 4).[77] The two isomers formed, **14a** and **14b**, with a ratio of 4:1, could be partly separated with flash chromatography, hence the low yield. The second step in the synthesis of the enantiomer of the proposed structure of ageloxime D **8d** and analogs (**8a**, **8b**, **8c**) was the introduction of a hydroxylamino group at C6, leading to the formation of the substituted purines **15a** and **15b**. Giner-Sorolla *et al.* described a hydroxylamination of 6-chloropurine (**13**),[74] but the literature procedure was not reproducible on our substrate, as we observed substantial formation of the hypoxanthine **16**. The formation of hypoxanthine **16** was believed to arise from the excess base used in this reaction. Exchanging the chloride with an OH-group utilizing a hydroxyl base such as KOH has been performed on nitrogen-containing heterocycles in literature,[78-80] though no example could be found for this particular substrate. To avoid the formation of the unwanted byproduct hypoxanthine **16** several conditions were tested. Decreasing the amount of base to equal quantities as the hydroxylamine salt increased the yield of the tautomers **15a** and **15b** from 30% to 84%. The ^{1}H NMR spectrum showed a ratio of 2:3 (**15b:15a**) amongst the two tautomers at room temperature in DMSO-d_6. Broadening of the peaks in the ^{1}H NMR spectrum obtained at 35 °C indicated rapid conversion between the two tautomers.

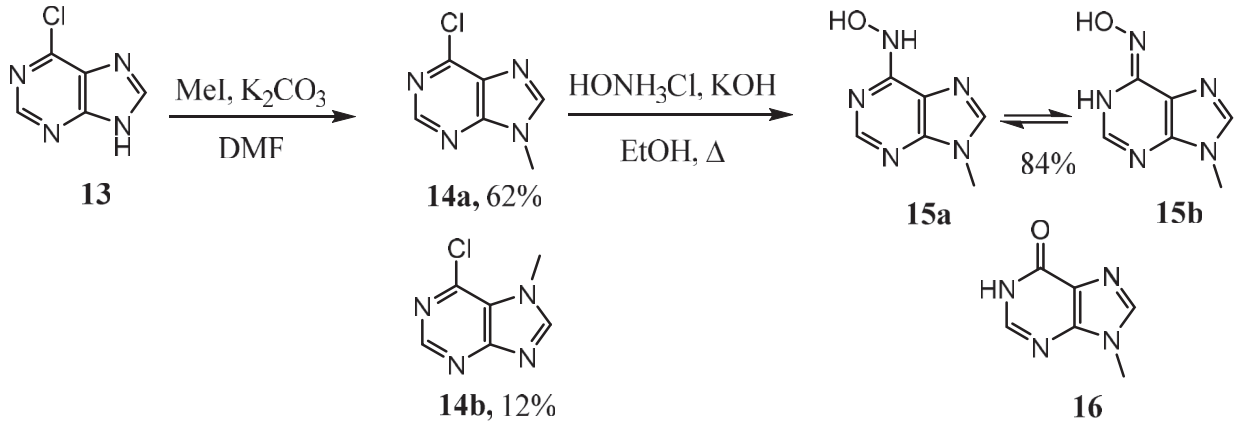

Scheme 4. Synthesis of hydroxylamine 15a/b via methylation of 6-chloropurine 13.

Alkylation of compound **15a/15b** with alkyl bromides at *N*7 has to the best of my knowledge not been performed previously. However, N^6-methoxy-agelasines on the have been synthesized

by alkylation of the purine moiety in DMA at 50 ºC (Scheme 1), which served as a natural starting point regarding conditions for the alkylation step (Scheme 5).[58]

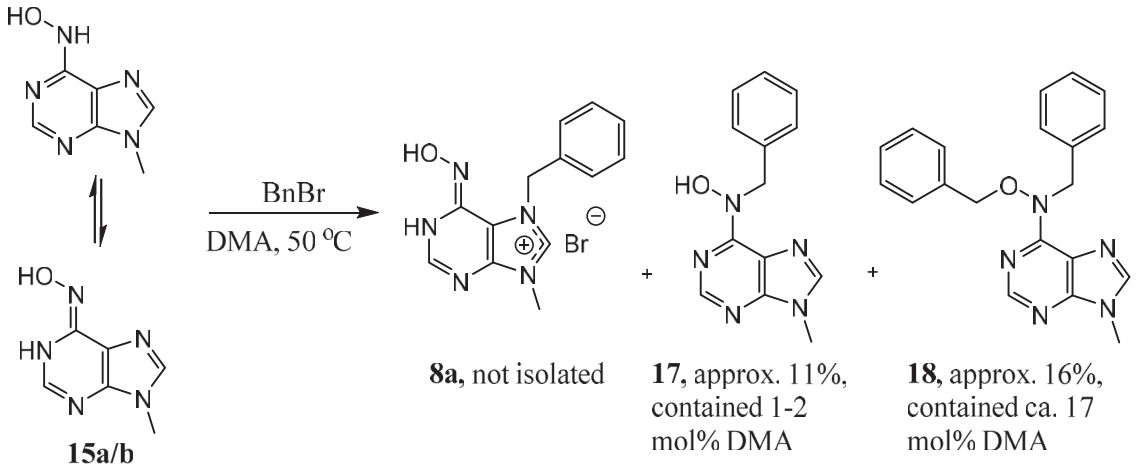

Scheme 5. Benzylation of the hydroxylamine purine 15a/15b with benzyl bromide as alkylating agent.

The ^{1}H NMR spectrum of the crude product of the benzylation of the hydroxylamine purine **15a**/**b** showed signals from at least three different compounds, and two compounds eluted from the column after purification with flash chromatography. Compound **17** was isolated in approx. 11% and contained 1-2 mol% DMA, although the ^{1}H NMR signals from this compound was not observed in the ^{1}H NMR of the crude product. This will be discussed below. Compound **18** was isolated in approx. 16%, which contained approx. 17 mol% DMA. Compound **8a** was not isolated, though it was suspected from the ^{1}H NMR spectrum of the crude product that this was the major product, as the NMR shifts matched the compound that was later isolated as pure benzyl-ageloxime **8a** in another synthetic route (Scheme 8). Other purification methods than flash chromatography were attempted, such as extraction and washing with a range of solvents, but were unsuccessful.

Due to the low selectivity in the alkylation reaction with benzyl bromide (Scheme 5), it became clear that a sterically demanding protecting group on the hydroxyl group was necessary. Previous synthesis of agelasines in our group have used different alkoxy groups as a directing group to enhance regioselectivity at *N*7 in the alkylation step.[58] Specifically, the *tert*-butoxy (*tert*-BuO) alkoxy group has proven to be a very good directing group for an increased selectivity in the alkylation reaction on *N*7 in the total synthesis of agelasine D (Scheme 1).[58] In the case of synthesizing agelasines, the *tert*-BuO is removed, but for the synthesis of ageloximes, only the *tert*-butyl was to be removed, and the oxygen needed to be retained. As

there are no known methods for retaining the oxygen in the reduction of alkoxy-agelasines to agelasines, a better suited option was to use a silyl protection group designed for alcohols. The choice fell on the *tert*-butyldimethylsilyl-group as protecting/directing group. Anders Vik tried to introduce O-(*tert*-butyldimethylsilyl)hydroxylamine at C6 in 6-chloro-9-methylpurine **13** without success.[28] Instead of introducing a protected hydroxylamine, protection of the hydroxyl group as a separate step was performed in this work, and this has not been reported in literature.

The introduction of the TBDMS-group resulted in products **19a** and **19b** which was isolated by extraction in 93% yield without the need of further purification (Scheme 6). The ratio between the two tautomers was 95:5 in ^{1}H NMR in DMSO-d_6 solution. The main tautomer formed was most likely the imino tautomer **19a**, as a coupling between the H2 and 1-NH protons was observed in the ^{1}H NMR spectrum. This coupling could also arise between H2 and 3-NH. Two articles published by prevoius members of our group, Bakkestuen *et al.*[62] and Roggen *et al.*[81] suggest that similar purine compounds exist as compound **19a** as the major tautomer.

Scheme 6. Introducing a TBDMS-protecting group on the hydroxylamine 15a/15b with TBDMS-Cl.

Originally, the alkylation reaction on similar alkoxy compounds (**2a** and **2b**) to **19a** and **19b** (hereby referred to as **19**) has, as previously stated, been carried out in DMA at 50 °C overnight with 1.5 equivalents of alkyl bromide (Scheme 1).[58] These reaction conditions provided only mediocre yields (54%) of the TBDMS-protected compound **20**.

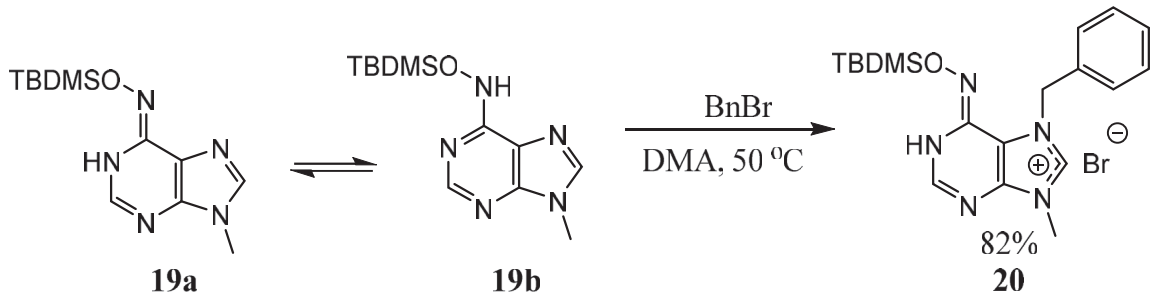

Scheme 7. Performing an alkylation reaction on TBDMS-protected hydroxylamine purine 19 utilizing benzyl bromide.

Both the dibenzylated product **18** and the N^6-isomer **17** was isolated in the initial reactions performed (Scheme 5). In an attempt to improve the yield of the desired TBDMS-protected benzyl-ageloxime **20**, and reduce the amount of byproducts, the equivalents of benzyl bromide used was decreased to 1.2. The formation of the dibenzylated product **18** was found to depend on the amount of benzyl bromide added in the reaction and decreased with decreasing amount of benzyl bromide. Conditions that led to limiting the formation of the N^6-alkylated isomer **17** and figuring out how it was formed was more of a mystery. The N^6-isomer **17** did not appear in the ^{1}H NMR spectrum of the off-white coloured crude product. After purification utilizing flash chromatography on silica gel, a purple compound eluted from the column. This purple compound turned out to be the N^6-isomer **17**. The TBDMS-protecting group is labile in acidic environments, and could become deprotected when it comes in contact with acidic silica, possibly explaining why N^6-isomer **17** was not observed in the ^{1}H NMR of the crude product. As the N^6-isomer exist after column chromatography of both the alkylation of hydroxylamine purine **15a**/**15b** and TBDMS-protected purine **19**, it is likely that the N^6 has acted as a nucleophile, and attacked the electrophilic site on the benzyl group attached at *N*7.

Reducing the reaction time from 21 h to 6 h, gave the most significant improvement of the yield of **20** from 54% to 82% (Scheme 7).

The deprotection step in this synthetic sequence proved to be challenging, and many reagents and methods were investigated (Scheme 8, Table 3). A TBDMS-group can in theory be removed with the use of acids[82, 83] or fluoride anions[82, 84-86], and this served as the starting point of the development of this deprotection step. In the following section some of the main attempts to deprotect compound **20** are discussed. The most important attempts are presented in Table 3 below.

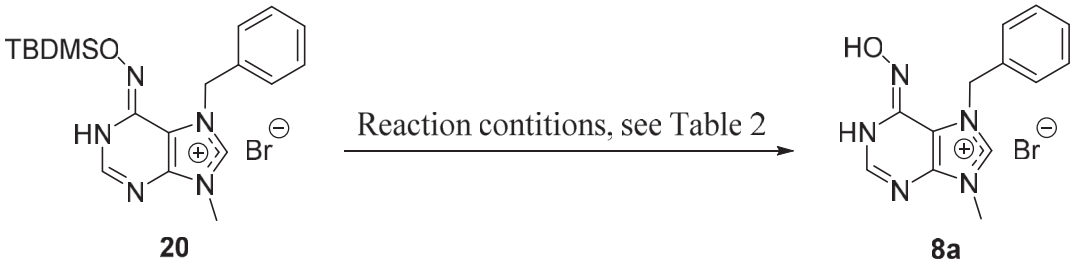

20 8a

Scheme 8. Removal of the TBDMS-group from compound 20 utilizing a variety of conditions, resulting in benzyl-ageloxime 8a.

Table 3. Reagents and conditions for the removal of TBDMS-group on TBDMS-protected benzyl-ageloxime 20.

Entry	Reagent	Time	Temperature	Solvent	Conversion (^{1}H NMR)
1	MeOH	2 h	reflux	MeOH	100% conversion
2	TBAF[1]	18 h	RT	THF	100% conversion[2]
3	TBAF[3]	48 h	RT	THF	50% conversion
4	TBAF	1 h	RT	MeCN/H_2O	100% conversion
5	CsF	2 h 45 min	RT	MeCN/H_2O	100% conversion
6	NH_4F	1 h	RT	MeCN/H_2O	100% conversion[4]

[1]Dry TBAF. [2]No starting material or product was observed on ^{1}H NMR of the crude product. [3]Undried TBAF. [4]Isolated yield 86%.

Recrystallization of compound **20** in methanol was explored as a purification method (entry 1). This conveniently turned out to deprotect the compound, and the recrystallization became a deprotection reaction with 100% conversion to benzyl-ageloxime **8a**. Pure methanol did not work as a deprotecting method for the TBDMS-protected *ent*-ageloxime D **29**, as it had for the TBDMS-protected benzyl-ageloxime (**20**). Catalytic amounts of HCl was added in an attempt to achieve 100% conversion to compound **8d**, but without success. As addition of HCl did not yield satisfactory results, other methods were explored. Silyl groups can be deprotected by fluoride ions, and there are a variety of reagents to choose from when in need of a fluoride source. Attempts to deprotect compound **20** utilizing a fluoride source is described in the following section.

Deprotection of compound **20** with tetra-n-butylammonium fluoride (TBAF) performed under dry conditions was explored (entry 2) but gave a complex mixture of unknown byproducts. TBAF is extremely hygroscopic.[87] Running the reaction with undried TBAF (entry 3) showed approx. 50% deprotection after 2 h according to ^{1}H NMR of the crude product. Running different reactions simultaneously, it was discovered that MeCN/H_2O was a suitable solvent regarding the solubility of both compounds **20** and **29**. A reaction was run with MeCN/H_2O as solvent in a 9:1 ratio (entry 4). The reaction went to completion in just 1 h. It was unfortunately difficult to separate the excess TBAF used in the reaction from compound **8a**. A new deprotecting reagent was therefore necessary.

CsF was tested as a deprotecting agent, being a rather "exotic" reagent for deprotecting a TBDMS-group (entry 5).[88] The idea of using this reagent was to be able to separate the inorganic salts from the benzyl-ageloxime **20**. Unfortunately, the ^{1}H NMR of the reaction mixture revealed unwanted byproducts, and the weight of the "purified" product was above 100%. As flash chromatography was not an option due to the fact that the compound would not elute, the purification attempts consisted of different washing/extraction methods. After many attempts in using different solvent and filtering techniques to purify the benzyl-ageloxime **8a**, it was concluded that the purification was not successful.

To summarize, TBAF (Scheme 8, Table 3, entry 4) and CsF (Scheme 8, Table 3, entry 5) deprotected the TBDMS-protected benzyl-ageloxime **20** under wet conditions, but purification was troublesome. Benzyl-ageloxime **8a** is too polar to elute from flash chromatography with silica gel, but as the other target compounds **8b**, **8c** and **8d** (Figure 16) are more lipofilic, this was not considered a major problem. Working simultaneously with the synthesis of geranylgeranyl-ageloxime **8c** (Scheme 11) and ageloxime D **8d** (Scheme 12), it became clear that flash chromatography was not a desirable purification method even for these lipofilic compounds, as new signals appeared on the ^{1}H NMR spectrum after column chromatography utilizing silica gel. It was therefore desirable to find a deprotection method that did not require flash chromatography as purification, and where no salts were formed as a byproduct from the deprotecting agent. In search of a reagent that would fulfil these requirements, ammonium fluoride, NH_4F, was selected as a fluoride source (see Table 3**,** entry 6).[89-91] Both byproducts formed in the deprotection reaction (TBDMS-F and NH_3) are volatile, and a pure product (**8a**) was achieved in 83% yield after work-up and evaporation.

The model system utilizing benzyl bromide as alkylation reagent was useful for establishing a synthetic pathway for the key alkylation and deprotection reactions required for the total synthesis of *ent*-ageloxime D and analogs.

2.3 Synthesis of geranyl-ageloxime

Geranyl-ageloxime (**8b**) was chosen as a target compund in addition to compounds with longer terpenoid *N*-7 substituents to see if the length of the chain was important for the biological activity towards *M. tuberculosis*. Geraniol was purchased and converted to geranyl bromide (**21**) in one step.[62] Alkylation of the TBDMS-protected purine **19** was performed at 50 ºC for 18 h, and yielded 70% of compound **22**. Deprotection was accomplished using both CsF (27%) and NH_4F (99%). Geranyl-ageloxime **8b** was as expected less water soluble than benzyl-ageloxime **8a**. This assumption led to the idea that the salt formed (CsBr) in the reaction performed with CsF could be removed with water. However, the yield was only 27%. Utilizing NH_4F the reaction time increased from 1 h for the TBDMS-protected benzyl-ageloxime (**20**), to 21.5 h for the geranyl-ageloxime (**8b**) indicating that the TBDMS-protected geranyl-ageloxime (**22**) was less reactive than the TBDMS-protected benzyl-ageloxime (**20**). After extensive drying of the compound *in vacuo*, the reaction had an essentially quantitative yield (Scheme 9).

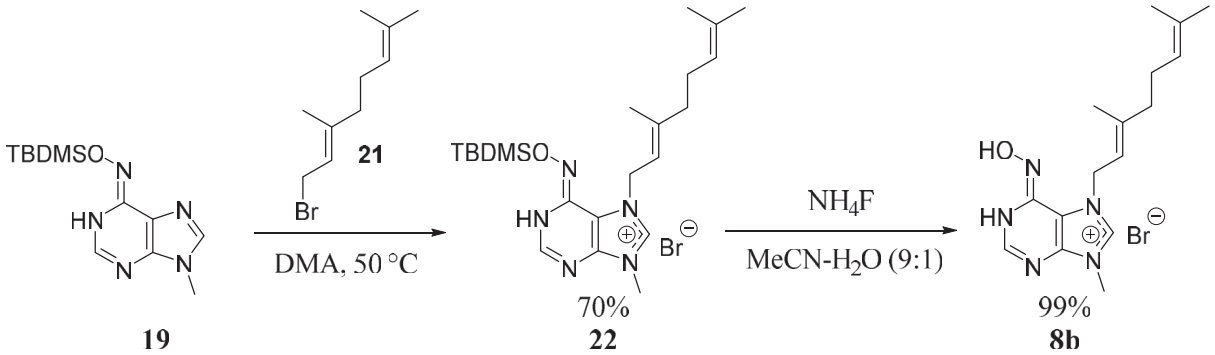

Scheme 9. Alkylation of TBDMS-protected purine 19 with geranyl bromide, followed by removal of the TBDMS-group, which resulted in target geranyl-ageloxime 8b.

2.4 Synthesis of geranylgeranyl-ageloxime

The geranylgeranyl-sidechain substituted on *N*7 on N^6-methoxy-agelasine (section 1.6.2, Figure 12) has proven to give biological activity against *M. tuberculosis*, and it was therefore of interest to synthesize this geranylgeranyl-ageloxime. Geranylgeraniol (**26**) was synthesized in three

steps from the inexpensive and readily available geranyllinalool **23** (Scheme 10).[62] The alcohol **26** was converted to the bromide **27** utilizing PBr_3.

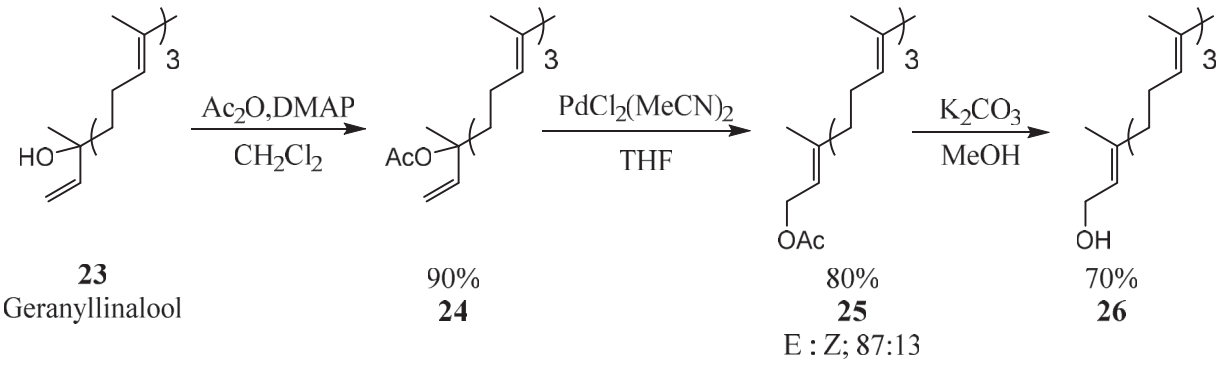

Scheme 10. Preparation of the geranylgeraniol 26 from geranyllinalool 23 in three steps.

The alkylation on *N*7 of the TBDMS-protected purine **19** with bromide **27** was performed under milder alkylating conditions compared to the TBDMS-protected benzyl-ageloxime (**20**) and TBDMS-protected geranyl-ageloxime (**22**) in order to avoid deprotection. Both the reaction time and temperature were reduced from 18 h and 50 ºC to 1 h and room temperature to yield 91% of the geranylgeranyl-ageloxime **8c**. The deprotection was performed similarly to the TBDMS-protected benzyl-ageloxime **20**, and gave a quantitative yield of the target compound **18** (Scheme 11).

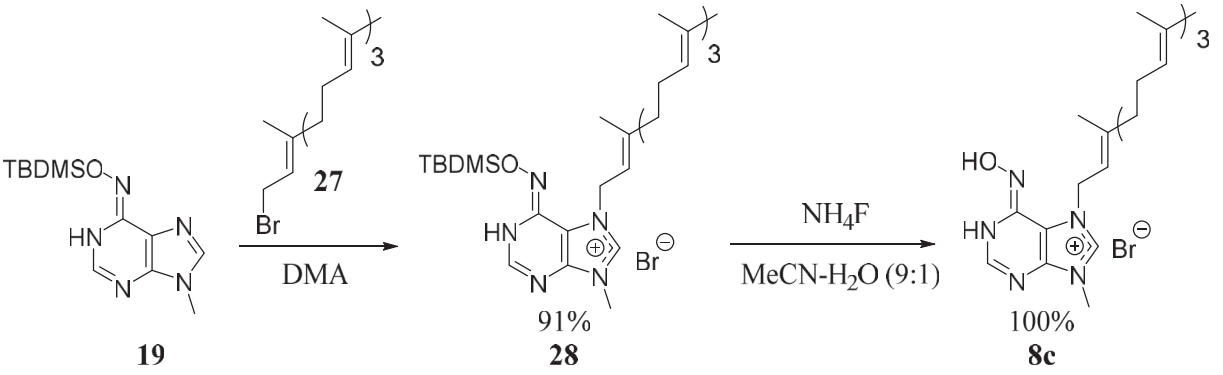

Scheme 11. Alkylation of TBDMS-protected purine 19 with geranylgeranyl bromide 27, followed by removal of the TBDMS-group with ammonium fluoride, which resulted in compound 8c.

2.5 Synthesis directed towards *ent*-ageloxime D

The first step in the synthesis of the proposed structure of *ent*-ageloxime D was alkylation on *N*7 on TBDMS-protected purine **19** with anticopalyl bromide **3**. Utilizing the same conditions as for the alkylation of the TBDMS-protected purine **19** with benzyl bromide, ^{1}H NMR of the crude product (**29**) indicated that the TBDMS-group had partially fallen of. To counteract the

unwanted partial deprotection of TBDMS-protected *ent*-ageloxime D (**29**), more gentle reaction conditions were necessary; the reaction time and temperature was adjusted from 21 h to 20 min, and 50 °C to room temperature in comparison with the alkylation performed with benzyl bromide. This lowered the amount of unwanted byproducts such as the desilylated N^6-substituted purine **30** (34% to 13%) and also the deprotected product **8d**, see Scheme 12. The adjusted alkylation conditions increased the yield from 23% in 70% of the desired TBDMS-protected *ent*-ageloxime D **29**. The reaction condition was similar to the one used for the geranylgeranyl-ageloxime (**18**), and both these more structurally complex substrates needed more gentle reaction conditions for the alkylation. The ^{1}H NMR of the off-white crude product showed no presence of the N^6-isomer (**30**), but it appeared after column chromatography as a purple solid. The formation of the N^6-isomer **30** is suspected to be because of a "rearrangement" of the location of the sidechain, where the lone pair on N^6 attacks the slightly electrophilic carbon in the sidechain, and the purine ends up as the leaving group. Since this seem to happen within seconds after loading the crude product on the silica gel (sudden color change from white to purple) it appears to be catalyzed by acidic conditions.

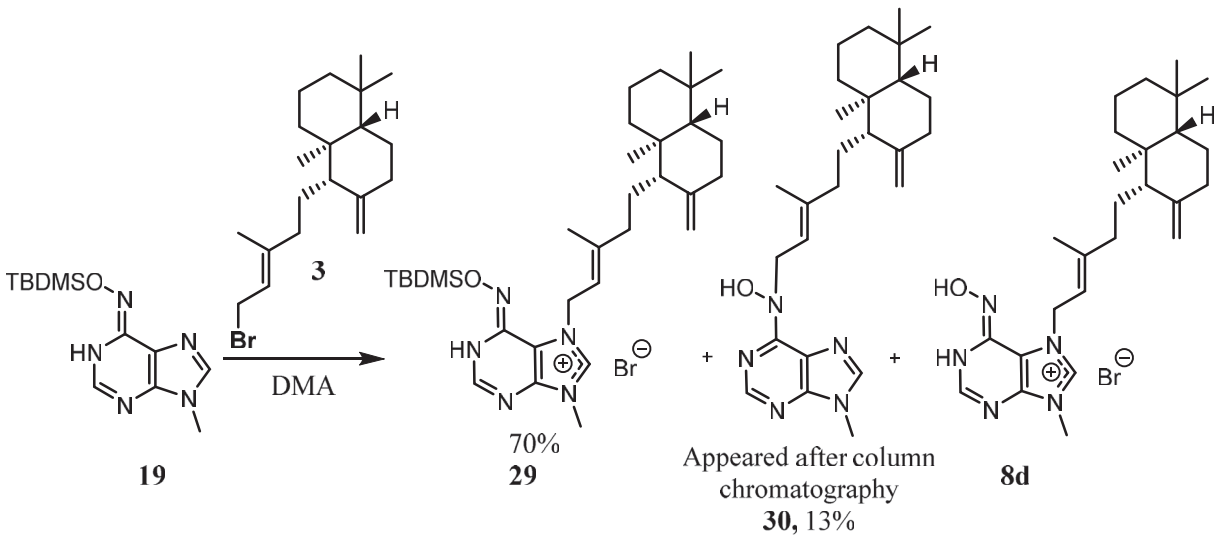

Scheme 12. Alkylation of TBDMS-protected purine 19 with anticopalol bromide 3. The formation of the N^6-isomer 30 is suspected to be because of a "rearrangement" of the location of the sidechain, where the lone pair on N^6 attacks the slightly electrophilic carbon in the sidechain, and the purine ends up as the leaving group

The TBDMS-protected benzyl-ageloxime (**20**) was, as discussed in section 3.2, desilylated by refluxing it in methanol and catalytic amounts of HCl for a two hours. The deprotection did not work as easily for TBDMS-protected *ent*-ageloxime D **29** as for the TBDMS-protected benzyl-ageloxime **20**. After refluxing TBDMS-protected *ent*-ageloxime D in MeOH and HCl for 70 h,

the ratio between starting material and desired product was only 3:7 and small amounts of byproducts were observed. Attempts to purify compound **8d** on silica (and reversed phase C18 with MeCN/H_2O) with flash chromatography employing sat. NH_3 in MeOH in CH_2Cl_2 as eluent resulted in new signals in the ^1H NMR spectrum, indicating that the reaction mixture of compound **8d** could not be purified with this method after deprotection. It is not clear why the deprotection of TBDMS-protected *ent*-ageloxime D **29** in HCl and MeOH was slower than for the TBDMS-protected benzyl-ageloxime (**20**). The time consumed when employing NH_4F (Scheme 13) as deprotecting reagent is not very different (1 h for TBDMS-protected benzyl-ageloxime **20** versus 40 min for TBDMS-protected *ent*-ageloxime D **8d**). Utilizing NH_4F as deprotecting agent gave quantitative yield of *ent*-ageloxime D (Scheme 13).

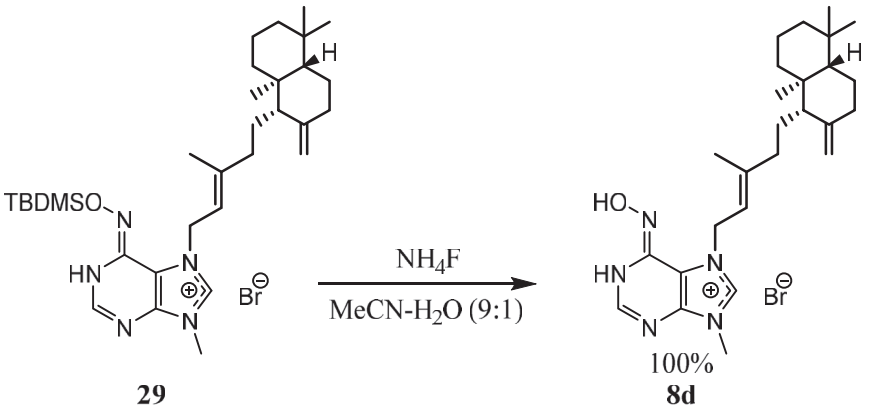

29 **8d**

Scheme 13. Removal of the TBDMS-group from compound 29 with NH_4F resulting in the proposed structure of ent-ageloxime D 8d in quantitative yields.

2.6 An unforeseen event – the new structure of ageloxime D

After successfully synthesizing the proposed structure of *ent*-ageloxime D (**8d**), we compared our spectra with those published by Hertiani *et al*[70], and found that our NMR data did not match the NMR spectra published for (-)-ageloxime D, see Figure 17. From the ^1H NMR spectrum, it seemed like the most significant difference in shift values could be found in the signals originating from the purine moiety. The next step was to figure out if the synthetically prepared *ent*-ageloxime D had the structure it was believed to have, or if the anomaly was located in the article published by Hertiani *et al*.[70]

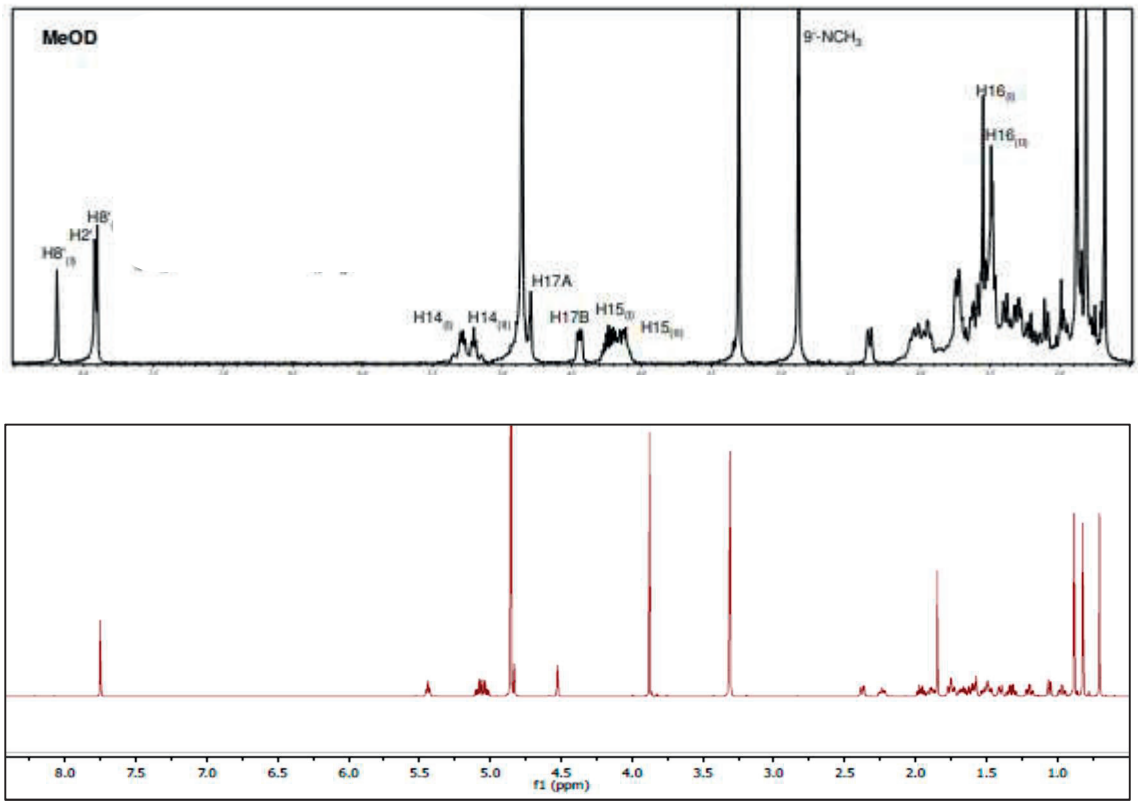

Figure 17. Comparison spectra recorded in CD_3OD. The top spectrum is from the article published by Hertiani *et al*,[70] and the bottom spectrum is of the synthetically prepared *ent*-ageloxime D.

A thorough structure elucidation was performed; ^{1}H-^{13}C HMBC and ^{1}H-^{15}N HMBC was used to determine both the position of the side chains, and the heterocyclic part of the synthesized molecule. As the most significant differences in shift values seemed to originate from the purine moiety, this will be the main focus in the structure elucidation discussion (Figure 18, Table 4). Key correlations found for the heterocyclic part from ^{1}H-^{13}C HMBC was between NCH_3 and C8', H8' to C15, H15 to C5'. Viewing the correlations found in the ^{1}H-^{15}N HMBC spectrum, some key correlations was between H8' to N7' and N9', H15 to N7', and NH1' to N6.

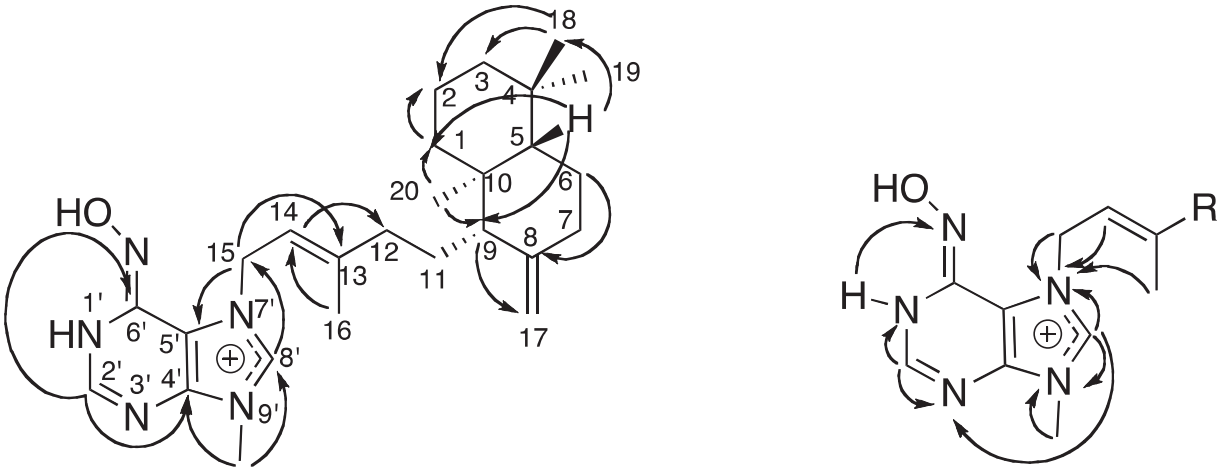

Figure 18. Key correlations found in the ^{1}H-^{13}C HMBC spectrum (left) and ^{1}H-^{15}N HMBC spectrum (right) of compound 8d.

Table 4. Overview of the correlations found in the ^{1}H-^{13}C HMBC spectra and assignments of signals in 1D spectra.

	^{1}H NMR[a]		^{13}C NMR[a]	^{15}N NMR[a]	Correlations
No.	δ[b]	Integration, multiplicity, J [Hz]	δ[c], DEPT	δ[d]	HMBC (H → C)[e]
1A, *eq*[f]	1.65-1.70	1H, m (u/o)[g]	38.4, CH_2		2,3,5,10,20
1B, *ax*[f]	0.88	1H, dt, 3.8, 13.0			2,3,9,10,20
2A, *ax*	1.48-1.54	1H, m (u/o)	18.8, CH_2		1,3,4,10
2B, *eq*	1.41-1.44	1H, m (u/o)			1,3,4,10
3A, *eq*	1.34	1H, br d, 13.4	41.6, CH_2		1,2,4,5,(6),19
3B, *ax*	1.11	1H, dt, 4.0, 13.4			1,2,4,5,18,19
4			33.2, C		
5	0.99	1H, dd, 2.6, 12.7	54.7, CH		1,4,6,7,9,10,18,19,20
6A, *eq*	1.65-1.70	1H, m (u/o)	23.9, CH_2		(5),(7),(10)
6B, *ax*	1.22	1H, dq, 4.2, 12.7			1,5,7,(4),10
7A, *eq*	2.32	1H, ddd, 3.4, 4.0, 12.7	37.6, CH_2		5,6,8,17
7B, *ax*	1.83-1.88	1H, m (u/o)			5,6,8,17
8			148.0, C		
9	1.48-1.54	1H, m (u/o)	55.1, CH		1,8,10,11,12,17,20
10			39.2, C		
11A	1.54-1.59	1H, m (u/o)	20.9, CH_2		8,9,10,13,14
11B	1.41-1.44	1H, m (u/o)			8,9,10,13,14
12A	2.11	1H, ddd, 4.0, 9.4, 14.0	37.7, CH_2		9,11,13,14,16
12B	1.83-1.88	1H, m (u/o)			9,11,13,14,16
13			144.1, C		
14	5.37	1H, qt, 1.0, 7.2	116.5, CH		12,15,16
15A	4.98	1H, dd, 7.2, 14.8	47.1, CH_2		(11),(12),13,14,(16),5′,8′
15B	4.94	1H, dd, 7.2, 14.8			(11),(12),13,14,(16),5′,8′
16	1.76	3H, d, 1.0	16.7, CH_3		12,13,14,(15)
17A	4.81	1H, td, 1.1, 1.5	106.4, CH_2		(6),7,(8),9
17B	4.48	1H, br s			7,(8),9
18	0.83	3H, s	33.3, CH_3		(2),3,4,5,19
19	0.75	3H, s	21.5, CH_3		3,4,5,18
20	0.61	3H, s	14.3, CH_3		1,5,9,10
1′-NH	11.00	1H, vbr (ca.800 Hz) s		-240.0	
2′	7.79	1H, s	148.9, CH		4′,5′,6′
3′-N				-179.5	
4′			140.7, C		
5′			110.6, C		
6′-NOH	10.58	1H, br (6.5 Hz) s	136.9, C	-105.5	6′
7′-N+				-208.5	
8′	9.26	1H, s	136.7, CH		4′,5′,N-CH3,15
9′-NCH_3	3.78	3H, s	31.6, CH_3	-218.5	4′, (5′),15

[a] ^{1}H NMR, ^{13}C NMR and ^{15}N NMR data were obtained at 600 MHz, 150 MHz and 60 MHz respectively, [b] ^{1}H chemical shift values are calibrated relative to internal $CD_2\underline{H}SOCD_3$ at 2.49 ppm, [c] ^{13}C chemical shift values are calibrated relative to internal $\underline{C}D_3SOCD_3$ at 39.50 ppm, [d] ^{15}N chemical shift values are calibrated relative to external $CH_3\underline{N}O_2$ / DMSO-d6 (9:1) at 0.00 ppm, [e] (x)= weak, [f] *eq*uatorial/*ax*ial positions in a (double) chair conformation, obtained by 2D NOESY/1D SELNOE, [g] unresolved/overlapping

The relative stereochemistry of the side chain was determined by extensive 2D NOESY and 1D SELNOE, and where found to match the expected structure. These spectra was also used for the determination of the position of the hydrogen in the purine moiety. As can be seen in Figure 19, correlations were found for the H2' to NH1', and NH1' to the OH (purple arrows). This gave strong evidence for a *syn* imine and that the heterocyclic NH is located on N1. The ^{13}C NMR of compound **8d** gave a triplet for the C8' in CD_3OD, indicating an acidic H8'. The orange arrows in Figure 19 highlights the correlations found from the NCH_3 to H8', and H8' to C15.

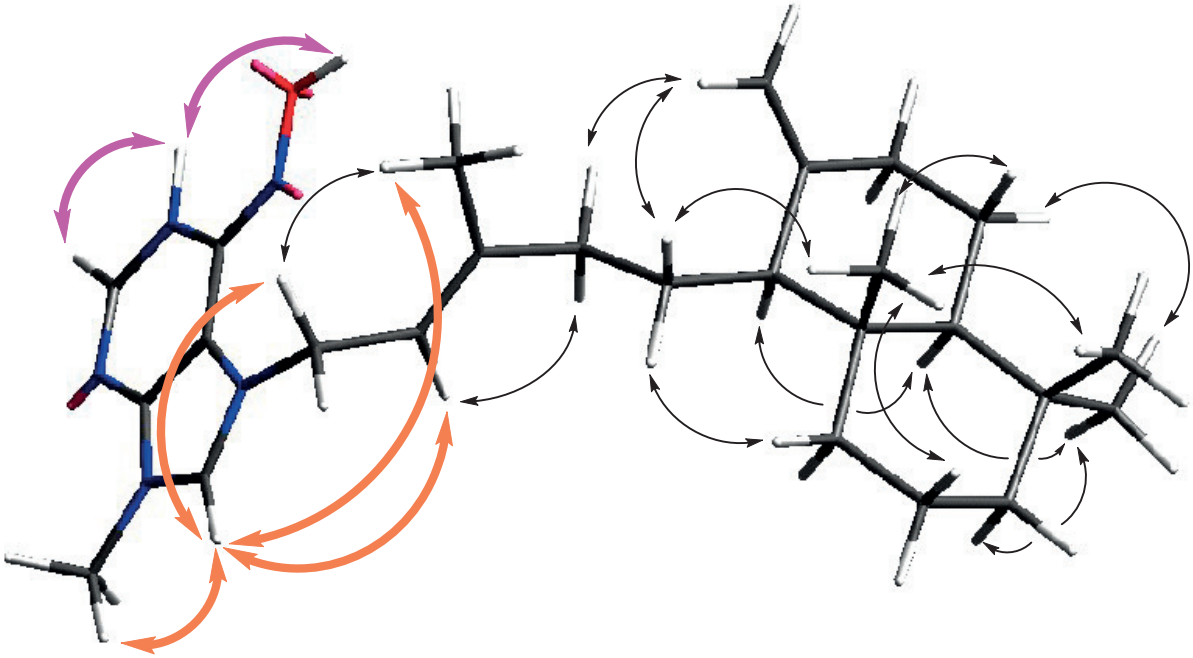

Figure 19. Key correlations found in the 2D NOESY/1D SELNOE spectra of compound 8d. Correlations between H2' to NH1', and NH1' to the OH are marked with purple arrows. The orange arrows highlights the correlations found from the NCH_3 to H8', and from H8' to C15.

The ^{1}H-^{13}C HMBC, ^{1}H-^{15}N HMBC and 2D NOESY/1D SELNOE spectra recorded were all in agreement with the proposed structure of (-)-ageloxime D.

The data provided in Hertiani's article[70] was significantly different on several points. They had obtained some of their NMR data from dissolving the compound in $CDCl_3$, but in our hands, compound **8d** was sparingly soluble in $CDCl_3$, and it was impossible to record a spectrum.

Significant shift changes were observed for particularly the C8' and the C6', see Table 5. The literature ^{13}C NMR data showed that the C8' gave rise to two signals at 165.9/166.5 ppm, and ours were a triplet at 137.3 ppm due exchange of proton with deuterium. Furthermore, the signal

for C6' also gave a double signal located at 97.2/99.2 ppm, whereas ours appeared at 137.9 ppm.

Table 5. An overview of two significant different shift values for the C8' and the C6'.

	Hertiani *et al.*[70]	Paulsen *et al.*[92]
C8' ^{13}C NMR	165.9/166.5 ppm	137.3 ppm (t)
C6' ^{13}C NMR	97.2/99.2 ppm	137.9 ppm

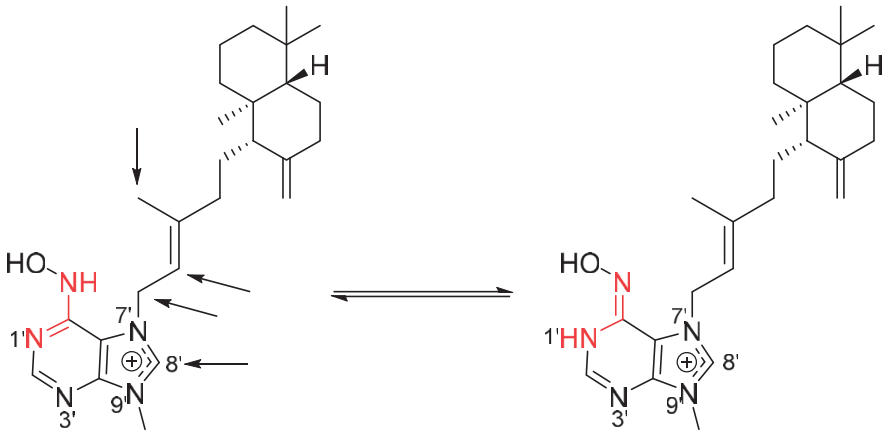

Figure 20. Tautomers of the proposed structure of ageloxime D with the affected area shown in red. The arrows indicate from which carbons the double signals have arisen from in the NMR spectra.

Hertiani *et al.*[70] reported seeing tautomers (amino and imino, marked in red in Figure 20) in spectra recorded in CD_3OD, giving double set of signals for H15, H14, H16 and H8' (see arrows in Figure 20). Seeing that the imino and amino tautomers were located at N1 and N^6 (marked in red in Figure 20), this seemed surprising as the imino/amino moiety are located far apart from the carbons giving rise to double signals in the molecule. Moreover, the extremely concentrated sample in $CDCl_3$ used when running NMR, resulted in no duplication of the signals for H15, H14, H16 and H8' in the spectra. The *N*9 was suggested to be protonated due to the solvent's acidity, explaining the doublet observed for the NCH_3 signal. As $CDCl_3$ is not particularly acidic,[93] it is not likely that protonation at *N*9 was due to protonation from the solvent. According to the ESI MS recorded by Hertiani *et al.*[70], a pseudo-molecular peak at m/z 440 $[M+H]^+$ was observed, which is unexpected for a molecule that is already carrying a positive charge, or two positive charges as they suggest, as the actual weight is 438 $[M]^+$.

The spectra recorded by Hertiani *et al.* lacked correlations in ^{1}H-^{13}C HMBC between NCH_3 and C8' in their spectra recorded in CD_3OD, but not in their oversaturated $CDCl_3$ spectra.[70] The

lack of HMBC correlation between NCH_3 and C8 in the spectra recorded in CD_3OD suggested a ring-opened structure. Searching the literature for clues gave an idea of what could have happened: Capon *et al*. isolated formamides after performing flash chromatography with silica gel and a basic eluent consisting of a 6:3:1 ratio of CH_2Cl_2/MeOH/NH_3 of the crude sponge extracts from the *Agelas* sponge.[45] These compounds could not be seen on the NMR of the crude sponge extracts, so they concluded that the formamides were artifacts formed during flash chromatography (Figure 21). Agelasines are known to hydrolyze to formamides under basic conditions.[42, 44] It should be noted that the eluent system used for purification of agelsines in our group has been saturated NH_3 in MeOH in CH_2Cl_2, and utilizing this has not lead to isolation of formamides.[58, 60, 62] However, Hertiani *et al*. did not use a basic eluent system.[70] One other group have isolated axistatins from the *Agelas* sponge, not claiming they were artifacts from column chromatography, including the formamide shown in Figure 21.[57]

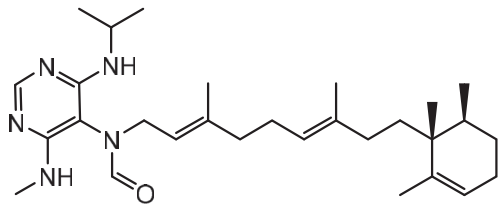

Figure 21. A formamide isolated after flash chromatography with silica gel and a basic eluent published by Capon *et al.*[45]

It is not clear if these formamides are artifacts from column chromatography, or if they exist in the *Agelas* sponge. Regardless of origin, it became clear that the formamides was a potential explanation. In order to verify the hypothesis, it was desirable to treat agelasine D to basic conditions. Luckily, another project had led to the synthesis of (+)-agelasine D (**31**),[58] which could be used for testing the hypothesis.

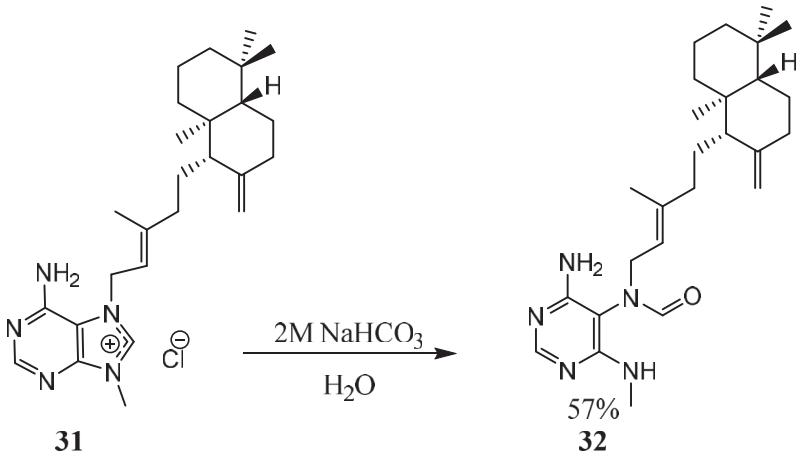

31 **32**

Scheme 14. Synthesis of formamide 25 from *ent*-agelasine D.

Performing the reaction led to the isolation of 57% yield of the ring-opened compound **32** (Scheme 14). After comparing NMR spectra of formamide **32** and Hertiani's spectra, they were found to be identical. The occurrence of these formamides explained why Hertiani recorded a *m/z* value of 440 which is the actual molecular weight of the formamide. Also, the two tautomers they report seeing in CD_3OD are most likely two rotamers, which can be explained by the restricted bond rotation of the amide bond.[94] Their observation of a protonated *N*9 is correct, but without a positive charge. The structure elucidation performed on the synthetic *ent*-ageloxime D matched the proposed structure of the compound, and after synthesizing the formamide **32** from (+)-agelasine D (**31**) it could be established that the compound published by Hertiani *et al.* was actually identical with the formamide **32**.

2.7 Biological testing

Even though the synthesized target compounds probably do not exist in nature, it was still desirable to test these compounds for biological activities. The compounds were screened for antimicrobial activities, along with biofilm inhibition and cytotoxicity against the microorganisms shown in Table 6.

The detailed results are presented in the article published by Paulsen *et al*., but a short summary will be presented below.[92]

The geranyl-ageloxime **8b** was virtually inactive against all microorganisms, in line with previous findings for the similar agelasine analog. Geranylgeranyl-ageloxime **8c** and *ent*-ageloxime D **8d** showed more interesting results, especially towards the protozoa causing Chagas disease (*T. cruzi*) and variants of leishmaniasis (*L. infantum*). The antibacterial effect

on the bacteria responsible for tuberculosis was also significant. It was interesting to investigate if the presence of a hydroxyl group on N^6 influenced the biological activity towards *M. tuberculosis*, when comparing *ent*-ageloxime D **8d** with previously published results for similar compounds (**4a** and **4b**). As mentioned in section 1.6.2, the minimum inhibitory concentration (MIC) value towards *M. tuberculosis* for *tert*-BuO-agelasine D **4b** was reported to be 3.13 µg/mL. For *ent*-ageloxime D **8d**, the MIC value was 3.00 µg/mL. This is essentially the same activity, and for this reason it does not seem like the hydroxyl-group resulted in an enhanced biological activity for towards *M. tuberculosis* (Figure 22). Unfortunately, geranylgeranyl-ageloxime **8c** and *ent*-ageloxime D **8d** also displayed very high toxicity towards mammalian fibroblast cell.

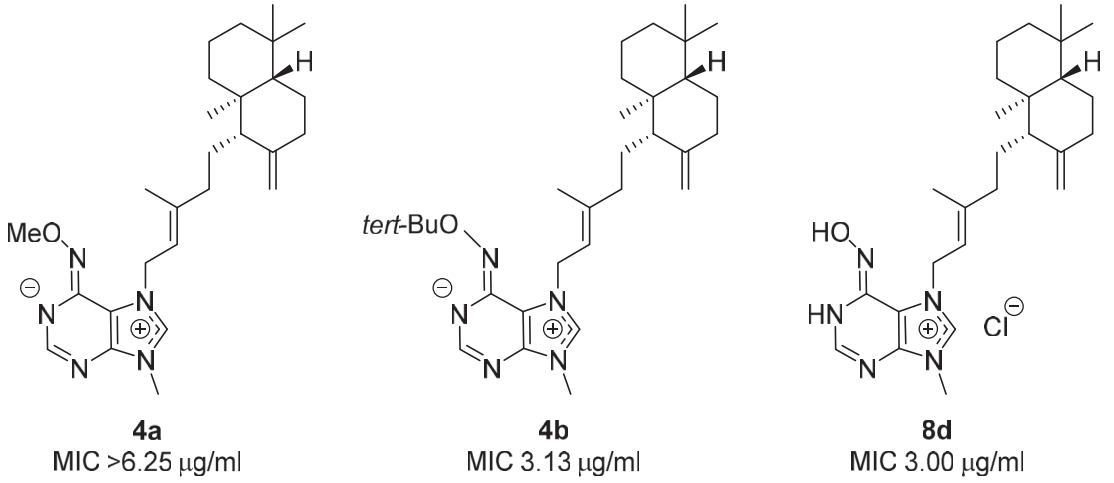

Figure 22. MIC of compound 4a, 4b and 8d towards *M. tuberculosis*.

Table 6. Overview of the biological activities obtained for compound 8b, 8c and 8d.

Compound	Bacteria IC_{50} (µM)		Fungi IC_{50} (µM)	Protozoa IC_{50} (µM)				*M. tuberculosis* MIC (µg/mL)		Toxicity IC_{50} (µM)
	S. aureus	*E. coli*	*C. albicans*	*T. cruzi,*	*T. brucei*	*T. rhodesiense*	*L. infantum*	MABA[1]	LORA[2]	MRC-5[3]
Compound **8b**	>64.0	>64.0	>64.0	11.5	28.0	8.06	20.3	>50.0	>50.0	>64.0
Compound **8c**	1.89	>64.0	2.00	0.54	2.01	0.50	2.16	11.3	15.3	1.90
Compound **8d**	1.84	>64.0	8.00	0.53	2.01	0.50	2.38	3.00	5.50	1.59
Drugs	Doxycycline 0.03	Doxycycline 0.58	Flucytosine 0.41	Benznidazol 2.69	Suramin 0.02	Suramine 0.03	Miltefosine 11.8	Isoniazid 0.48	Isoniazid >128	Tamoxifen 11.23

[1] MABA stands for Microplate Alamar Blue Assay. [2] LORA stands for Low Oxygen Recovery Assay. [3] MRC-5 is short for Medical Research Council cell strain 5 (human lung fibroblast cells).

3 Synthesis of (-)-agelasine F

3.1 Introduction

(-)-Agelasine F was isolated from the *Agelas* sponge in 1984.[43] This compound has shown interesting activity against some drug resistant strains of *M. tuberculosis in vitro,* in addition to inhibition of Na,K-ATPase.[43, 52] Both the racemic mixture and the enantiomer of the naturally occurring agelasine F, have been synthesized previously.[61, 67] The enantiomer has been synthesized by Proszenyàk *et al*; a previous member of our group.[61] This 12 step total synthesis was the starting point of the last part of the PhD (Scheme 15). The goal was to synthesize the naturally occurring enantiomer of agelasine F, to improve the yield in some of the key steps in this synthesis, and to find an inexpensive starting material. In the published synthesis by Proszenyàk *et al,*[61] the starting material was (*R*)-pulegone (577 NOK for 5 g)[95], being a low-cost alternative to the (*S*)-enantiomer of pulegone required for the synthesis of (+)-agelasine F.

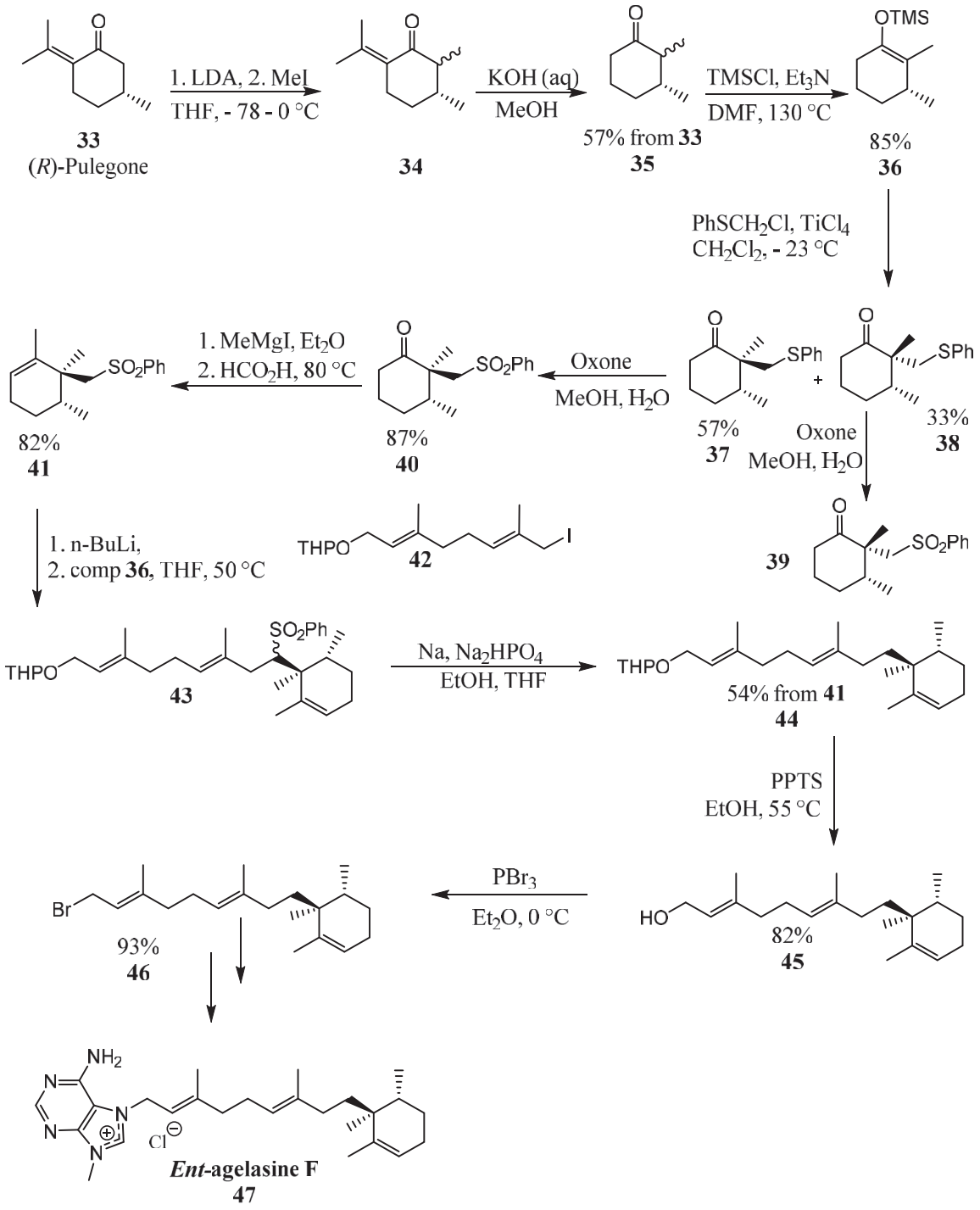

Scheme 15. The total synthesis of *ent*-agelasine F published by Proszenyàk *et al* .[61] starting from (*R*)-pulegone.

Proszenyàk *et al.*[61], introduced a methyl group to the alpha carbon in the first step, and followed by removal of the propenyl moiety, giving rise to a diastereomeric mixture of the (2*R*,3*R*)- and (2*S*,3*R*)-2,3-dimethylcyclohexanone (**35**).[61] This mixture was converted into the thermodynamic product of the silyl enol ether **36**, before it was alkylated with chloromethyl

phenyl sulfide in the presence of $TiCl_4$. This gave a diastereomeric mixture of sulfide **37** and **38**. These sulfides can be separated using flash chromatography, and further oxidized to sulfones **39** and **40** with oxone as reagent.

The stereochemistry of sulfone **39** has previously been verified by X-ray crystallography.[61] After introducing the last methyl group with methylmagnesium bromide on the sulfone **40**, formic acid-mediated regioselective water elimination gave the methylated sulfone **41**. Compound **41** was treated with *n*-BuLi and reacted with a modified THP-protected geranyl iodide **42**, before reducing the compound (**43)** with sodium to remove the SO_2Ph-group. After removal of THP using PPTS, compound **45** was reacted with PBr_3 to yield the bromide **46**. The alkylation of the purine with the bromide **46**, could take place on both N^6 and $N7$. To ensure a good stereoselectivity for the attachment of the sidechain to the $N7$ in the purine moiety, the bulky *tert*-butylhydroxy-group was used as a directing group. This was later reduced to the target compound, *ent*-agelasine F (**47**).

As can be seen in Scheme 15, there are some steps in the synthesis that could be improved. Overall, it was desirable to find a way to make the (*S*)-enantiomer of the monocyclic sidechain of agelasine F in an inexpensive way without starting from the expensive (*S*)-pulegone (2180 NOK pr 1 ml)[95]. An alternative way of synthesizing the substituted cyclohexene building block could be to start from (*S*)-carvone **48** or 2-methylcyclohex-2-en-1-one **51** (Scheme 16).

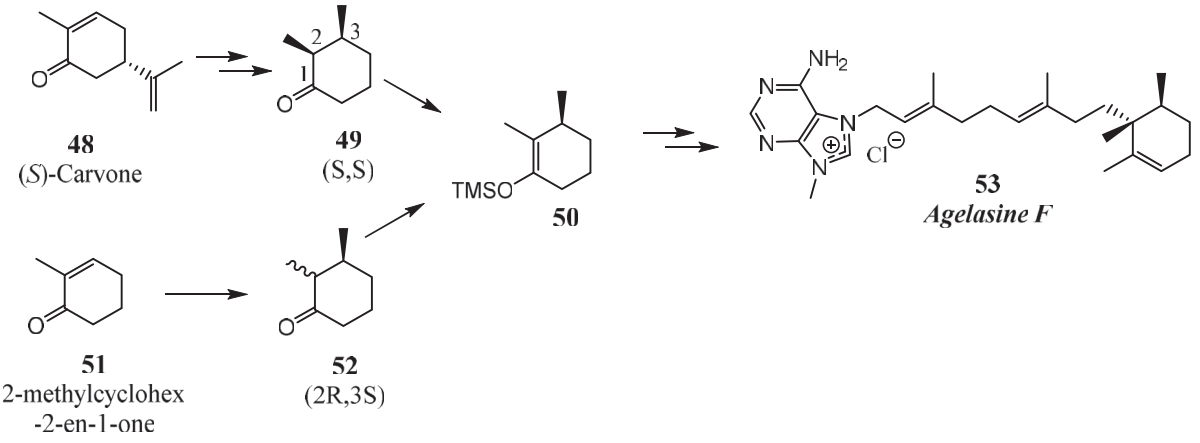

Scheme 16. Potential starting materials (48 and 51) and routes to the total synthesis of agelasine F.

Using one of these as starting material, it was assumed to be possible to omit the moderately yielding initial two-step conversion (Scheme 15) of (*R*)-pulegone **33** to ketone **35**.

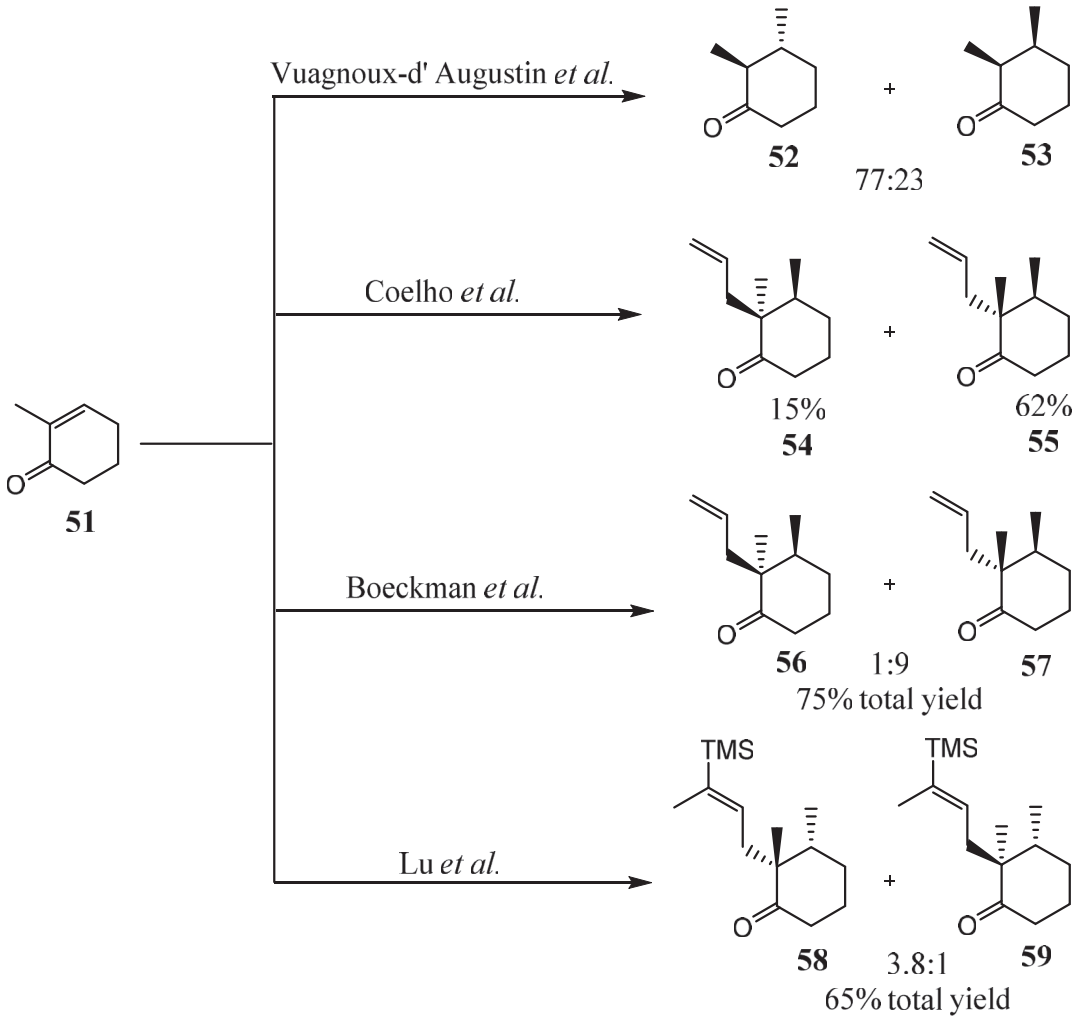

Scheme 17. An overview of different possible synthetic routes starting from 2-methylcyclohex-2-en-1-one 51.

If the simpler 2-methylcyclohex-2-en-1-one (**51**) of the two starting materials was used, it was assumed that methylation using a chiral ligand in order to obtain the sterically correct methyl at C3 was possible. Vuagnoux-d' Augustin *et al*. reported a cupper-catalyzed asymmetric conjugate addition (A.C.A) of R_3Al to 2-methylcyclohex-2-en-1-one (Scheme 17).[96] This resulted in a ratio of 77:23 between **52**:**53**, with the lowest amount of the desired compound **53**. Direct synthesis of the enantiomers of compounds similar to sulfones **39** and **40** from 2-methylcyclohex-2-en-1-one **51** has been reported by Boeckman *et al*.[97] and Lu *et al*.[98], though with the use of toxic HMPA and an allylic halide. Coelho *et al*. performed the methylation and alkylation using in situ prepared cuprate reagent and alkyl halide without HMPA, but with the possibility of explosion of the RCu salts formed in the reaction.[99] Even though this starting material is a simple structure, it is quite expensive, costing 1530 NOK per gram[100]. Therefore, (*S*)-carvone **48** was chosen as the preferred starting material, being relatively inexpensive (624

NOK for 24 g)[95] and not requiring HMPA in the methylation and alkylation at C3. In addition, the isopropenyl-group acts as a directing group, helping to achieve the correct stereochemistry when introducing the methyl group in the first step.

The non-selective alkylation of the silyl enol ether (**36**) gave rise to a mixture of the two sulfides **37** and **38**. The total yield was good, but the stereoselectivity between the two isomers was less than desired. This challenge will also be addressed in the following sections. Two different synthetic routes from (*S*)-carvone (**48**) will be presented, and their pros and cons will be discussed (Scheme 18). The main differences for these two pathways, is that in pathway 1, the first step is a methylation, and the introduction of the phenyl sulfide is performed later in the process, taking advantage of the formation of a silyl enol ether. In pathway 2, the introduction of the phenyl sulfide happens directly after the methylation, as an enolate is formed in the methylation reaction.

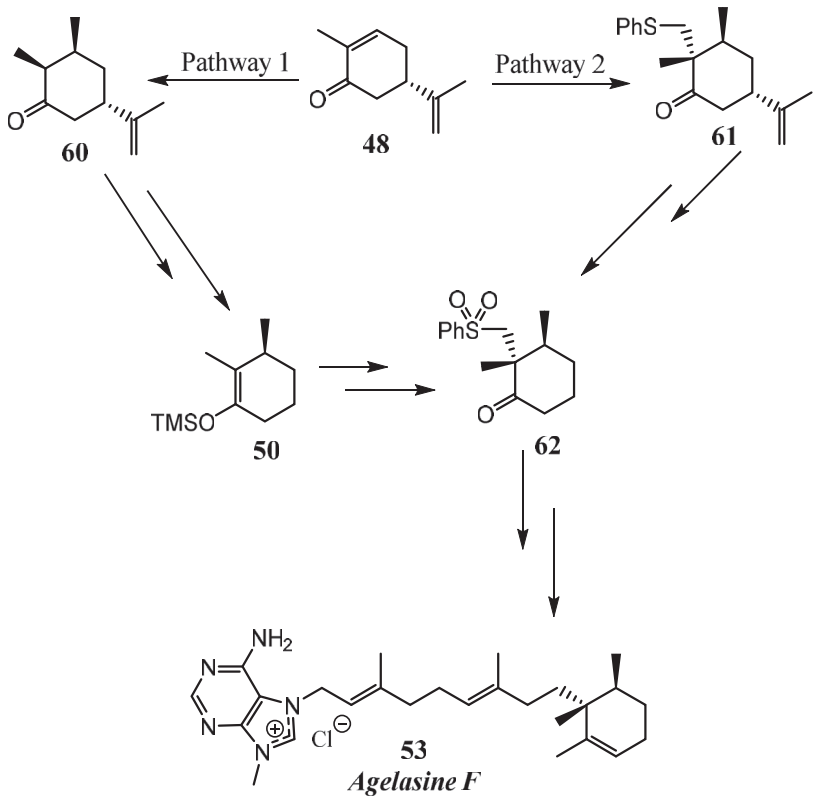

Scheme 18. Overview of the two synthetic pathways described in this thesis for the total synthesis of (-)-agelasine F.

3.2 Synthesis of the monocyclic side chain of (-)-agelasine F

Following the procedure published by Ebert *et al*, (*S*)-carvone **48** was methylated using an *in situ* prepared cuprate reagent giving a stereoselective introduction of the methyl group at C3, resulting in a high yield and excellent diastereomeric ratio of compound **60** (Scheme 19).[101] As mentioned in section 3.1, the isopropenyl-group acts as a directing group by helping to achieve the correct stereochemistry when introducing the methyl group at C3. The isopropenyl-group is effectively blocking one side of the molecule, forcing the rather voluminous cuprate reagent to attack from above. A sterically demanding proton source was utilized to give a cis relationship between the two methyl groups. The isopropenyl moiety was removed by ozonolysis followed by an iron/copper promoted fragmentation of the hydroperoxide formed (hereby referred to as modified ozonolysis).[102-104] This mild oxidation method gave two products (**63** and **64**) which both seemed to be volatile, and care had to be taken when evaporating the solvent. In the article published by Ebert *et al.*, the hydrogenation was performed in petroleum ether with rhodium on charcoal (5%) at ambient pressure for three hours.[101] The authors report substantial epimerization at C2 when the reaction was performed in diethylether. In our hands, using the same catalyst, it did not yield the desired product, and thus the reaction was altered. Two different solvents were tested, as well as different catalysts. Diethyl ether as solvent contributed to unwanted epimerization at C2, in line with findings published by Ebert *et al*.[101] The reason for the epimerization was probably due to higher polarity of the solvent than pentane. In reactions where enolization can occur, a polar solvent can influence the equilibrium and push it towards the enol form, thus causing epimerization at C2.[105] This resulted in pentane being the preferred solvent, yielding a ratio of 94:6 between the cis-trans diastereomers **49** and **65**. The successful reaction was performed with Pd/C as catalyst.

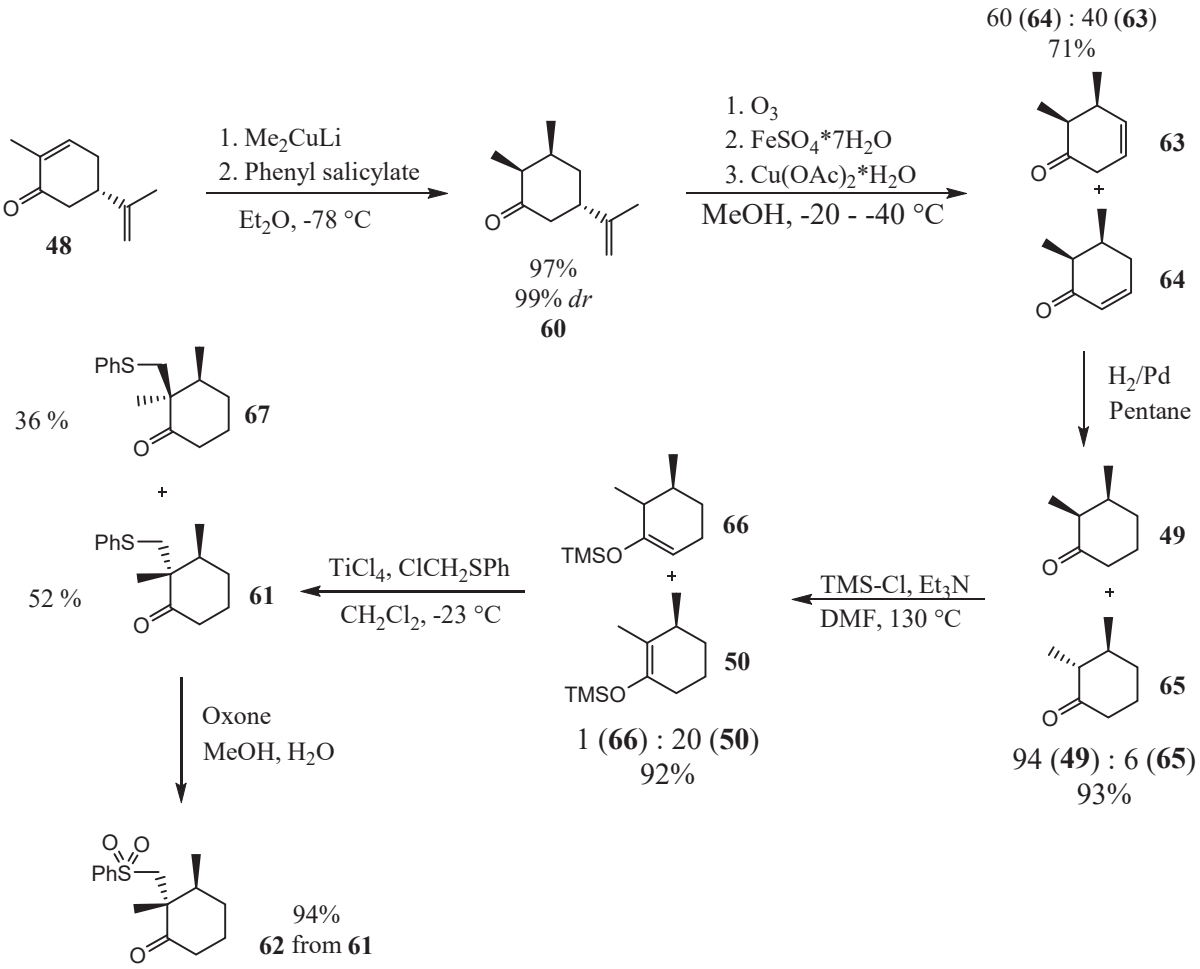

Scheme 19. Summary of the first six steps in the total synthesis of agelasine F.

The next step in the synthesis towards agelasine F was the formation of the silyl enol ether **50**, which had variable reproducibility according to Proszenyàk.[106] There are two main products that form in this reaction, as the double bond of the silyl enol ether has two possible positions. The thermodynamic (**50**) and kinetic (**66**) product ratio varied from 7:3 to 20:1, yields ranging from 50% to 92%, the desired product being the thermodynamic **50**. The lifetime of this compound was very limited and had to be used directly in the next step. The alkylation was performed in the presence of a Lewis acid, and $TiCl_4$ was used in the original synthesis.[61] In order to affect the ratio of the two sulfides **61** and **67**, attempts to vary the time and temperature from – 78 ºC to room temperature and 20 min to 1 h, resulted in no change in the ratio between the two diastereomeric sulfides. An overall summary of the work is presented in Table 7. Changing the Lewis acid to Et_2AlCl did not give a substantial change in the ratio either. However, when changing the Lewis acid to the softer $ZnBr_2$,[107] and changing the solvent to THF for solubility reasons, the ratio shifted in favor to the wanted isomer: from 1:0.54 to 1:0.26. Performing this reaction over longer time and starting at – 78 ºC did not impact the ratio of the

isomers. Varying the halogen did not impact the ratio either, and running the reaction with ZnI_2, $ZnCl_2$ and $ZnBr_2$ under identical conditions gave no change in the ratio observed for the two diastereomers. Even though these Zn-containing Lewis acids gave better selectivity with respect to the ratio of the two isomers, the total yield was sabotaged by what is believed to be alkylation of the kinetic product of the silyl enol ether (**68**), hydrolysation of the silyl enol ether (**49**), and epimerization of the hydrolyzed silyl enol ether (**65**) (Scheme 20).

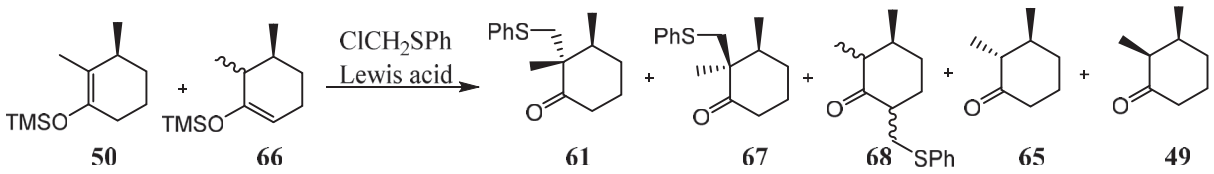

Scheme 20. Suspected products from the alkylation with chloromethyl phenyl sulfide of the silyl enol ether 50/66: the alkylation of the kinetic product of the silyl enol ether (68), hydrolysation of the silyl enol ether (49), and epimerization of the hydrolyzed silyl enol ether (65).

Table 7. Alkylation of silyl enol ether

Lewis acid	Solvent	Temp.	Time	Ratio **61**:**67**[a]
$TiCl_4$	CH_2Cl_2	RT	30 min	1:0.55
$TiCl_4$	CH_2Cl_2	0 °C	1 h	1:0.56
$TiCl_4$	CH_2Cl_2	-23 °C	1 h	1:0.55
$TiCl_4$	CH_2Cl_2	-78 °C	1h 20 min	1:0.51
Et_2AlCl	CH_2Cl_2/toluene	0 °C	20 min	1:0.51
$ZnBr_2$	THF	RT	4 h	1:0.26
$ZnBr_2$	THF	-78 °C → RT	21 h	1:0.26
ZnI_2	THF	RT	3 h	1:0.28
$ZnCl_2$	THF	RT	3 h	1:0.30

(a) Determined by ^{1}H NMR of the crude reaction mixture.

Since the alkylation reaction with the silyl enol ether gave such intricate results, it was desirable to avoid this step completely.

3.3 Alternative synthetic pathway to the monocyclic side chain of (-)-agelasine F

In search of finding new methods to synthesize the key sulfone **62**, an article published by Liffert *et al*. suggested a conjugate addition of methyl cuprate to γ-hydroxy-protected carvone, and trapping the enolate with a TMS-group (Scheme 21).[108] Although the starting materials were different, the idea was alluring. Initial attempts in performing this reaction with (*S*)-carvone **48** as starting material resulted in methylated product, but no TMS-group trapping the enolate. This lead to the decision to not trap the enolate at all, but to add the electrophile directly in the reaction mixture after methylation had occurred.

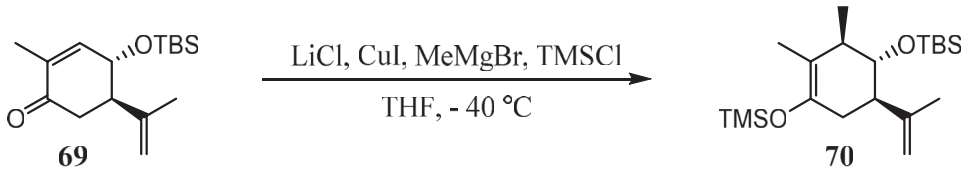

69 **70**

Scheme 21. Methylation of compound 69 with an in situ prepared cuprate followed by a trapping of the enolate with TMSCl resulting in compound 70 published by Liffert *et al*.[108]

The intermediate enolate **71** was utilized directly by adding the alkylating agent to this mixture (Scheme 22). Two different electrophiles were tested. Using chloromethyl phenyl sulfone as alkylating agent gave no preferred sulfone product (**72**), agreeing with unpublished results by Proszenyàk.[106] Utilizing chloromethyl phenyl sulfide yielded sulfide (**73**) in 54%. The ratio was approximately 3:1 in the crude mixture between the two diastereomers **73** and (what is presumed to be) **74** (Scheme 22).

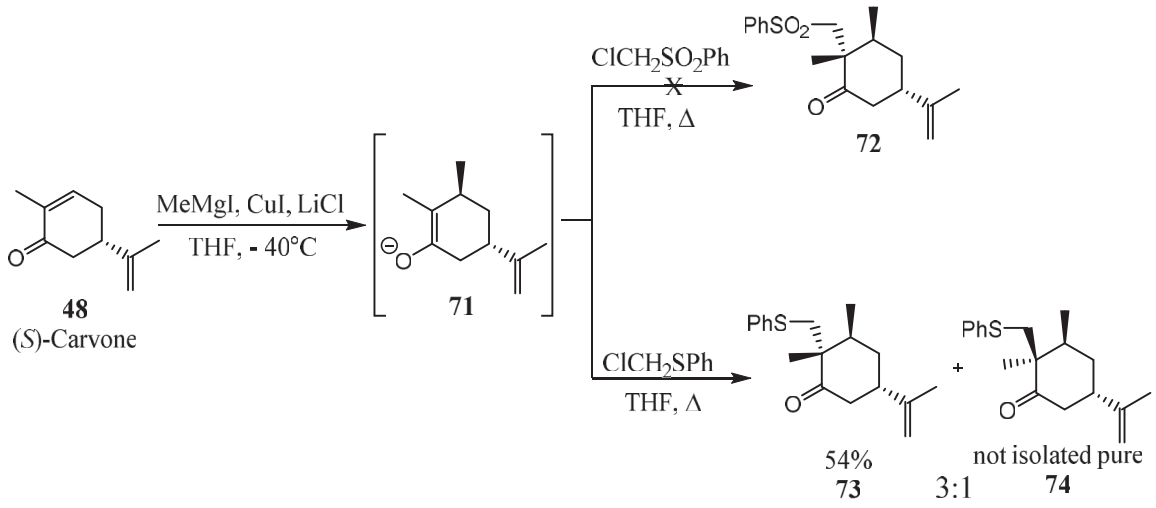

48 (*S*)-Carvone **71** **72** **73** **74**

Scheme 22. Reaction conditions for the two different alkylating agents used for alkylating the enolate 71.

Now there were to possible ways to proceed: either oxidize the sulfide to the sulfone before removing the isopropenyl group with the modified ozonolysis, or the other way around (Scheme 23).

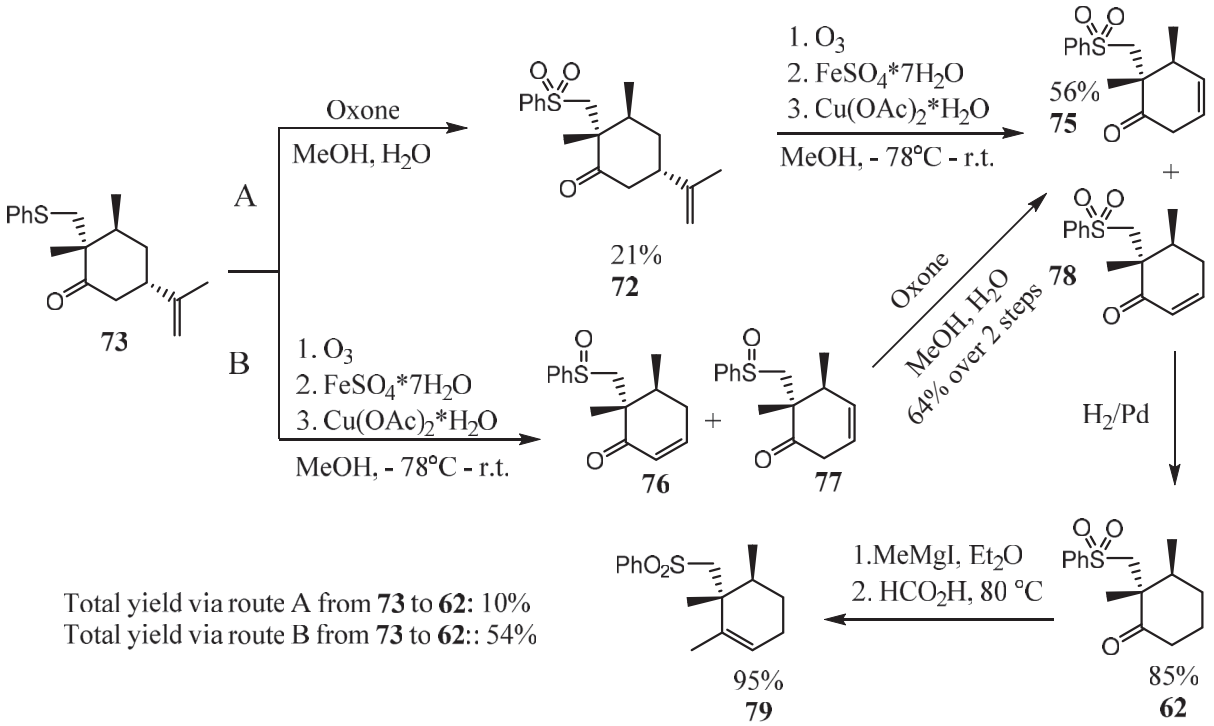

Scheme 23. Oxidation of the sulfide 73 to the sulfone 72 before removing the isopropenyl group with a modified ozonolysis (route A), or the other way around (route B).

In the original reaction sequence from the article published by Proszenyàk *et al*[61], the reaction time in the oxidation-reaction of the sulfide **37** (Scheme 15) was 19 h, which was also used for the oxidation of the sulfide in Pathway 1. In the case of oxidation of compound **37**, it was no other functional group that could easily be oxidized. As the reaction sequence changed, the oxidation had to be performed in the presence of a double bond. Ferraz *et al*. reported oxidation on similar substrates which indicated that both the endocyclic and the exocyclic double bonds was prone to epoxidation (Scheme 24), but with the ketone or alcohol moiety determining which bond is most prone to attack by oxone.[109]

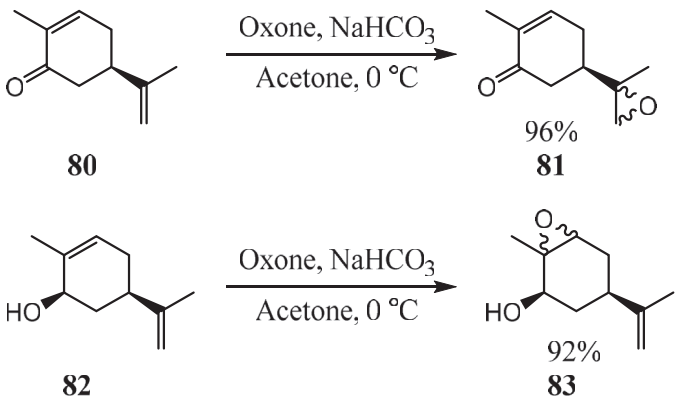

Scheme 24. Examples of oxidation of endocyclic and exocyclic double bonds on similar substrates as 58/59 and 60 published by Ferraz *et al.*[109]

In an attempt to avoid oxidation of the exocyclic double bond in compound **73**, possibly yielding epoxides in route A in Scheme 23, the reaction time was 2.5 h, and the temperature was 0 °C. Even with these changes, the reaction gave poor yields of 21 %, with no trace of starting material on ^{1}H NMR of the crude product, indicating formation of unwanted byproducts. This was not satisfactory, and it was desirable to explore the possibility that the endocyclic double bonds in compounds **76** and **77** in route B would be less prone to oxidation.[109] The isopropenyl group on compound **73** was removed with modified ozonolysis which resulted in both the *R* and *S*-conjugated and *R* and *S*-unconjugated (*R* and *S* are with respect to the sulfur) sulfoxides **76** and **77**. This complex mixture was directly oxidized to the corresponding sulfones, with an overall yield of 64%. The hydrogenation of sulfone **75** and **78** gave a high yield of **62** (85%). The last step in the synthesis of the monocyclic part of the terpenoid side chain, was the introduction of the last methyl group and elimination of water to obtain compound **79**. This was achieved with the same reaction conditions published by Proszenyàk *et al*.[61]

With this new route, several problems were avoided. Both the handling of the volatile compounds **63**, **64** and **65**, and the formation of the unstable silyl enol ether **50**/**66** were avoided. To sum up, Proszenyàk's route was 5 steps and gave a total yield of 24% from (*R*)-pulegone **33** to sulfone **40** (equivalent to sulfone **62**). Pathway 1 had 5 steps and gave an increased yield to 29% from (*S*)-carvone to sulfone **62.** Pathway 2 route B had 4 steps from (S)-carvone **48** to sulfone **62**, and had also a yield of 29% (see Scheme 18 for pathways and Scheme 23 for routes).

The final part of the total synthesis of agelasine F contained five steps (see Scheme 25 from compound **79**). The iodide **42** was synthesized in three steps by protecting geraniol with DHP,[110] before introducing a hydroxyl group trans to the terminal allylic double bond with

SeO_2 and *tert*-butylhydroperoxide[111, 112] which was then reacted with I_2 to give the desired compound.[61] The purification of the iodide **42** was reported to be by column chromatography to remove of the triphenylphosphine oxide, but this gave a doubling of signals on ^{13}C NMR. One can only speculate why the doubling of signals is observed, but the working hypothesis was that the iodide had rearranged, but the exact structure is not known. This was avoided if the purification was altered: instead of purifying the compound by column chromatography, the compound could be sufficiently purified by dissolving the crude product in a small amount of Et_2O which made the $POPh_3$ precipitate. The precipitate was removed by filtration. Lithiation of the sulfone **79** and reaction with iodide **42** resulted in compound **84**. The sulfonyl group was reductively removed with sodium, and removal of THP using PPTS yielded compound **86**. Reacting the alcohol **86** with PBr_3 resulted in bromide **87**, which was reacted with the adenine derivative **88**. The *tert*-butoxy group was reductively removed to yield agelasine F **(53)** (Scheme 25).

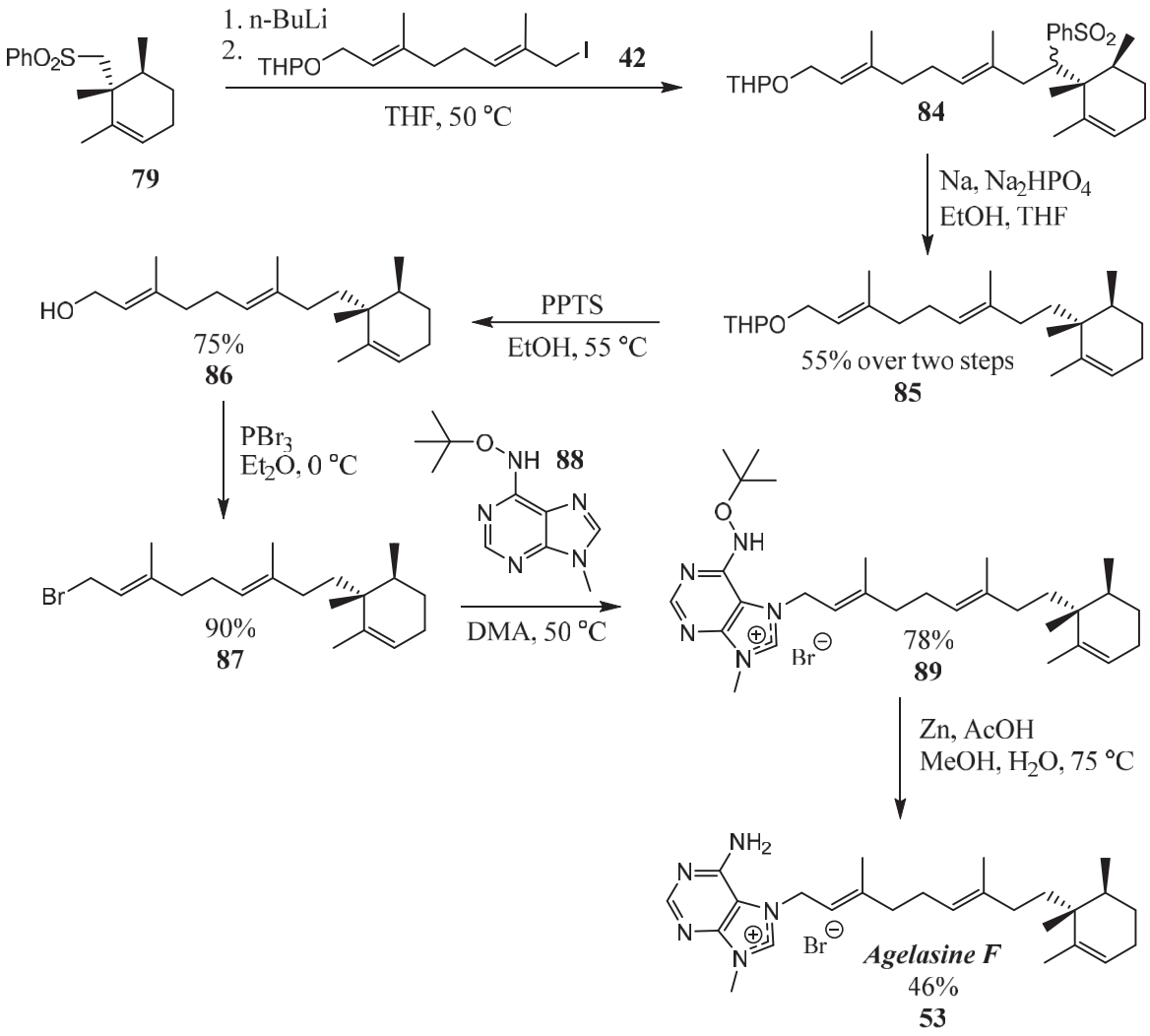

Scheme 25. The final part of the total synthesis of agelasine F.

4 Conclusion

The recorded NMR spectra for the synthesized proposed structure of *ent*-ageloxime D did not match the published NMR-spectra for the compound. The proposed structure was incorrect, and was in fact a ring opened formamide, and not an ageloxime. This underlines the importance of verifying structurally elucidated compounds found in nature with synthesis of the compound in question.

The N^6-hydroxyagelasine D and analogs were tested for biological activities, and compound **8c** and **8d** were found to have several interesting activities. The most prominent being activities towards the protozoa causing Chagas disease and variants of Leishmaniasis. The antibacterial effect on the bacteria responsible for tuberculosis was also significant. Unfortunately, the said compounds also displayed very high toxicity towards mammalian fibroblast cells.

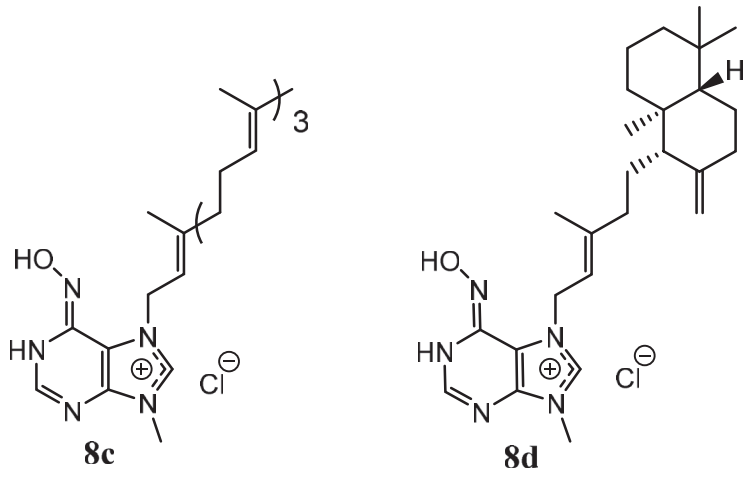

Figure 23. Target structure 8c and 8d displaying high antimicrobial activities.

(-)-Agelasine F (**53**) was successfully synthesized from the relatively low-cost and commercially available *S*-carvone **48** with three different routes. The first route (Pathway 1, Scheme 19) followed the literature synthesis performed by Ebert *et al*,[101] in the three first steps, then altering the literature synthesis performed by Proszenyàk *et al*[61] by varying the Lewis acid, time and temperature in the alkylation of the silyl enol ether. As this did not yield satisfactory yields, the reaction sequence was altered, and two different routes was employed (Scheme 23). The alkylation alpha to the carbonyl with chloromethyl phenyl sulfide was performed in a one-pot procedure with the methylation (**73**), utilizing the formation of the enol (**71**). As the modified ozonolysis followed by oxidation had the best yield, this was the preferred route to achieve sulfone **62**.

5 Future work

As the proposed structure of ageloxime D did not match the actual structure Hertiani *et al*. had isolated from the Agelas sponge, it would be of interest to find a way to synthesize the formamide. Seeing as this is a ring-opened agelasine, and these can be synthesized by treating the agelsine with basic conditions, it is tempting to suggest that the formamide can be synthesized in this manner.

The modified ozonolysis of the sulfide **55** was performed at – 78 ºC resulting in sulfoxides **58** and **59**. According to Maggiolo *et al*.,[113] performing the reaction at higher temperatures can

lead to formation of sulfones. This is very interesting, as finding a temperature that could give sulfones while still being a safe reaction would be desirable.

The enantiomers of both sulfones (**32** and **33**) are interesting building blocks for a variety of natural products, see Figure 24.

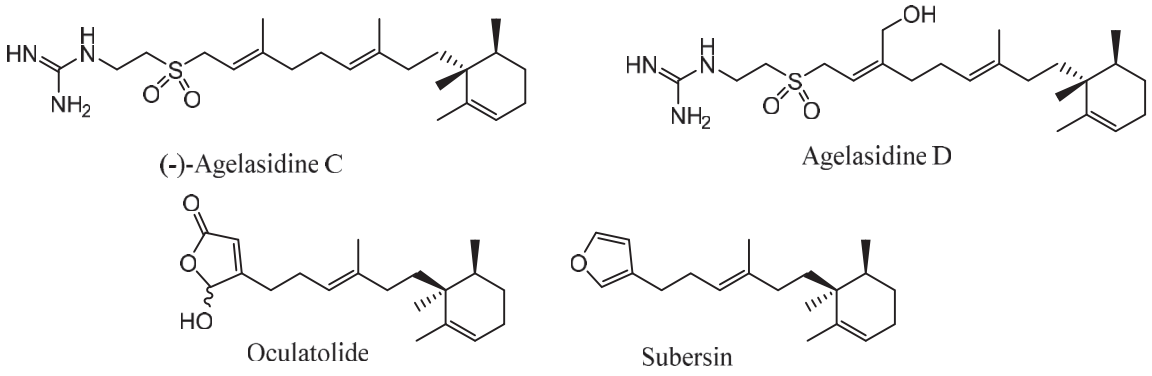

Figure 24. Examples of natural products that can be synthesized from sulfones 32 and 33.

6 References

1. IACG, No time to wait: securing the future from drug-resistant infections. UN Member States, 2019.
2. Fleming, A., *Br. J. Exp. Pathol*, **1929,** *10* (3), 226-236.
3. PEW https://www.pewtrusts.org/-/media/assets/2019/08/arp_antibiotics_currently_in_global_clinical_development_data_table_v2.pdf?la=nb&hash=9C1D5A2E99B265FBC608542A3B116C13FD2B919A (accessed 31.03.2020).
4. WHO *Antibacterial agents in clinical development: an analysis of the antibacterial clinical development pipeline*; 2019.
5. WHO *Prioritization of pathogens to guide discovery, research and development of new antibiotics for drug-resistant bacterial infections, including tuberculosis.*; 2017.
6. WHO *Latent tuberculosis infection: updated and consolidated guidelines for programmatic management*; 2018.
7. WHO *Global tuberculosis report*; 2019.
8. Donlan, R. M., *Clin. Infect. Dis.*, **2001,** *33* (8), 1387-1392.
9. Jamal, M.; Ahmad, W.; Andleeb, S.; Jalil, F.; Imran, M.; Nawaz, M. A.; Hussain, T.; Ali, M.; Rafiq, M.; Kamil, M. A., *J. Chin. Med. Assoc.*, **2018,** *81* (1), 7-11.
10. Wu, H.; Moser, C.; Wang, H. Z.; Hoiby, N.; Song, Z. J., *Int. J. Oral. Sci.*, **2015,** *7* (1), 1-7.
11. Hellio, C.; Yebra, D., *Advances in marine antifouling coatings and technologies*. Woodhead Publishing Limited: Cambrigde, 2009.
12. Vietti, P. *New Hull Coatings Cut Fuel Use, Protect Environment*; Office of Naval Research Corporate Strategic Communications: September, 2009.
13. Torres-Guerrero, E.; Quintanilla-Cedillo, M. R.; Ruiz-Esmenjaud, J.; Arenas, R., *F1000Res*, **2017,** *6*, 1-15.
14. Chakravarty, J.; Sundar, S., *J. Glob. Infect. Dis.*, **2010,** *2* (2), 167-76.

15. Sales Junior, P. A.; Molina, I.; Fonseca Murta, S. M.; Sanchez-Montalva, A.; Salvador, F.; Correa-Oliveira, R.; Carneiro, C. M., *Am. J. Trop. Med. Hyg.*, **2017,** *97* (5), 1289-1303.
16. WHO *WHO interim guidelines for the treatment of gambiense human African trypanosomiasis*; 2019.
17. Baker, N.; de Koning, H. P.; Maser, P.; Horn, D., *Trends Parasitol*, **2013,** *29* (3), 110-118.
18. WHO *Global action plan on antimicrobial resistance*; 2015.
19. Newman, D. J.; Cragg, G. M., *J. Nat. Prod.*, **2016,** *79* (3), 629-661.
20. García, P. A.; Valles, E.; Díez, D.; Castro, M.-Á., *Mar. Drugs*, **2018,** *16* (6), 1-32.
21. WHO, *WHO Drug Information*, **2014,** *28* (2).
22. WHO *Artemisinin resistance and artemisinin-based combination therapy efficacy*; 2018.
23. Veeresham, C., *J. Adv. Pharm. Technol. Res.*, **2012,** *3* (4), 200-1.
24. Proksch, P.; Edrada-Ebel, R.; Ebel, R., *Mar. Drugs*, **2003,** *1* (1), 5-17.
25. Blunt, J. W.; Copp, B. R.; Hu, W. P.; Munro, M. H.; Northcote, P. T.; Prinsep, M. R., *Nat. Prod. Rep.*, **2009,** *26* (2), 170-244.
26. Blunt, J. W.; Copp, B. R.; Keyzers, R. A.; Munro, M. H.; Prinsep, M. R., *Nat. Prod. Rep.*, **2016,** *33* (3), 382-431.
27. Skropeta, D.; Wei, L., *Nat. Prod. Rep.*, **2014,** *31* (8), 999-1025.
28. Vik, A. Synthetic studies directed towards bioactive purine-contaning marine natural products and analogs. PhD, UiO, 2007.
29. Rosemeyer, H., *Chem. Biodivers.*, **2004,** *1* (3), 361-401.
30. Cappelletti, S.; Piacentino, D.; Sani, G.; Aromatario, M., *Curr. Neuropharmacol.*, **2015,** *13* (1), 71-88.
31. Moffatt, B. A.; Ashihara, H., *Purine and pyrimidine nucleotide synthesis and metabolism*. 2002/01/01 ed.; 2002; Vol. 1.
32. Schantz, E. J.; Lynch, J. M.; Vayvada, G.; Matsumoto, K.; Rapoport, H., *Biochemistry*, **1966,** *5* (4), 1191-1195.
33. Osterbauer, P. J., Neurobiological Weapons. In *Clinical Neurotoxicology*, Dobbs, M., Ed. Elsevier: 2009; Vol. 1, p 720.
34. Strichartz, G., *J. Gen. Physiol.*, **1984,** *84* (2), 281-305.
35. Cusick, K. D.; Sayler, G. S., *Mar. Drugs*, **2013,** *11* (4), 991-1018.
36. Sivonen, K., *Cyanobacterial Toxins*. Elsevier: Oxford, 2009.
37. Mitchell, S. S.; Whitehill, A. B.; Trapido-Rosenthal, H. G.; Ireland, C. M., *J. Nat. Prod.*, **1997,** *60* (7), 727-728.
38. Parra-Velandia, F. J.; Zea, S.; Van Soest, R. W., *Zootaxa*, **2014,** *3794*, 301-43.
39. Zhang, H.; Dong, M.; Chen, J.; Wang, H.; Tenney, K.; Crews, P., *Mar. Drugs*, **2017,** *15* (11), 1-29.
40. Welsch, M. E.; Snyder, S. A.; Stockwell, B. R., *Curr. Opin. Chem. Biol.*, **2010,** *14* (3), 347-61.
41. Gordaliza, M., *Mar. Drugs*, **2009,** *7* (4), 833-849.
42. Cullen, E.; Devlin, J. P., *Can. J. Chem.*, **1975,** *53* (11), 1690-1691.
43. Wu, H.; Nakamura, H.; Kobayashi, J. i.; Ohizumi, Y.; Hirata, Y., *Tetrahedron Lett.*, **1984,** *25* (34), 3719-3722.
44. Wu, H.; Nakamura, H.; Kobayashi, J. i.; Kobayashi, M.; Ohizumi, Y.; Hirata, Y., *Bull. Chem. Soc. Jpn.*, **1986,** *59*, 2495-2504.
45. Capon, R. J.; Faulkner, D. J., *J. Am. Chem. Soc.*, **1984,** *106* (6), 1819-1822.

46. Appenzeller, J.; Mihci, G.; Martin, M. T.; Gallard, J. F.; Menou, J. L.; Boury-Esnallt, N.; Hooper, J.; Petek, S.; Chevalley, S.; Valentin, A.; Zaparucha, A.; Al-Mourabit, A.; Debitus, C., *J. Nat. Prod.*, **2008,** *71* (8), 1451-1454.
47. Nakamura, H.; Wu, H.; Ohizumi, Y.; Hirata, Y., *Tetrahedron Lett.*, **1984,** *25* (28), 2989-2992.
48. Ishida, K.; Ishibashi, M.; Shigemori, H.; Sasaki, T.; Kobayashi, J., *Chem. Pharm. Bull.*, **1992,** *40* (3), 766-767.
49. Hattori, T.; Adachi, K.; Shizuri, Y., *J. Nat. Prod.*, **1997,** *60* (4), 411-413.
50. Fu, X.; Schmitz, F. J.; Tanner, R. S.; Kelly-Borges, M., *J. Nat. Prod.*, **1998,** *61* (4), 548-50.
51. Iwagawa, T.; Kaneko, M.; Okamura, H.; Nakatani, M.; van Soest, R. W. M., *J. Nat. Prod.*, **1998,** *61* (10), 1310-1312.
52. Mangalindan, G. C.; Talaue, M. T.; Cruz, L. J.; Franzblau, S. G.; Adams, L. B.; Richardson, A. D.; Ireland, C. M.; Concepcion, G. P., *Planta Med*, **2000,** *66* (4), 364-365.
53. Kubota, T.; Iwai, T.; Takahashi-Nakaguchi, A.; Fromont, J.; Gonoi, T.; Kobayashi, J., *Tetrahedron*, **2012,** *68* (47), 9738-9744.
54. Calcul, L.; Tenney, K.; Ratnam, J.; McKerrow, J. H.; Crews, P., *Aust. J. Chem.*, **2011,** *64* (6), 915-921.
55. Stout, E. P.; Yu, L. C.; Molinski, T. F., *Eur. J. Org. Chem.*, **2012,** *2012*, 5131-5135.
56. Hong, L.-L.; Sun, J.-B.; Yang, F.; Liu, M.; Tang, J.; Sun, F.; Jiao, W.-H.; Wang, S.-P.; Zhang, W.; Lin, H.-W., *RSC Adv.*, **2017,** *7* (39), 23970-23976.
57. Pettit, G. R.; Tang, Y.; Zhang, Q.; Bourne, G. T.; Arm, C. A.; Leet, J. E.; Knight, J. C.; Pettit, R. K.; Chapuis, J. C.; Doubek, D. L.; Ward, F. J.; Weber, C.; Hooper, J. N., *J. Nat. Prod.*, **2013,** *76* (3), 420-424.
58. Vik, A.; Hedner, E.; Charnock, C.; Samuelsen, O.; Larsson, R.; Gundersen, L. L.; Bohlin, L., *J. Nat. Prod.*, **2006,** *69* (3), 381-386.
59. Yang, F.; Hamann, M. T.; Zou, Y.; Zhang, M.-Y.; Gong, X.-B.; Xiao, J.-R.; Chen, W.-S.; Lin, H.-W., *J. Nat. Prod.*, **2012,** *2012* (75), 774-778.
60. Utenova, B. T.; Gundersen, L.-L., *Tetrahedron Lett.*, **2004,** *45* (22), 4233-4235.
61. Proszenyak, A.; Braendvang, M.; Charnock, C.; Gundersen, L. L., *Tetrahedron*, **2008,** *65* (1), 194-199.
62. Bakkestuen, A.; Gundersen, L.-L.; Petersen, D.; Utenova, B.; Vik, A., *Org. Biomol. Chem.*, **2005,** *3* (6), 1025-1033.
63. Bakkestuen, A. K.; Gundersen, L.-L., *Tetrahedron*, **2003,** *59* (1), 115-121.
64. Piers, E.; Breau, M. L.; Han, Y.; Plourde, G. L.; Yeh, W.-L., *J. Chem. Soc., Perkin Trans. 1*, **1995,** (8), 963-966.
65. Piers, E.; Roberge, J. Y., *Tetrahedron Lett.*, **1992,** *33* (46), 6923-6926.
66. Marcos, I. S.; García, N.; Sexmero, M. J.; Basabe, P.; Díez, D.; Urones, J. G., *Tetrahedron*, **2005,** *61* (49), 11672-11678.
67. Asao, K.; Iio, H.; Tokoroyama, T., *Tetrahedron Lett.*, **1989,** *30* (46), 6401-6404.
68. Vik, A.; Proszenyak, A.; Vermeersch, M.; Cos, P.; Maes, L.; Gundersen, L. L., *Molecules*, **2009,** *14* (1), 279-288.
69. Sjogren, M.; Dahlstrom, M.; Hedner, E.; Jonsson, P. R.; Vik, A.; Gundersen, L. L.; Bohlin, L., *Biofouling*, **2008,** *24* (4), 251-258.
70. Hertiani, T.; Edrada-Ebel, R.; Ortlepp, S.; van Soest, R. W.; de Voogd, N. J.; Wray, V.; Hentschel, U.; Kozytska, S.; Muller, W. E.; Proksch, P., *Bioorg. Med. Chem.*, **2010,** *18* (3), 1297-1311.
71. Maziarz, E. K.; Perfect, J. R., *Infect. Dis. Clin. North. Am.*, **2016,** *30* (1), 179-206.
72. Nicolaou, K. C.; Snyder, S. A., *Angew. Chem. Int. Ed. Engl.*, **2005,** *44* (7), 1012-1044.
73. Robins, R. K.; Lin, H. H., *J. Am. Chem. Soc.*, **1957,** *79* (2), 490-494.

74. Giner-Sorolla, A.; Bendich, A., *J. Am. Chem. Soc.*, **1958,** *80* (15), 3932-3937.
75. Giner-Sorolla, A.; O'Bryant, S. A.; Nanos, C.; Dollinger, M. R.; Bendich, A.; Burchenal, J. H., *J. Med. Chem.*, **1968,** *11* (3), 521-523.
76. Giner-Sorolla, A.; O'Bryant, S.; Burchenal, J. H.; Bendich, A., *Biochemistry*, **1966,** *5* (9), 3057-3061.
77. Barlin, G. B.; Chapman, N. B., *J. Chem. Soc.*, **1965**, 3017-3022.
78. Jafar, N. N.; Al-Masoudi, N. A.; Baqir, S. J.; Leyssen, P.; Pannecouque, C., *Antivir. Chem. Chemother.*, **2012,** *23* (3), 103-112.
79. Xu, H.; Maga, G.; Focher, F.; Smith, E. R.; Spadari, S.; Gambino, J.; Wright, G. E., *J. Med. Chem.*, **1995,** *38* (1), 49-57.
80. Kovačková, S.; Dračínský, M.; Rejman, D., *Tetrahedron*, **2011,** *67* (7), 1485-1500.
81. Gundersen, L.-L.; Görbitz, C. H.; Neier, L.; Roggen, H.; Tamm, T., *Theoretical Chemistry Accounts*, **2010,** *129* (3-5), 349-358.
82. Holton, R. A.; Kim, H. B.; Somoza, C.; Liang, F.; Biediger, R. J.; Boatman, P. D.; Shindo, M.; Smith, C. C.; Kim, S., *J. Am. Chem. Soc.*, **1994,** *116* (4), 1599-1600.
83. Nakanishi, M.; Mori, M., *Angew. Chem. Int. Ed. Engl.*, **2002,** *41* (11), 1934-1936.
84. Corey, E. J.; Venkateswarlu, A., *J. Am. Chem. Soc.*, **1972,** *94* (17), 6190-6191.
85. Holton, R. A.; Juo, R. R.; Kim, H. B.; Williams, A. D.; Harusawa, S.; Lowenthal, R. E.; Yogai, S., *J. Am. Chem. Soc.*, **1988,** *110* (19), 6558-6560.
86. Evans, D. A.; Barrow, J. C.; Leighton, J. L.; Robichaud, A. J.; Sefkow, M., *J. Am. Chem. Soc.*, **1994,** *116* (26), 12111-12112.
87. Albanese, D.; Landini, D.; Penso, M., *J. Org. Chem.*, **1998,** *63* (25), 9587-9589.
88. Cirillo, P. F.; Panek, J. S., *J. Org. Chem.*, **1990,** *55* (25), 6071-6073.
89. Crich, D.; Hermann, F., *Tetrahedron Lett.*, **1993,** *34* (21), 3385-3388.
90. Zhang, W.; Robins, M. J., *Tetrahedron Lett.*, **1992,** *33* (9), 1177-1180.
91. White, J. D.; Amedio, J. C.; Gut, S.; Jayasinghe, L., *J. Org. Chem.*, **1989,** *54* (18), 4268-4270.
92. Paulsen, B.; Fredriksen, K. A.; Petersen, D.; Maes, L.; Matheeussen, A.; Naemi, A. O.; Scheie, A. A.; Simm, R.; Ma, R.; Wan, B.; Franzblau, S.; Gundersen, L. L., *Bioorg. Med. Chem.*, **2019,** *27* (4), 620-629.
93. Margolin, Z.; Long, F. A., *J. Am. Chem. Soc.*, **1973,** *95* (9), 2757-2762.
94. Siddall Iii, T. H.; Garner, R. H., *Can. J. Chem.*, **1966,** *44* (20), 2387-2394.
95. Sigmaaldrich.com https://www.sigmaaldrich.com/catalog/product/aldrich/435759?lang=en&region=NO (accessed 28.03.2020).
96. Vuagnoux-d'Augustin, M.; Alexakis, A., *Chemistry*, **2007,** *13* (34), 9647-9662.
97. Boeckman, R. K., *J. Org. Chem.*, **1973,** *38* (26), 4450-4452.
98. Lu, Z.; Li, H.; Bian, M.; Li, A., *J. Am. Chem. Soc.*, **2015,** *137* (43), 13764-13767.
99. Coelho, F.; Diaz, G., *Tetrahedron*, **2002,** *58* (9), 1647-1656.
100. https://www.1clickchemistry.com/product/product-detail?id=2C61367&index=0 (accessed 31.03.2020).
101. Ebert, S.; Krause, N., *Eur. J. Org. Chem.*, **2001,** (20), 3831-3835.
102. Audran, G.; Marque, S. R. A.; Santelli, M., *Tetrahedron*, **2018,** *74* (43), 6221-6261.
103. Schreiber, S., *J. Am. Chem. Soc.*, **1980,** *102* (19), 6163-6165.
104. Schreiber, S.; Hulin, B.; Liew, W.-F., *Tetrahedron*, **1986,** *42* (11), 2945-2950.
105. Charif, I. E.; Mekelleche, S. M.; Villemin, D., *J. Theor. Comput. Chem.*, **2011,** *09* (06), 1021-1032.
106. Proszenyàk, A., Semester report. 2008.
107. Pearson, R. G., *J. Am. Chem. Soc.*, **1963,** *85* (22), 3533-3539.

108. Liffert, R.; Linden, A.; Gademann, K., *J. Am. Chem. Soc.*, **2017,** *139* (45), 16096-16099.
109. Ferraz, H. M. C.; Muzzi, R. M.; de O. Vieira, T.; Viertler, H., *Tetrahedron Lett.*, **2000,** *41* (26), 5021-5023.
110. Chen, A.; Chen, A. P. C.; Chen, Y.-H.; Liu, H.-P.; Li, Y.-C.; Chen, C.-T.; Liang, P.-H., *J. Am. Chem. Soc.*, **2002,** *124* (51), 15217-15224.
111. Chappe, B.; Musikas, H.; Marie, D.; Ourisson, G., *Bull. Chem. Soc. Jpn.*, **1988,** *61* (1), 141-148.
112. Ippoliti, F. M.; Barber, J. S.; Tang, Y.; Garg, N. K., *J. Org. Chem.*, **2018,** *83* (18), 11323-11326.
113. Maggiolo, A.; Blair, A., *Adv. Chem.*, **1959**.

Paper 1

Synthesis and antimicrobial activities of N6-hydroxyagelasine analogs and revision of the structure of ageloximes.

Paulsen, B.; Fredriksen, K. A.; Petersen, D.; Maes, L.; Matheeussen, A.; Naemi, A. O.; Scheie, A. A.; Simm, R.; Ma, R.; Wan, B.; Franzblau, S.; Gundersen, L. L., *Bioorg. Med. Chem.* **2019,** *27* (4), 620-629.

Bioorganic & Medicinal Chemistry 27 (2019) 620–629

Contents lists available at ScienceDirect

Bioorganic & Medicinal Chemistry

journal homepage: www.elsevier.com/locate/bmc

Synthesis and antimicrobial activities of N^6-hydroxyagelasine analogs and revision of the structure of ageloximes

Britt Paulsen[a], Kim Alex Fredriksen[a], Dirk Petersen[a], Louis Maes[b], An Matheeussen[b], Ali-Oddin Naemi[c], Anne Aamdal Scheie[c], Roger Simm[c], Rui Ma[d], Baojie Wan[d], Scott Franzblau[d], Lise-Lotte Gundersen[a,*]

[a] Department of Chemistry, University of Oslo, P.O.Box 1033, Blindern, 0315 Oslo, Norway
[b] Laboratory of Microbiology, Parasitology and Hygiene (LMPH), University of Antwerp, Wilrijk, Belgium
[c] Institute of Oral Biology, University of Oslo, P.O. Box 1052, Blindern, 0316 Oslo, Norway
[d] Institute for Tuberculosis Research, University of Illinois at Chicago, 833 S. Wood St., Chicago, IL, USA

ARTICLE INFO

Keywords:
Agelasine
Ageloxime
Antimicrobial activity
Structure elucidation

ABSTRACT

(+)-N^6-Hydroxyagelasine D, the enantiomer of the proposed structure of (−)-ageloxime D, as well as N^6-hydroxyagelasine analogs were synthesized by selective N-7 alkylation of N^6-[*tert*-butyl(dimethyl)silyloxy]-9-methyl-9*H*-purin-6-amine in order to install the terpenoid side chain, followed by fluoride mediated removal of the TBDMS-protecting group. N^6-Hydroxyagelasine D and the analog carrying a geranylgeranyl side chain displayed profound antimicrobial activities against several pathogenic bacteria and protozoa and inhibited bacterial biofilm formation. However these compounds were also toxic towards mammalian fibroblast cells (MRC-5). The spectral data of N^6-hydroxyagelasine D did not match those reported for ageloxime D before. Hence, a revised structure of ageloxime D was proposed. Basic hydrolysis of agelasine D gave (+)-*N*-[4-amino-6-(methylamino) pyrimidin-5-yl]-*N*-copalylformamide, a compound with spectral data in full agreement with those reported for (−)-ageloxime D.

1. Introduction

Several bioactive secondary metabolites from marine sponges can be classified as purine-terpene hybrids. Important sub-classes are agelasines and ageloximes (Fig. 1). Agelasines are isolated from marine sponges of the genus *Agelas* and are associated with bioactivities like antimicrobial and cytotoxic effects as well as contractive responses of smooth muscles and inhibition of Na,K-ATPase.[1] Ageloximes, also isolated from *Agelas* sp., are claimed to be N^6-hydroxyagelasines. To date isolation of (−)-ageloxime B[2] from *A. mauritania* and (−)-ageloxime D[3] from *A. nakamurai* has been reported (Fig. 1). The ageloximes are named after the corresponding agelasines, purinium salts with a primary amino group in the purine 6-position.

(−)-Ageloxime D was reported to inhibit biofilm formation from *Staphylococcus epidermidis*, but did not inhibit the growth of the planktonic bacteria (MIC > 45 μM). (−)-Agelasine D, on the other hand, did not inhibit biofilm formation, but displayed potent growth inhibition against *S. epidermidis* (MIC < 0.09 μM),[3] indicating that the oxime substituent on C-6 in ageloximes is important for biofilm inhibition and at the same time reduces toxicity towards the bacteria. However, it was later reported that both (−)-ageloxime B and (−)-ageloxime D displayed antimicrobial activity against other microorganisms (*Cryptococcus neoformans* and *Staphylococcus aureus*; MICs ca. 10 μg/mL (ca. 23 μM, calculated from the Mw's of the revised structures).[2] Bacteria capable of forming biofilms are often less sensitive to antibiotics compared to planktonic organisms and there is a current need for efficient and non-toxic biofilm inhibitors.[4]

We have previously showed that synthetic analogs of agelasines, carrying a simpler terpenoid side chain (*i.e.* geranylgeranyl) and/or an alkoxy substituent at N^6 display just as high antimicrobial activities as the natural products.[5] Thus we wanted to develop an efficient synthetic route to ageloximes and analogs and compare their antimicrobial activity as well as ability to inhibit biofilm formation with the corresponding agelasines and N^6-alkoxyagelasines. As a continuance of our synthetic studies towards bioactive purine-terpene hybrids,[5,6] we now report the first synthesis of N^6-alkoxyagelasine analogs and their antimicrobial activities. We also propose a revised structure of ageloxime D.

* Corresponding author.
E-mail address: l.l.gundersen@kjemi.uio.no (L.-L. Gundersen).

https://doi.org/10.1016/j.bmc.2019.01.002
Received 18 October 2018; Received in revised form 20 December 2018; Accepted 3 January 2019
Available online 04 January 2019

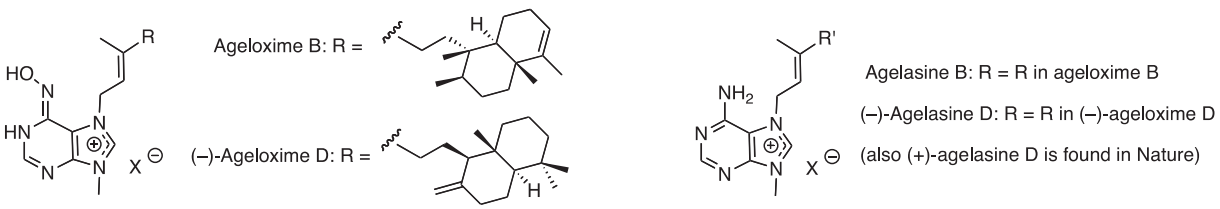

Fig. 1. Proposed structures of ageloximes B and D and structures of agelasine B and D.

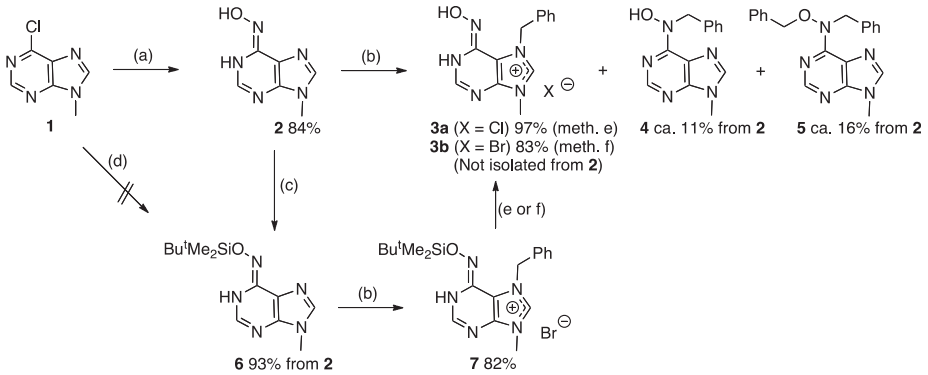

Scheme 1. Reagents and conditions: (a) $HONH_2$·HCl, KOH, EtOH; (b) $PhCH_2Br$, DMA, 50 °C; (c) Bu^tMe_2SiCl, imidazole, DMF; (d) $Bu^tMe_2SiONH_2$, Et_3N, *n*-BuOH, Δ; (e) HCl(aq), MeOH, Δ; (f) NH_4F, MeCN, H_2O.

2. Results and discussion

2.1. Chemistry

First we looked into methods for selective introduction of a side chain at N-7 on 6-hydroxylamino-9-methylpurine (**2**). Benzyl bromide was used as alkylating agent in these model reactions. Compound **2** was synthesized from the 6-chloropurine **1** by a modified procedure from literature (Scheme 1).[7] In this procedure, hydroxylamine was generated *in situ* by treating $HONH_2$·HCl with an excess of KOH in ethanol. However, we found that excess base resulted in partial hydrolysis of the starting material to give 9-methylhypoxanthine[8] whereby the desired product **2** could only be isolated in ca. 30% yield. When hydroxylamine was generated using exactly equal amounts of $HONH_2$·HCl and KOH, the oxime **2** was produced in 84% yield. We also attempted the substitution with commercially available hydroxylamine in water, but again hydrolysis of the starting material took place. Compound **2** existed as an almost 1:1 mixture of the imino (oxime; shown in Scheme 1) and amino (hydroxylamine) tautomer in DMSO-d_6 at ambient temperature. Benzylation of the oxime **2** resulted in at least three compounds; the desired product **3**, the N^6-benzylated isomer **4** and the dibenzylated compound **5**. Unfortunately we were not able to isolate the ageloxime analog **3** in pure form from this mixture. We have previously shown that a bulky alkoxy group at N^6 prevents alkylation of the exocyclic nitrogen,[6b] and we protected the hydroxyl group in compound **3** with the sterically demanding *tert*-butyldimethylsilyl (TBDMS) group to give the O-silylated derivative **6**. An attempt to synthesize compound **6** from chloropurine **1** by reaction with $Bu^tMe_2SiONH_2$ failed,[9] probably due to decomposition of the hydroxylamine derivate under reaction conditions normally used for similar reactions with alkoxyamines.[4] Compound **6** was selectively benzylated at N-7 and the O-protecting group was easily removed under acidic conditions to give the desired product **3a** in high yield. Unfortunately, acidic deprotection was more complicated when compounds with other N-7 side chains where the targets (*vide infra*), and we searched for other ways to deprotect the benzylpurinium salt **7**. TBAF mediated cleavage turned out to be sluggish and purification of the salt **3** was more complicated. CsF led to quantitative conversion into the target **3**, but removal of inorganic salts from the polar purinium salt **3** turned out to be difficult. NH_4F was initially introduced as an economical alternative to TBAF for cleavage of silyl ethers[10] and is often used for selective cleavage of *tert*-butyldiphenylsilyl ethers in the presence of TBDMS-ethers.[10,11] To our delight we found that the protecting group in compound **7** could be removed by treatment with one equivalent NH_4F in MeCN and water and pure target compound **3b** (bromide) was isolated in high yield after crystallization from MeCN. The reaction proceeded readily at ambient temperatures whereas most known examples of TBDMS ether cleavage using NH_4F have been performed at elevated temperatures (typically 40–75 °C).[12]

Next we synthesized ageloxime analogs **10** with terpenoid side chains on N-7 (Scheme 2). Compounds **10a–c** were easily formed by selective N-7 alkylation employing geranyl bromide, geranylgeranyl bromide or *anti*-copalyl bromide (the latter easily synthesized from commercially available (+)-manool via (+)-copalol/*anti*-copalol).[6a,6b] The N-alkylations could be performed at lower reaction temperatures and shorter reaction times compared to what has been used in related reactions before,[5,6a,6b,6e,6f,13] and in the syntheses of compounds **10b** and **10c** these milder reaction conditions were required in order to avoid unwanted side reactions. When compound **6** was reacted with *anti*-copalyl bromide for only 20 min at ambient temperature, ca. 13% of the desilylated N^6-substituted purine **9c** was formed together with the desired product **8c**. If the reaction mixture was allowed to stir over night, the yield of compound **8c** decreased (23%) and the yield of the by-product **9c** increased (ca. 34%). Also the desilylated product **10c** as well as unidentified compounds were observed. Compounds **9** were probably formed in minor amounts in the syntheses of compounds **8a** and **8b**, but were not isolated.

The N-7 benzylpurinium salt **7** was, as discussed above, quantitatively desilylated when treated with HCl in refluxing methanol for a couple of hours. Unfortunately, acidic deprotection of compounds **8** turned out to be more sluggish. For instance, when the copalyl derivative **8c** was reacted with acid in refluxing methanol for 70 h, the ratio between starting material **8c** and desired product **10c** was ca. 3:7 and minor amounts of an unknown product was observed. However, NH_4F mediated deprotections of compounds **8** gave all targets **10** in quantitative yields.

The structure of the target compound **10c** was established by NMR spectroscopy (Figs. 2 and 3, Table 1). The identity of the heterocyclic

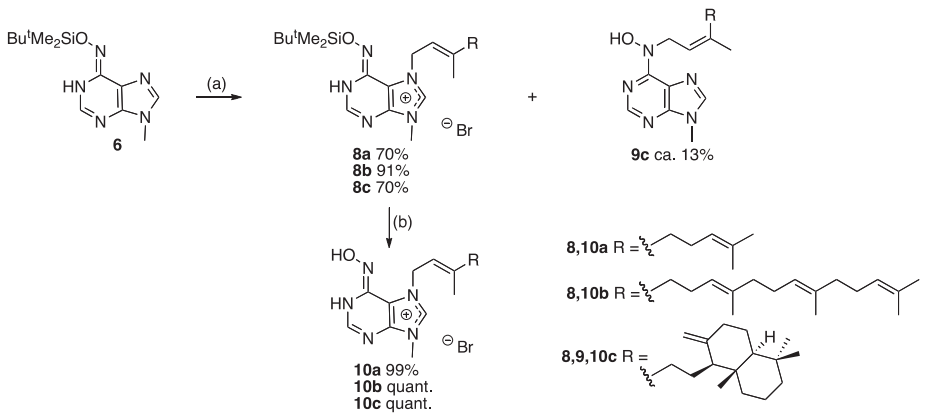

Scheme 2. Reagents and conditions: (a) R-Br, DMA, r.t. or 50 °C; (b) NH_4F, MeCN, H_2O.

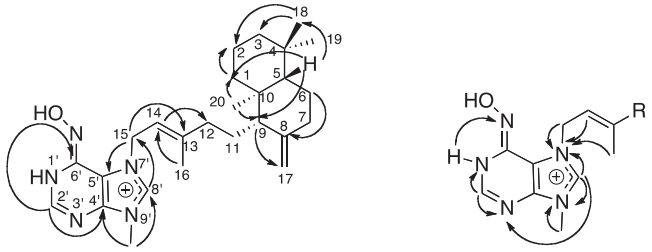

Fig. 2. Key correlations found in the ^{1}H-^{13}C HMBC spectrum (left) and ^{1}H-^{15}N HMBC spectrum (right) of compound **10c**.

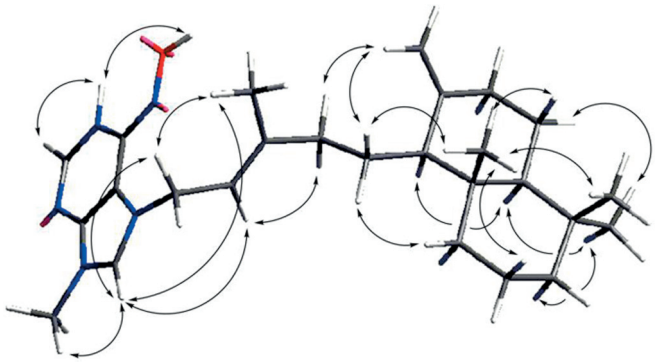

Fig. 3. Key correlations found in the 2D NOESY/1D SELNOE spectra of compound **10c**.

part of the molecule as well as the attachment of the side chains were determined from HMBC (^{1}H-^{13}C as well as ^{1}H-^{15}N) spectroscopy (Fig. 2) and the relative stereochemistry of the terpene side chain was established by 2D NOESY/1D SELNOE (Fig. 3). The heterocyclic NH was found to be localized at N-1 and the ^{13}C and ^{15}N NMR shifts of the atoms in the heterocycle were in good agreement with those reported before for 1*H*-imino tautomers of previously synthesized N^6-alkoxy agelasine analogs.[5,6b] Compounds **6**, **8** and **10** are all drawed as *syn* imines, since calculations and spectroscopic studies have shown the *syn* form of related molecules to be favored over the *anti* form.[14] Furthermore, SELNOE irradiating the NH showed that compound **10c** exists as *syn* imine in DMSO-d_6 (Fig. 3).

However, we were surprised to see that the NMR spectra of compound **10c** did not match those published for (−)-ageloxime D.[3] Literature ^{13}C NMR data (CD_3OD) are included in Table 1 for comparison. It was reported that ageloxime D exists as two tautomers in CD_3OD. Our ^{1}H NMR and ^{13}C NMR spectra of compound **10c** did only show one tautomer and looked substantially different from those published before, especially the signals from the heterocyclic part. One interesting difference was the signals for the purine H-8′/C-8′. The literature reported the H-8′ to appear at 7.95, but we could not see a signal for H-8′ in the CD_3OD ^{1}H NMR spectrum of compound **10c**. This indicated a very acidic proton at this site, being exchanged by deuterium. We also observed a triplet (^{13}C-^{2}H-coupling) for C-8′ in the ^{13}C NMR spectrum, not mentioned in the literature, which supported this observation. The acidity of H-8′ in the proposed imidazolium cation structure was also believed to be quite high. Furthermore, ageloxime B and D were reported to be protonated at N-9 in $CDCl_3$.[2,3] We found protonation of an imidazolium cation quite unlikely in a relatively weak acidic solution, and also that compound **10c** was almost insoluble in $CDCl_3$. Last but not least, the molecular ions reported for ageloxime B and D were *m/z* 440,[2,3] which corresponds to $C_{26}H_{40}N_5O+2$, whereas the molecular ion found for compound **10c** was 438 (M^+).

We suspected that the previously isolated ageloximes were in fact not N^6-hydroxyagelasines. Ageloxime D[2,3] seemed to have the same (enantiomeric) terpene side chain as our compound **10c**, but it was not likely that the heterocyclic parts were identical. Capon et al.[15] isolated formamides **12a** and **12b** (Fig. 4) and stated that they were artifacts formed during silica gel chromatography of crude sponge extracts containing the corresponding ageline A (agelasine F; **11a**) and ageline B (**11b**). Furthermore, they showed that ageline A and B could be converted to the corresponding formamides **12** when treated with aqueous base. Also other agelasines have been hydrolyzed to formamides using this protocol.[16]

Two formamidopyrimidines with terpene side chains, named axistatin 1 and 2 were isolated from the marine sponge *Agelas axifera* Hentschel.[17] The proposed structure of axistatin 2 (**12c**) is shown in Fig. 4. We found the NMR data reported for axistatin 2 and ageloxime B[2] to be essentially identical.* This led us to believe that the previously isolated ageloxime B has the same structure as axistatin 2 and that ageloxime D is the ring opened form of agelasine D. This would explain the molecular ion found for the ageloximes and the coupling between the CH_3N protons and the NH previously explained by N-9 protonation. Furthermore, presence of double NMR signals in CD_3OD could be explained by restricted rotation around the amide bond rather than the presence of two tautomers. The affected protons in the CD_3OD ^{1}H NMR spectrum[3] were those close to the formamide group earlier mistaken to be the purine H-8′. Thus we hydrolized our previously synthesized (+)-agelasine D (**11d**)[6a,6b] and obtained the formamide **12d** (Scheme 3). The spectral data for compound **12d** were identical with those previously reported for (−)-ageloxime D[3] and the optical rotation confirmed that this compound is the enatiomer of the previously reported (−)-ageloxime D. Thus we have also confirmed the absolute stereochemistry of the ageloxime reported by Hertiani et al. who just

* A table with literature NMR data of ageloxime B and axistatin 2 can be found in the Supplementary material.

Table 1
NMR data of compound **10c**. ^{13}C NMR data in CD_3OD reported for ageloxime D is included for comparison.

No.[a]	DMSO-d_6				CD_3OD			
	^{1}H NMR[b]		^{13}C NMR[c]	^{15}N NMR[d]	^{1}H NMR[b]		^{13}C NMR[c]	^{13}C NMR Ageloxime D[3]
	δ	Integration, multiplicity, *J* (Hz)	δ, DEPT		δ	Integration, multiplicity, *J* (Hz)	δ, DEPT	δ
1A, eq[e]	1.65–1.70	1H, m[f]	38.4, CH_2		1.72–1.77	1H, m[f]	40.3, CH_2	40.7
1B, ax[e]	0.88	1H, td, 3.8, 13.0			0.96	1H, td, 3.8, 13.0		
2A, ax[e]	1.48–1.54	1H, m[f]	18.8, CH_2		1.57–1.63	1H, m[f]	20.4, CH_2	20.4
2B, eq[e]	1.41–1.44	1H, m[f]			1.46–1.54	1H, m[f]		
3A, eq[e]	1.34	1H, br d, 12.9	41.6, CH_2		1.39–1.41	1H, m[f]	43.3, CH_2	43.3
3B, ax[e]	1.10	1H, td, 4.0, 13.4			1.19	1H, td, 4.0, 13.5		
4			33.2, C				34.5, C	40.2
5	0.99	1H, dd, 2.6, 12.6	54.7, CH		1.05	1H, dd, 2.7, 12.6	57.0, CH	56.8
6A, eq[e]	1.65–1.70	1H, m[f]	23.9, CH_2		1.72–1.77	1H, m[f]	25.6, CH_2	25.6
6B, ax[e]	1.22	1H, dq, 4.2, 12.9			1.31	1H, dq, 4.2, 12.9		
7A, eq[e]	2.33	1H, ddd, 3.4, 4.0, 12.7	37.6, CH_2		2.36	1H, ddd, 3.4, 4.0, 12.7	39.4, CH_2	39.4
7B, ax[e]	1.83–1.88	1H, m[f]			1.88	1H, ddd, 5.0, 13.0, 13.0		
8			148.0, C				149.7, C	149.8
9	1.48–1.54	1H, m[f]	55.1, CH		1.57–1.64	1H, m[f]	57.1, CH	58.3
10			39.2, C				40.7, C	34.5
11A	1.54–1.59	1H, m[f]	20.9, CH_2		1.65–1.70	1H, m[f]	22.5, CH_2	41.6
11B	1.41–1.44	1H, m[f]			1.46–1.54	1H, m[f]		
12A	2.11	1H, ddd, 4.0, 9.4, 14.0	37.7, CH_2		2.23	1H, ddd, 4.3, 9.1, 14.0	39.2, CH_2	25.6
12B	1.83–1.88	1H, m[f]			1.96	1H, dt, 8.1, 14.0		
13			144.1, C				147.2, C	145.4/144.4[g]
14	5.37	1H, qt, 1.0, 7.2	116.5, CH		5.43	1H, qt, 1.0, 7.2	117.4, CH	117.9/118.4
15A	4.98	1H, dd, 7.2, 14.8	47.1, CH_2		5.01–5.10	2H, m	49.0, CH_2	45.9/41.6
15B	4.94	1H, dd, 7.2, 14.8						
16	1.76	3H, d, 1.0	16.7, CH_3		1.84	3H, d, 1.0	17.0, CH_3	16.0/16.2
17A	4.81	1H, td, 1.1, 1.5	106.4, CH_2		4.82	1H, q, 1.5	107.0, CH_2	107.0
17B	4.48	1H, br s			4.52	1H, q 1.0		
18	0.83	3H, s	33.3, CH_3		0.87	3H, s	34.1, CH_3	34.1
19	0.75	3H, s	21.5, CH_3		0.81	3H, s	22.1, CH_3	20.4
20	0.61	3H, s	14.3, CH_3		0.69	3H, s	15.0, CH_3	15.1
1′ NH	11.00	1H, br s		−240.0	–[h]			
2′	7.79	1H, s	148.9, CH		7.74	1H, s	149.9, CH	157.7/157.3
3′				−179.5				
4′			140.7, C				142.5, C	161.5/160.6
5′			110.6, C				112.9, C	97.2/99.2
6′			136.9, C				137.9, C	162.0/160.6
6′-NOH	10.58	1H, br s		−105.5	–[h]			
7′				−208.5				
8′	9.26	1H, s	136.7, CH		–[h]		137.3, C[i]	165.9/166.5
9′				−218.5				
9′-CH_3	3.78	3H, s	31.6, CH_3				32.1	28.2

[a] For numbering of the atoms, see Fig. 2.
[b] ^{1}H NMR data were obtained at 600 MHz.
[c] ^{13}C NMR data were obtained at 150 MHz.
[d] ^{15}N NMR data were obtained at 60 MHz.
[e] Equatorial/axial positions in a (double) chair conformation, obtained by 2D NOESY/1D SELNOE.
[f] Unresolved or overlapping.
[g] Double set of signals were observed and explained by tautomery.[3]
[h] Exchangeable H not seen in CD_3OD.
[i] The carbon resonance appeared as a triplet.

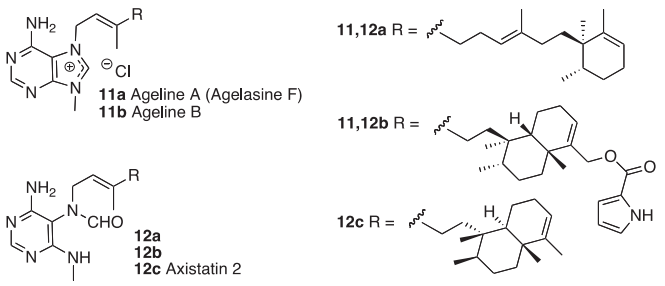

Fig. 4. Structures of agelasines **11** and ring opened derivatives/axistatins **12**.

assumed that the compound they named (−)-ageloxime D would have the same absolute stereochemistry as (−)-agelasine D.[3]

2.2. Biology

Even though the synthetic products **10** turned out not to be *ent*-ageloxime D and analogs, we chose to examine their activities against a variety of microorganisms (Table 2). The geranyl derivative **10a** was essentially inactive against bacteria (*S. aureus*, *Escherichia coli* and *Mycobacterium tuberculosis*) and yeast (*Candida albicans*) and showed only a modest inhibitory activity against protozoa (*Trypanosoma cruzi*, *T. brucei*, *T. rhodesiense* and *Leishmania infantum*). This is in line with our previous findings; a certain size of the lipophilic substituent on N-7 is required for antimicrobial activities of agelasine analogs.[5,18]

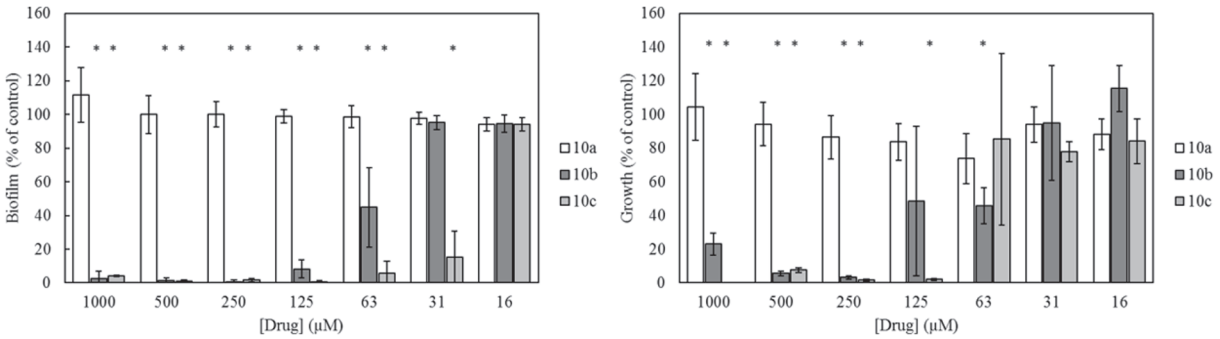

Fig. 5. Effect of compounds **10a**, **10b** and **10c** on biofilm (left) and growth (right) of *S. epidermidis*. Shown are averages and 95% confidence intervals of at least two independent experiments carried out in at least two technical replicates per experiment. * indicates statistical significant difference compared to the control (two-tailed students *t*-test, $p < 0.05$).

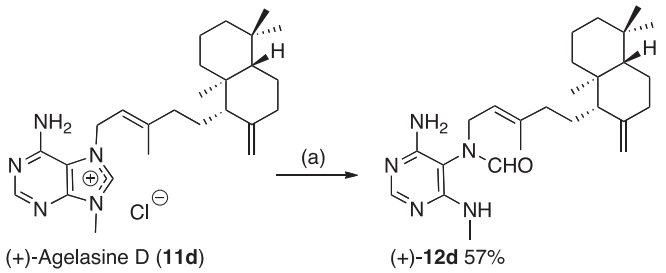

Scheme 3. Reagents and conditions: (a) $NaHCO_3$, H_2O.

Table 2
Antimicrobial activities of compounds **10**.

	Compound **10a**	Compound **10b**	Compound **10c**
S. aureus, IC_{50} (μM)[a]	> 64.0	1.89	1.84
E. coli, IC_{50} (μM)[b]	> 64.0	> 64.0	> 64.0
C. albicans, IC_{50} (μM)[c]	> 64.0	2.00	8.00
T. cruzi, IC_{50} (μM)[d]	11.5	0.54	0.53
T. brucei, IC_{50} (μM)[e]	28.0	2.01	2.01
T. rhodesiense, IC_{50} (μM)[f]	8.06	0.50	0.50
L. infantum IC_{50} (μM)[g]	20.3	2.16	2.38
M. tuberculosis MIC (μg/mL) MABA assay[h]	> 50.0	11.3	3.00
M. tuberculosis MIC (μg/mL) LORA assay[i]	> 50.0	15.3	5.50
MRC-5 IC_{50} (μM)[j]	> 64.0	1.90	1.59

[a] IC_{50} doxycycline 0.03 μM.
[b] IC_{50} doxycycline 0.58 μM.
[c] IC_{50} flucytosine 0.41 μM.
[d] IC_{50} benznidazol 2.69 μM.
[e] IC_{50} suramin 0.02 μM.
[f] IC_{50} suramine 0.03 μM.
[g] IC_{50} miltefosine 11.8 μM.
[h] MIC isoniazid 0.48 μg/mL.
[i] MIC isoniazid > 128 μg/mL.
[j] IC_{50} tamoxifen 11.23 μM.

Compounds **10b** and **10c**, containing larger lipophilic side chains, displayed good to very good activities towards all microorganisms examined except for *E. coli*. The IC_{50} or MIC values are comparable with those found for other agelasine analogs with a diterpenoid side chain. As also seen for related compounds, the N^6-hydroxyagelasine analogs **10b** and **10c** were not only toxic to microorganisms but also to mammalian MRC-5_{sv2} (human lung fibroblast) cells.[5,18]

The activity of compounds **10a**, **10b** and **10c** were also tested against biofilm formation and compared to the effect on growth under the same conditions. Compound **10a** did not have any significant effect on biofilm formation or growth of *S. epidermidis*, *Pseudomonas aeruginosa* or *E. coli*,[19] with the exception of a 50% reduction in biofilm formation for *P. aeruginosa* at the highest concentration tested (1 mM) (Fig. 6). These results correlate with the antibacterial activity of the compounds measured as reduced metabolic activity (Table 2). The N^6-hydroxyagelasine analogs **10b** and **10c** reduced biofilm formation of the Gram-positive bacterium *S. epidermidis* by 90% at 125 μM and 63 μM, respectively. In comparison, growth was reduced by 50% at 125 μM and 15% at 63 μM for **10b** and **10c**, respectively.

For the Gram-negative bacteria *P. aeruginosa* and *E. coli*, the effect on biofilm formation was less pronounced. For *P. aeruginosa* (Fig. 6), compounds **10b** and **10c** only inhibited biofilm formation by 40–50% at 250 μM and reached 60% and 70%, respectively at the highest concentration tested (1 mM). However, growth was only inhibited by 20–30% at this concentration.

Similarly, compounds **10b** and **10c** inhibited biofilm formation of *E. coli* by 70% at 500 μM, but only reduced growth by approximately 20% at this concentration (Fig. 7). These results indicate a small inhibitory effect of compounds **10b** and **10c** on biofilm formation. However, since the inhibition of biofilm formation is accompanied by a reduction in growth, it is not possible to conclude from these experiments whether it is a specific anti-biofilm effect or a more general growth mediated effect. In addition, the results (Table 2 and Fig. 5) suggest that Gram-positive bacteria are more susceptible to the antibacterial effects of the compounds.

3. Conclusions

We have synthesized (+)-N^6-hydroxyagelasine D and other N^6-hydroxyagelasine by selective N-7 alkylation of N^6-[*tert*-butyl(dimethyl) silyloxy]-9-methyl-9*H*-purin-6-amine followed by efficient cleavage of the silyl ether by NH_4F. However, the spectral data of synthetically prepared (+)-N^6-hydroxyagelasine D did not match those reported for the naturally occurring (−)-ageloxime D. Instead we found that when (+)-agelasine D was treated with aqueous base, ring opening of the imidazole ring took place to give a 4-amino-6-(methylamino)pyrimidin-5-ylformamide with spectral data essentially identical to those reported for (−)-ageloxime D before. This led us to propose a revised structure for (−)-ageloxime D. This pyrimidinylformamide may be found in *Agelas* sp. or alternatively the compound is an artifact from isolation of (−)-agelasine D. The work presented herein demonstrates the value of total synthesis in order to prove, or disprove, the structure of natural products.[20] N^6-Hydroxyagelasine analogs carrying a diterpenoid side chain at N-7, displayed toxicity towards both microorganisms as well as mammalian cells. These compounds also inhibited bacterial biofilm formation, but the data indicate that this effect is likely a result of the antibacterial properties of the compounds causing reduced bacterial growth rather than a specific anti-biofilm property.

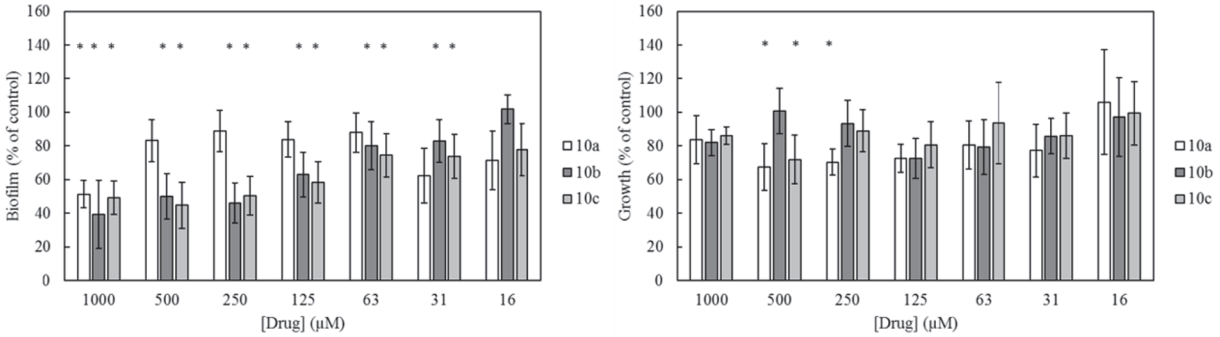

Fig. 6. Effect of compounds **10a**, **10b** and **10c** on biofilm (left) and growth (right) of *P. aeruginosa*. Shown are averages and 95% confidence intervals of at least two independent experiments carried out in at least two technical replicates per experiment. * indicates statistical significant difference compared to the control (two-tailed students *t*-test, $p < 0.05$).

4. Experimental section

4.1. Chemistry

^{1}H NMR spectra were recorded at 600 MHz on a Bruker AV 600 MHz or a Bruker AVII 600 MHz, at 400 MHz on a Bruker AVII 400 instrument. The decoupled ^{13}C NMR spectra were recorded at 150 or 100 MHz using the instruments mentioned above or at 125 MHz on a Bruker AVII 500 MHz. ^{15}N NMR spectra were recorded at 60 or 50 MHz using instruments mentioned above. ^{1}H chemical shift values are calibrated relative to internal CD_2HSOCD_3 at 2.49 ppm, CD_2HOD at 3.30 ppm or $CHCl_3$ at 7.24 ppm. ^{13}C chemical shift values are calibrated relative to internal $(CD_3)_2SO$ at 39.50 ppm, CD_3OD at 49.00 ppm or $CDCl_3$ at 77.00 ppm. ^{15}N chemical shift values are calibrated relative to external CH_3NO_2/DMSO-d_6 (9:1) at 0.00 ppm. Assignments of ^{1}H, ^{13}C and ^{15}N resonances are inferred from 1D ^{1}H NMR, 1D ^{13}C NMR, DEPT or APT, and 2D NMR (COSY, HMQC, HMBC and/or NOESY) spectroscopic data. ESI MS spectra were obtained on a Waters Micromass QTOF 2 W instrument. Melting points were determined on a Büchi Melting Point B-545 apparatus. Dry DMF were obtained from a solvent purification system, MB SPS-800 from MBraun, Garching, Germany. DMA was distilled over BaO prior to use, and *n*-BuOH was distilled over BaO and stored over 3 Å molecular sieves. Triethylamine was distilled from CaH_2 and stored over molecular sieves (3 Å). Flash chromatography was performed on silica gel Merck, Darmstadt, Germany (Merck No. 09385). Compounds available by literature methods: Geranyl bromide,[5a] geranylgeranyl bromide,[5a] 6-chloro-9-methyl-9*H*-purine (**1**),[21] *anti*-copalyl bromide,[6a,6b] (+)-agelasine D (**11d**).[6a,6b]

4.1.1. 6-Hydroxylamino-9-methyl-9H-purine (2)

A warm solution of KOH (3.270 g, 58.28 mmol) in EtOH (abs., 80 mL) was added to a boiling solution of $HONH_2$·HCl (4.035 g, 58.07 mmol) in EtOH (abs., 80 mL). Immediately upon mixing of the two solutions, precipitation of KCl was observed. The resulting mixture was stirred and maintained near the boiling point for an additional 10 min. The hot reaction mixture was filtered and 6-chloro-9-methyl-9*H*-purine (**1**) (1.241 g, 8.027 mmol) in EtOH (abs., 70 mL) was added to the hydroxylamine solution. The resulting solution was kept at reflux for 4 h. The reaction mixture was cooled to ambient temperature and the precipitated product was collected by filtration. The crystals were washed with EtOH (abs., 15 mL) and dried *in vacuo*; yield 992 mg (84%), colorless crystals, mp 233–234 °C. (lit.[8] 244 °C). ^{1}H NMR (400 MHz, DMSO-d_6) δ 10.96, 10.24 (s, 1H, OH taut. A and B), 9.49, 9.00 (s, H, NH taut. A and B), 8.25, 8.11, 7.71, 7.52 (s, 1H, H-2 and H-8, taut A and B), 3.73, 3.62 (br s, 3H, CH_3 taut. A and B); HRMS (ESI) found 166.0732, calcd for $C_6H_8N_5O^+$ 166.0723.

4.1.2. N^6-Benzyl-N^6-hydroxy-9-methyl-9H-purin-6-amine (4) and N^6-benzyl-N^6-benzyloxy-9-methyl-9H-purin-6-amine (5)

Compound **2** (81 mg, 0.49 mmol) was dissolved in dry DMA (8 mL) at ambient temperature under Ar atm before benzyl bromide (0.09 mL, 0.7 mmol) was added. The mixture was stirred at 50 °C for 18 h and evaporated *in vacuo*. The products were separated by flash chromatography eluting with 5–10% MeOH saturated with NH_3 in CH_2Cl_2; yield 13 mg (ca. 11%, contained 1–2 mol% DMA) of compound **4**, purple waxy material, and 29 mg (ca. 16%, contained ca. 17 mol% DMA) of compound **5**, pale greenish oil. **4**; ^{1}H NMR (400 MHz, $CDCl_3$) δ 8.22 (s, 1H, H-2), 7.39 (s, 1H, H-8), 7.49–7.32 (s, 5H, Ph), 6.24 (s, 1H, OH), 5.32 (s, 2H, CH_2), 3.57 (s, 3H, CH_3); MS ESI found 240.2, calcd for $C_{13}H_{14}N_5^+$-OH 240.1. **5**; ^{1}H NMR (400 MHz, $CDCl_3$) δ 8.54 (s, 1H, H-8), 7.85 (s, 1H, H-2), 7.47–7.25 (m, 10*H*, Ph), 5.23 (s, 2H, NCH_2), 5.01 (s, 2H, OCH_2), 3.85 (s, 3H, NCH_3); HRMS (ESI) found 346.1683, calcd for $C_{20}H_{20}N_5O^+$ 346.1662. Spectral data were in good agreement with those reported before.[6b]

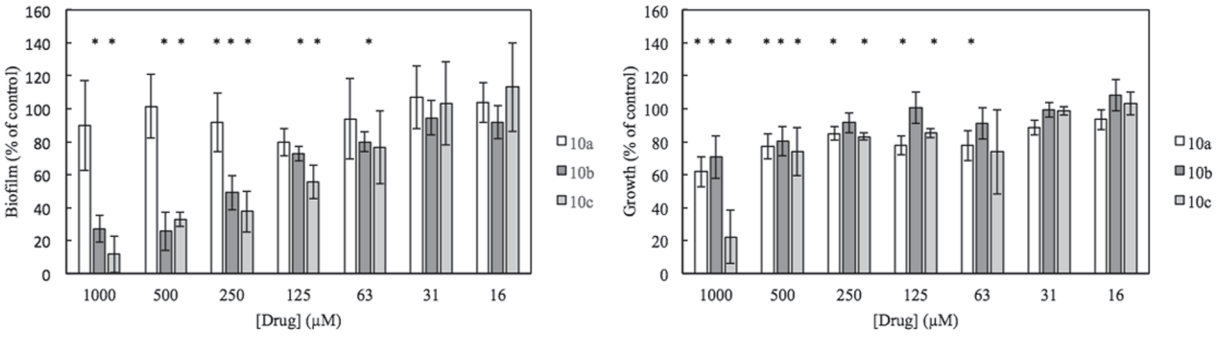

Fig. 7. Effect of compounds **10a**, **10b** and **10c** on biofilm (left) and growth (right) of *E. coli*. Shown are averages and 95% confidence intervals of at least two independent experiments carried out in at least two technical replicates per experiment. * indicates statistical significant difference compared to the control (two-tailed students *t*-test, $p < 0.05$).

*4.1.3. N^6-[tert-Butyl(dimethyl)silyloxy]-9-methyl-9H-purin-6-amine (**6**)*

A mixture of 6-hydroxylamino-9-methyl-9*H*-purine (**2**) (302 mg, 1.94 mmol), imidazole (329 mg, 4.84 mmol) and dry DMF (2.7 mL) was stirred under Ar atm before *tert*-butyldimethylsilyl chloride (307 mg, 2.03 mmol) was added. The reaction mixture was stirred at ambient temperature for 22 h, diluted with EtOAc (150 mL) and washed with water (3 × 30 mL) and brine (40 mL). The organic phase was dried (Na_2SO_4) and evaporated *in vacuo*; yield 317 mg (93%); colorless solid, mp 216–217 °C. ^{1}H NMR (400 MHz, DMSO-d_6) δ 10.91 (br s, 1H, NH), 7.78 (s, 1H, H-8), 7.65 (s, 1H, H-2), 3.64 (s, 3H, NCH_3), 0.95 (s, 9H, Bu^t), 0.15 [s, 6H, $Si(CH_3)_2$]; ^{13}C NMR (100 MHz, DMSO-d_6) δ 144.3 (C-6), 144.1 (C-2), 141.6 (C-4), 138.8 (C-8), 118.1 (C-5), 29.5 (NCH_3), 26.2 (CH_3 in Bu^t), 18.0 (C in Bu^t), −5.0 [$Si(CH_3)_2$]; HRMS (ESI) found 280.1597, calcd for $C_{12}H_{22}N_5OSi^+$ 280.1588.

*4.1.4. 7-Benzyl-6-tert-butyl(dimethyl)silyloxyamino-9-methyl-7H-purinium bromide (**7**)*

Benzyl bromide (0.037 mL, 0.31 mmol) was added to a stirring solution of compound **6** (100 mg, 0.283 mmol) in dry DMA (5 mL) under Ar atm. The resulting mixture was stirred at ambient temperature for 1 h, and at 50 °C for 6 h and evaporated *in vacuo*. The crude product was purified by flash chromatography eluting with 5–10% MeOH in CH_2Cl_2; yield 104 mg (82%), colorless solid, mp 249–251 °C. ^{1}H NMR (400 MHz, DMSO-d_6) δ 11.87 (br s, 1H, NH), 9.33 (s, 1H, H-8), 7.86 (s, 1H, H-2), 7.39–7.34 (m, 5H, Ph), 5.65 (s, 2H, CH_2), 3.79 (s, 3H, NCH_3), 0.89 (s, 9H, Bu^t), 0.08 [s, 6H, $Si(CH_3)_2$]; ^{13}C NMR (100 MHz, DMSO-d_6) δ 148.9 (C-2), 141.4 (C-4), 139.9 (C-6), 138.5 (C-8), 134.5 (C in Ph), 128.7 (CH in Ph), 128.4 (CH in Ph), 127.4 (CH in Ph), 110.6 (C-5), 52.1 (CH_2), 31.9 (NCH_3), 25.9 (CH_3 in Bu^t), 17.9 (C in Bu^t), −5.3 [$Si(CH_3)_2$]; HRMS (ESI) found 370.2057, calcd for $C_{19}H_{28}N_5OSi^+$ 370.2058.

*4.1.5. 7-Benzyl-6-hydroxylamine-9-methyl-9H-purin-7-ium chloride (**3a**)*

Compound **7** (127 mg, 0.283 mmol) was dissolved in methanol (2 mL) and 1 M HCl (aq) (1 drop) was added. The solution was stirred at reflux for 2.5 h, cooled to ambient temperature, washed with hexane (3 × 3 mL) and evaporated *in vacuo*; yield 92 mg (97%); colorless solid, mp 219–222 °C. ^{1}H NMR (400 MHz, DMSO-d_6) δ 11.96 (br s, 1H, NH), 10.65 (s, 1H, OH), 9.39 (s, 1H, H-8), 7.82 (s, 1H, H-2), 7.41–7.37 (m, 5H, Ph), 5.63 (s, 2H, CH_2), 3.81 (s, 3H, NCH_3); ^{13}C NMR (100 MHz, DMSO-d_6) δ 148.9 (C-2), 140.8 (C-4), 137.5 (C-8), 136.6 (C-6), 134.5 (C in Ph), 128.88 (CH in Ph), 128.58 (CH in Ph), 127.92 (CH in Ph), 110.8 (C-5), 51.9 (CH_2), 31.79 (NCH_3); HRMS (ESI) found 256.1193, calcd for $C_{13}H_{14}N_5O^+$ 256.1193.

*4.1.6. 7-Benzyl-6-hydroxylamine-9-methyl-9H-purin-7-ium bromide (**3b**)*

Compound **7** (20.5 mg, 0.0453 mmol) was dissolved in MeCN-H_2O (9:1, 0.5 mL) and transferred to a vial containing NH_4F (1.3 mg, 0.035 mmol). Additional MeCN-H_2O (9:1, 0.5 mL) was used to transfer the starting material to the reaction vial. The clear and colorless solution stirred for 60 min at ambient temperature and was evaporated *in vacuo*. Dry MeCN (2 mL) was added and the resulting heterogeneous mixture was agitated by a spatula for 2 min while gently heating the solution with a heating gun. The crystals were allowed to settle by gravity (2 min) before the MeCN-phase was removed by a glass pipette. This process was repeated once more with MeCN (1 mL). The crystals were dried *in vacuo*; yield 12.7 mg (83% based on the amount of comp. **7**), colorless solid, mp 244–245 °C. Spectral data as reported for the chloride **3a** above.

*4.1.7. 6-(tert-Butyldimethylsilyloxyimino)-7-[(E)-3,7-dimethylocta-2,6-dienyl]-9-methyl-6,9-dihydro-1H-purin-7-ium bromide (**8a**)*

Geranyl bromide (265 mg, 1.12 mmol) was added dropwise over 1 min to a stirring solution of compound **6** (283 mg, 1.02 mmol) in dry DMA (10 mL) under Ar atm. The resulting mixture was stirred at ambient temperature for 10 min and at 50 °C for 18 h and evaporated *in vacuo*. The crude product was purified by flash chromatography eluting with 5–10% MeOH in CH_2Cl_2; yield 348 mg (70%), colorless solid, mp 196–197 °C. ^{1}H NMR (400 MHz, DMSO-d_6) δ 11.90 (br s, 1H, NH), 9.37 (s, 1H, H-8 in purine), 7.92 (s, 1H, H-2 in purine), 5.49–5.46 (m, 1H, H-2), 5.07–5.03 (m, 1H, H-6), 4.97 (d, J = 7.0 Hz, 2H, H-1), 3.81 (s, 3H, NCH_3), 2.10–2.05 (m, 2H, H-5), 2.05–2.01 (m, 2H, H-4), 1.77 (s, 3H, CH_3 at C-3), 1.62 (s, 3H, H-8), 1.54 (s, 3H, CH_3 at C-7), 0.96 (s, 9H, Bu^t), 0.20 [s, 6H, $Si(CH_3)_2$]; ^{13}C NMR (100 MHz, DMSO-d_6) δ 148.8 (C-2 in purine), 143.0 (C-3), 141.2 (C-4 in purine), 140.0 (C-6 in purine), 137.6 (C-8 in purine), 131.2 (C-7), 123.5 (C-6), 116.8 (C-2), 110.1 (C-5 in purine), 47.3 (C-1), 38.9 (C-4), 31.7 (NCH_3), 26.0 (CH_3 in Bu^t), 25.7 (C-5), 25.4 (C-8), 18.0 (C in Bu^t), 17.5 (CH_3 at C-7), 16.5 (CH_3 at C-3), −5.2 [$(Si(CH_3)_2$]; HRMS (ESI) found 416.2840, calcd for $C_{22}H_{38}N_5OSi^+$ 416.2840.

*4.1.8. 6-(tert-Butyldimethylsilyloxyimino)-9-methyl-7-[(2E,6E,10E)-3,7,11,15-tetramethylhexadeca-2,6,10,14-tetraenyl]-6,9-dihydro-1H-purin-7-ium bromide (**8b**)*

Geranylgeranyl bromide (95 mg, 0.27 mmol) was dissolved in dry DMA (3 mL) under Ar atm and compound **6** (68 mg, 0.24 mmol) was added. The resulting mixture was stirred at ambient temperature for 1 h and evaporated *in vacuo*. The crude product was purified by flash chromatography eluting with 5–10% MeOH in CH_2Cl_2; yield 140 mg (91%), colorless solid, mp 170–171 °C. ^{1}H NMR (600 MHz, DMSO-d_6) δ 11.88 (br s, 1H, NH), 9.34 (s, 1H, H-8 in purine), 7.91 (s, 1H, H-2 in purine), 5.46 (qt, J = 7.0 and 1.1, Hz, 1H, H-2), 5.05–5.02 (m, 3H, H-6, H-10, H-14), 4.96 (d, J = 7.0 Hz, 1H, H-1), 3.79 (s, 3H, NCH_3), 2.08–1.96 (m, 8H, H-4, H-5, H-9, H-13), 1.92–1.88 (m, 4H, H-8, H-12), 1.76 (s, 3H, CH_3 at C-3), 1.61 (s, 3H, H-16), 1.53 (s, 6H, CH_3 at C-7 and C-15), 1.52 (s, 3H, CH_3 at C-11) 0.95 (s, 9H, Bu^t), 0.18 [s, 6H, Si $(CH_3)_2$]; ^{13}C NMR (150 MHz, DMSO-d_6) δ 148.7 (C-2 in purine), 143.0 (C-3), 141.2 (C-4 in purine), 139.9 (C-6 in purine), 137.6 (C-8 in purine), 134.8 (C-7), 134.3 (C-11), 130.6 (C-15), 124.0 (C-14), 123.8 (C-10), 123.3 (C-6), 116.7 (C-2), 110.1 (C-5 in purine), 47.2 (C-1), 39.2 (2 × C, C-8 and C-12), 38.9 (C-4), 31.7 (NCH_3), 26.2 (2 × C, C-9 and C-13), 26.0 (CH_3 in Bu^t), 25.6 (C-5), 25.5 (C-16), 18.0 (C in Bu^t), 17.5 (CH_3 at C-15), 16.5 (CH_3 at C-3), 15.8 (2 × C, CH_3 at C-7 and C-11), −5.3 [$(Si(CH_3)_2$]; HRMS (ESI) 552.4090, calcd for $C_{32}H_{54}N_5O^+$ 552.4092.

*4.1.9. (+)-6-(tert-Butyldimethylsilyloxyimino)-9-methyl-7-{(E)-3-methyl-6-[(1S,4aS,8aS)-5,5,8a-trimethyl-2-methylenedecahydronaphthalen-1-yl] hex-2-enyl}-6,7-dihydro-1H-purin-9-ium bromide (**8c**) and (E)-N-{3-methyl-5-[(1S,4aS,8aS)-1,5,5,8a-tetramethyl-2-methylenedecahydronaphthalen-1-yl]pent-2-enyl}-N-(9-methyl-9H-purin-6-yl)hydroxylamine (**9c**)*

anti-Copalyl bromide (93 mg, 0.26 mmol) was dissolved in dry DMA (3.3 mL) under Ar atm and compound **6** (67 mg, 0.24 mmol) was added. The resulting mixture was stirred at ambient temperature for 20 min and evaporated *in vacuo*. The crude product was purified by flash chromatography eluting with 5–10% MeOH in CH_2Cl_2; yield 108 mg (70%) **8c**, colorless solid, and 15 mg (ca. 13%, contained ca. 30 mol% DMA) **9c**, waxy purple solid. **8c**; mp 194–196 °C. ^{1}H NMR (400 MHz, DMSO-d_6) δ 11.89 (s, 1H, NH), 9.36 (s, 1H, H-8 in purine), 7.92 (s, 1H, H-2 in purine), 5.43 (qt, J = 7.2, 1.0 Hz, 1H, H-14), 5.01–4.91 (m, 2H, H-15), 4.79 (s, 1H, H-17_A), 4.47 (s, 1H, H-17_B), 3.80 (s, 3H, NCH_3), 2.32 (ddd, J = 12.7, 4.0, 3.4 Hz, 1H, H-7_A), 2.10 (ddd, J = 14.0, 9.4, 4.0 Hz, 1H, H-12_A), 1.88–1.78 (m, 2H, H-7_B, H-12_B), 1.75 (d, J = 1.0 Hz, 3H, H-16), 1.69–1.63 (m, 2H, H-1_A, H-6_A), 1.56–1.47 (m, 3H, H-11_A, H-2_A, H-9), 1.43–1.39 (m, 2H, H-2_B, H-11_B), 1.35 (br d, 1H, J = 12.9 Hz, H-3_A), 1.22 (dq, J = 12.9, 4.2 Hz, 1H, H-6_B), 1.09 (dt, J = 13.4, 4.0 Hz, 1H, H-3_B), 0.90–1.00 (m, 1H, H-5), 0.95 (s, 9H, Bu^t), 0.82–0.87 (m, 1H, H-1_B), 0.83 (s, 3H, H-18), 0.75 (s, 3H, H-19), 0.61 (s, 3H, H-20), 0.18 [s, 6H, Si $(CH_3)_2$]; ^{13}C NMR (100 MHz, DMSO-d_6) δ 148.8 (C-2 in purine), 147.9 (C-8), 143.7 (C-13), 141.3 (C-4 in purine), 140.0 (C-6 in purine), 137.6 (C-8 in purine), 116.7 (C-14), 110.0 (C-5 in purine), 106.4 (C-17), 55.2 (C-9), 54.8 (C-5), 47.2 (C-15), 41.7 (C-3), 39.1 (C-10), 38.5 (C-1) 37.7

(C-12), 37.6 (C-7), 33.3 (C-18), 33.2 (C-4), 31.7 (NCH_3), 26.0 (CH_3 in Bu^t), 23.9 (C-6), 21.5 (C-19), 20.9 (C-11), 18.8 (C-2), 18.0 (C in Bu^t), 16.7 (C-16), 14.3 (C-20), −5.2 [$Si(CH_3)_2$]; ^{15}N NMR (50 MHz, DMSO-d_6) δ −239.5 (N-1), −218.5 (N-9), −208.5 (N-7), −176.0 (N-3), N^6 was hidden; HRMS (ESI) found 552.4092, calcd for $C_{32}H_{54}N_5OSi^+$ 552.4092, $[\alpha]_D^{25}$ = +4.2 (*c* 0.26 MeOH). **9c**; ^{1}H NMR (600 MHz, DMSO-d_6) *δ* 9.81 (br s, 1H, OH), 8.27 (s, 1H, H-2 in purine), 8.15 (s, 1H, H-8 in purine), 5.27–5.29 (m, 1H, H-14), 4.77–4.81 (m, 1H, H-15$_A$), 4.76 (br s, 1H, H-17$_A$), 4.61–4.65 (m, 1H, H-15$_B$), 4.44 (br s, 1H, H-17$_B$), 3.72 (s, 3H, NCH_3), 2.25 (br d, *J* = 11.7 Hz, 1H, H-7$_A$), 2.01–2.04 (m, 1H, H-12$_A$), 1.71–1.79 (m, 2H, H-12$_B$, H-7$_B$), 1.69 (s, 3H, H-16), 1.58–1.64 (m, 2H, H-1$_A$, H-6$_A$), 1.46–1.52 (m, 2H, H-11$_A$, H-9), 1.29–1.37 (m, 3H, H-2$_B$, H-3$_A$, H-11$_B$), 1.17 (q, *J* = 12.6 Hz, 1H, H-6$_B$), 1.05 (t, *J* = 12.5 Hz, 1H, H-3$_B$), 0.90 (d, *J* = 12.4 Hz, 1H, H-5), 0.81 (s, 3H, H-18), 0.73 (s, 3H, H-19), 0.58 (s, 3H, H-20); ^{13}C NMR (125 MHz, DMSO-d_6) *δ* 155.1 (C-6 in purine), 151.5 (C-2 in purine), 150.7 (C-4 in purine), 148.0 (C-8), 141.3 (C-8 in purine), 138.8 (C-13), 119.2 (C-14), 117.8 (C-5 in purine), 106.2 (C-17), 54.7 (C-9), 54.5 (C-5), 49.7 (C-15), 41.5 (C-3), 39.0 (C-10), 38.3 (C-1), 37.6 (C-12), 37.5 (C-7), 33.2 (C-18), 33.1 (C-4), 29.4 (NCH_3), 23.9 (C-6), 21.5 (C-19), 20.9 (C-11), 18.8 (C-2), 16.4 (C-16), 14.3 (C-20); ^{15}N NMR (50 MHz, DMSO-d_6) δ −229.6 (N-9), −152.2 (N-3), −148.6 (N-1), −136.8 (N-7), N^6 was hidden; HRMS (ESI) found 438.3227, calcd for $C_{26}H_{40}N_5O^+$ 438.3227.

*4.1.10. 7-[(E)-3,7-Dimethylocta-2,6-dienyl]-6-(hydroxyimino)-9-methyl-6,9-dihydro-1H-purin-7-ium bromide (**10a**)*

Compound **8a** (54 mg, 0.11 mmol) was dissolved in MeCN-H_2O (9:1, 1 mL) and transferred to a vial containing NH_4F (4 mg, 0.1 mmol) in MeCN-H_2O (9:1, 1 mL). Additional MeCN-H_2O (9:1, 0.5 mL) was used to transfer the starting material to the reaction vial. The resulting solution was stirred for 22 h at ambient temperature and evaporated *in vacuo*; yield 41 mg (99%), colorless solid, mp 187–188 °C (dec.). ^{1}H NMR (400 MHz, DMSO-d_6) *δ* 11.92 (br s, 1H, NH), 10.62 (s, 1H, OH), 9.22 (s, 1H, H-8 in purine), 7.80 (s, 1H, H-2 in purine), 5.44–5.41 (m, 1H, H-2), 5.08–5.05 (m, 1H, H-6), 4.97 (d, *J* = 7.1 Hz, 2H, H-1), 3.79 (s, 3H, NCH_3), 2.10–2.06 (m, 2H, H-5), 2.04–2.02 (m, 2H, H-4), 1.77 (s, 3H, CH_3 at C-3), 1.62 (s, 3H, H-8), 1.56 (s, 3H, CH_3 at C-7); ^{13}C NMR (100 MHz, DMSO-d_6) *δ* 148.8 (C-2 in purine), 143.5 (C-3), 140.6 (C-4 in purine), 136.7 (C-6 in purine), 131.2 (C-7), 123.5 (C-6), 116.5 (C-2), 110.7 (C-5 in purine), 47.1 (C-1), 38.9 (C-4) 31.6 (NCH_3), 25.7 (C-5), 25.4 (C-8), 17.6 (CH_3 at C-7), 16.5 (CH_3 at C-3); ^{15}N NMR (50 MHz, DMSO-d_6) δ −240.0 (N-1), −218.4 (N-9), −209.2 (N-7), −179.4 (N-3), −105.5 (N^6); HRMS (ESI) found 302.1975, calcd for $C_{16}H_{24}N_5O^+$ 302.1975.

*4.1.11. 6-(Hydroxyimino)-9-methyl-7-[(2E,6E,10E)-3,7,11,15-tetramethylhexadeca-2,6,10,14-tetraenyl]-6,9-dihydro-1H-purin-7-ium bromide (**10b**)*

Compound **8b** (118 mg, 0.19 mmol) was dissolved in MeCN-H_2O (9:1, 4 mL) and NH_4F (6.9 mg, 0.19 mmol) was added as a powder. The vial previously containing NH_4F was rinsed with MeCN-H_2O (9:1, 2 mL). The resulting solution was stirred for 40 min and evaporated *in vacuo*; yield 99 mg (> 99%), colorless solid, mp 188–189 °C. ^{1}H NMR (600 MHz, DMSO-d_6) *δ* 11.70 (br s, 1H, NH), 9.25 (s, 1H, H-8 in purine), 7.78 (s, 1H, H-2 in purine), 5.41 (qt, *J* = 7.1, 1.1 Hz, 1H, H-2), 5.03–5.08 (m, 3H, H-6, H-10, H-14), 4.97 (d, *J* = 7.1 Hz, 1H, H-1), 3.78 (s, 3H, NCH_3), 2.10–2.07 (m, 2H, H-5), 2.05–2.02 (m, 2H, H-4), 2.00–1.96 (m, 4H, H-9, H-13), 1.91–1.89 (m, 4H, H-8, H-12), 1.77 (s, 3H, CH_3 at C-3), 1.62 (s, 3H, H-16), 1.54 (s, 3H, CH_3 at C-7), 1.53 (s, 3H, CH_3 at C-15), 1.52 (s, 3H, H-18); ^{13}C NMR (125 MHz, DMSO-d_6) *δ* 148.9 (C-2 in purine), 143.5 (C-3), 140.7 (C-4 in purine), 136.8 (C-6 in purine), 136.7 (C-8 in purine), 134.8 (C-7), 134.3 (C-11), 130.6 (C-15), 124.1 (C-14), 123.8 (C-10), 123.4 (C-6), 116.5 (C-2), 110.7 (C-5 in purine), 47.1 (C-1), 39.2 (C-12), 39.1 (C-8), 38.9 (C-4), 31.6 (NCH_3), 26.2 (C-13), 26.0 (C-9), 25.6 (C-5), 25.5 (C-16), 17.5 (CH_3 at C-15), 16.6 (CH_3 at C-3), 15.8 (CH_3 at C-7), 15.7 (CH_3 at C-11); ^{15}N NMR (50 MHz, DMSO-d_6) δ −239.9 (N-1), −218.4 (N-9), −208.7 (N-7), −178.5 (N-3), −105.5 (N^6); HRMS (ESI) 438.3226, calcd for $C_{26}H_{40}N_5O^+$ 438.3227.

*4.1.12. (+)-6-(Hydroxyimino)-9-methyl-7-{(E)-3-methyl-6-[(1S,4aS,8aS)-5,5,8a-trimethyl-2-methylenedecahydronaphthalen-1-yl]hex-2-enyl}-6,7-dihydro-1H-purin-9-ium bromide [(+)-N^6-Hydroxyagelasine D bromide, **10c**]*

Compound **8c** (108 mg, 0.171 mmol) was dissolved in MeCN-H_2O (9:1, 3 mL) and NH_4F (6.3 mg, 0.17 mmol) was added as a powder. The vial previously containing NH_4F was rinsed with MeCN-H_2O (9:1, 2 mL). The resulting solution was stirred for 1 h 30 min and evaporated *in vacuo*; yield 88.5 mg (> 99%), colorless solid, mp 188–189 °C. ^{1}H NMR, ^{13}C NMR and ^{15}N NMR data are presented in Table 1. HRMS (ESI) found 438.3228, calcd for $C_{26}H_{40}N_5O^+$ 438.3227; $[\alpha]_D^{20}$ = +6.2 (*c* 0.26 MeOH).

*4.1.13. N-[4-Amino-6-(methylamino)pyrimidin-5-yl]-N-{(E)-3-methyl-5-[(1S,4aS,8aS)-5,5,8a-trimethyl-2-methylenedecahydronaphthalen-1-yl]pent-2-enyl}formamide (**12d**)*

(+)-Agelasine D (**11d**) (25 mg, 0.050 mmol) was treated with 2 M $NaHCO_3$ solution (12.5 mL) for 20 min at ambient temperature, before the mixture was extracted with CH_2Cl_2 (3 × 50 mL), and evaporated *in vacuo*. The crude product was purified by flash chromatography eluting with 2–10% MeOH in CH_2Cl_2. Due to a low yield, the extraction was performed a second time on the basic water solution with CH_2Cl_2 (2 × 4 mL) yielding more product; total yield 13 mg (57%), pale yellow waxy solid. ^{1}H NMR (600 MHz, $CDCl_3$) *δ* 8.14 (s, 1H, H-2 in pyrimidine), 7.95 (s, 1H, NCHO), 5.30 (t, *J* = 7.7 Hz, 1H, H-14), 4.95 (br s, 2H, NH_2), 4.87 (br s, 1H, NH), 4.79 (s, 1H, H-17$_A$), 4.40 (s, 1H, H-17$_B$), 4.14–4.12 (m, 2H, H-15), 2.98–2.96 (m, 3H, NCH_3), 2.37–2.34 (m, 1H, H-7$_A$), 2.12–2.07 (m, 1H, H-12$_A$), 1.92 (ddd, *J* = 14.0, 13.4, 4.8 Hz, 1H, H-7$_A$), 1.76–1.67 (m, 3H, H-6$_A$, H-1$_A$, H-12$_B$), 1.60 (d, *J* = 5.0 Hz, 3H, H-16), 1.55–1.44 (m, 4H, H-9, H-11$_A$, H-2$_A$, H-2$_B$), 1.38–1.36 (m, 1H, H-3$_A$), 1.34–1.25 (m, 2H, H-11$_B$, 1H, H-6$_B$), 1.15 (ddd, *J* = 13.5, 13.4, 4.1 Hz, 13.4, 1H, H-3$_B$), 1.04 (dd, *J* = 12.7, 2.6 Hz, 1H, H-5), 0.93–0.96 (m, 1H, H-1$_B$), 0.85 (s, 3H, H-18), 0.77 (s, 3H, H-19), 0.64 (s, 3H, H-20); ^{13}C NMR (125 MHz, $CDCl_3$) *δ* 164.3 (NCHO), 160.5 (C-4 in pyrimidine), 158.9 (C-6 in pyrimidine), 156.4 (C-2 in pyrimidine), 148.5 (C-8), 144.2 (C-13), 117.0 (C-14), 106.2 (C-17), 99.3 (C-5 in pyrimidine), 56.4 (C-9), 55.5 (C-5), 42.1 (C-3), 41.4 (C-15), 39.7 (C-10), 39.1 (C-1), 38.6 (C-12), 38.3 (C-7), 33.6 (2×C, C-4, C-18), 28.1 (NCH_3), 24.4 (C-6), 21.9 (C-11), 21.7 (C-19), 19.4 (C-2), 16.4 (C-16), 14.5 (C-20); HRMS (ESI) found 440.3385, calcd for $C_{26}H_{42}N_5O^+$ 440.3384; $[\alpha]_D^{25}$ = +5.6 (*c* 0.50 MeOH). The spectral data and absolute value for optical rotation were in good agreement with those reported for (−)-ageloxime D before.[3]

4.2. Biology

4.2.1. Activity against M. tuberculosis

MICs against replicating and non-replicating *M. tuberculosis* H37Rv were determined using the Microplate Alamar Blue Assay and Low Oxygen Recovery Assay, respectively.[22]

4.2.2. Activity against S. aureus, E. coli, C. albicans, L. infantum, T. cruzi, T. brucei, T. rhodesiense and MRC-5 cells

4.2.2.1. Compounds and reagents. Compounds stock solutions were prepared in 100% DMSO at 20 mM. The compounds were serially pre-diluted (2-fold or 4-fold) in DMSO followed by a further dilution in demineralized water to assure a final in-test DMSO concentration of < 1%.

4.2.2.2. Bacteria, fungi, parasite and cell cultures. *S. aureus* ATCC6538 and *E. coli* ATCC8739 were cultured in MHT (Mueller Hinton Broth) and maintained on TSA (Tryptone Soy Agar). *C. albicans* (azole

resistant) was cultured in RPMI-1640 medium supplemented with Mops buffer and glucose and maintained on PDA (Potato Dextrose Agar). *L. infantum* MHOM/MA(BE)/67 was maintained in the golden hamster. Amastigotes were collected from the spleen of an infected donor hamster using three centrifugation purification steps and spleen parasite burdens are assessed using the Stauber technique.[23] Primary peritoneal mouse macrophages were used as host cell and were collected 2 days after peritoneal stimulation with 2% potato starch suspension. *T. cruzi*, Tulahuen CL2 galactosidase strain (nifurtimox-sensitive),[24] was maintained on MRC-5_{sv2} (human lung fibroblast) cells in MEM medium, supplemented with 200 mM L-glutamine, 16.5 mM $NaHCO_3$, and 5% inactivated fetal calf serum. *T. b. brusei* Squib 427 strain (suramine-sensitive) *and T. b. rhodesiense* STIB-900 strain were maintained in Hirumi (HMI-9) medium, supplemented with 10% inactivated fetal calf serum. MRC-5_{sv2} cells were cultured in MEM + Earl's salts-medium, supplemented with L-glutamine, $NaHCO_3$, and 5% inactivated fetal calf serum. All cultures were conducted at 37 °C under an atmosphere of 5% CO_2.

4.2.2.3. Activity against S. aureus, E. coli, C. albicans and MRC-5 cells. The assays were performed at 37 °C in sterile 96-well microtiter plates, each well containing the aqueous compound (10 µL) dilution together with bacterial/fungal/MRC-5 inoculum (190 µL; 5×10^3 CFU/mL). The MRC-5 assay was performed under an atmosphere of 5% CO_2. The compounds were tested at 64, 16, 4, 1 and 0.25 µM. Bacterial/fungal/MRC-5 growth was compared to untreated-control wells (100% growth) and medium-control wells (0% cell growth). After 17 h (*S. aureus* and *E. coli*), 24 h (*C. albicans*) or 3 days (MRC-5) incubation, viability was assessed fluorimetrically after addition of resazurin. After 0.5 h (*S. aureus, E. coli* and *C. albicans*) or 4 h (MRC-5) at 37 °C, fluorescence was measured (λ_{ex} 550 nm, λ_{em} 590 nm). The results are expressed as % reduction in growth/viability compared to control wells and an IC_{50} (50% inhibitory concentration) was calculated. Doxycycline was used as positive control for *S. aureus* and *E. coli*, flucytosine for *C. albicans* and tamoxifen for MRC-5 cells.

4.2.2.4. Activity against L. infantum. The assay was performed at 37 °C under an atmosphere of 5% CO_2 in sterile 96-well microtiter plates, each well containing the aqueous compound (10 µL) dilution together with macrophage/parasite inoculum (190 µL; $3{\cdot}10^4$ cells + $4.5{\cdot}10^5$ parasites/well). The inoculum was prepared in RPMI-1640 medium, supplemented with 200 mM L-glutamine, 16.5 mM $NaHCO_3$, and 5% inactivated fetal calf serum. The macrophages were infected after 48 h and the compounds were added after 2 h of infection. The compounds were tested at 64, 16, 4, 1 and 0.25 µM. Parasite multiplication was compared to untreated-infected controls and uninfected controls. After 5 days, parasite burdens (number of amastigotes/macrophage) were microscopically assessed after staining with a 10% Giemsa solution. The results were expressed as % reduction in parasite burden compared to control wells and an IC_{50} was calculated. Miltefosine was used as positive control.

4.2.2.5. Activity against T. cruzi. The assay was performed at 37 °C under an atmosphere of 5% CO_2 in sterile 96-well microtiter plates, each well containing the aqueous compound (10 µL) dilution together with MRC-5 cell/parasite inoculum (190 µL; $4{\cdot}10^3$ cells/well + $4{\cdot}10^4$ parasites/well). The compounds were tested at 64, 16, 4, 1 and 0.25 µM. Parasite growth was compared to untreated-infected controls and uninfected controls. After 7 days incubation, parasite burdens were assessed after adding the substrate CPRG [chlorophenolred β-D-galactopyranoside; 50 µL/well of a solution of CPRG (15.2 mg) and Nonidet (250 µL) in PBS (100 mL)]. The color change was measured spectrophotometrically at 540 nm after 4 h. The results were expressed as % reduction in parasite burden compared to control wells and an IC_{50} was calculated. Benznidazole was used as positive control.

4.2.2.6. Activity against T. brucei, and T. rhodesiense. The assay was performed at 37 °C under an atmosphere of 5% CO_2 in sterile 96-well microtiter plates, each well containing the aqueous compound (10 µL) dilution together with the parasite suspension [190 µL; 1.5×10^3 parasites/well (*T. brucei*) or 4×10^3 parasites/well (*T. rhodesiense*)]. The compounds were tested at 64, 16, 4, 1 and 0.25 µM. Parasite growth was compared to untreated-infected controls and uninfected controls. After 3 days incubation, parasite growth was assessed fluorimetrically after addition of resazurin [50 µL; 50 µg/mL in phosphate buffer] to each well. After 6 h (*T. rhodesiense*) or 24 h (*T. brucei*) at 37 °C, fluorescence was measured (λ_{ex} 550 nm, λ_{em} 590 nm). The results were expressed as % reduction in parasite growth/viability compared to control wells and an IC_{50} was calculated. Suramin was used as positive control.

4.2.3. Activity against biofilm formation of S. epidermidis, E. coli and P. aeruginosa.

Biofilm assays were optimized for each of the strains: *E. coli* (2006-22-1153-55-2),[19] *P. aeruginosa* (CCUG 56489) and *S. epidermidis* (ATCC 35984). The biofilm assays were performed in 96-well microtiter plates under ambient atmosphere in Brain Heart Infusion (BHI) medium (BD Biosciences) at 37 °C for 17 h (*S. epidermidis* and *P. aeruginosa*) or in LB broth without salt [LB^-; Yeast extract (10 g/L), Tryptone (5 g/L)] at 28 °C for 24 h (*E. coli*). Bacteria were grown overnight in shaken preculture (200 rpm) in BHI broth (*S. epidermidis, P. aeruginosa*) or LB broth (*E. coli*). For the biofilm assays, bacteria were diluted 1:100 in the indicated medium to give an approximate starting OD_{600} of 0.025. Two-fold serially diluted test compounds were added to the wells and biofilms were grown for the indicated optimized times before the medium was removed, the wells were washed 2 times with 0.9% NaCl solution and the biofilms were stained with safranin (0.1%) for 20 min. Following staining, the wells were washed 3 times with 0.9% NaCl solution and the biofilms were dissolved in 30% acetic acid for 10 min. Absorbance was measured at 530 nm using a Citation 3 Multi Cell Imaging Multi-Mode Reader (BioTek Instruments). Growth was recorded by measuring the OD_{600} of 50 µL of the growth medium. All experiments were performed at least three times and each condition was tested in duplicates in each experiment. In each experiment, the absorbance values were normalized against the untreated control sample and the effect of the different test compounds were reported as average percent biofilm formation compared to the untreated control with 95% confidence intervals.

Acknowledgments

The Norwegian Research Council is gratefully acknowledged for financial support (Grant No. 209330) to BP and for partly financing the NMR instruments used.

Appendix A. Supplementary data

Supplementary data to this article can be found online at https://doi.org/10.1016/j.bmc.2019.01.002.

References

1. (a) For reviews on agelasines and other terpene-adenine hybrids, see for instance: Gundersen L-L. Synthesis and biological activities of marine terpene-adenine hybrids and synthetic analogs. *Phytochem Rev.* 2013;12:467–486;

   (b) García PA, Valles E, Díez D, Castro MÁ. Marine alkylpurines: a promising group of bioactive marine natural products. *Mar Drugs.* 2018;16:6–37.
2. Yang F, Hamann MT, Zou Y, et al. Antimicrobial metabolites from the Paracel Islands sponge Agelas mauritania. *J Nat Prod.* 2012;75:774–778.
3. Hertiani T, Edrada-Ebel R, Ortlepp S, et al. From anti-fouling to biofilm inhibition: new cytotoxic secondary metabolites from two Indonesian Agelas sponges. *Bioorg Med Chem.* 2010;18:1297–1311.
4. Algburi A, Comito N, Kashtanov D, Dicks LMT. Control of biofilm formation:

antibiotics and beyond. *Appl Environ Microbiol.* 2017;83:e02508–16 and references therein.

5. (a) Bakkestuen AK, Gundersen L-L, Petersen D, Utenova BT, Vik A. Synthesis and antimycobacterial activity of agelasine E and analogs. *Org Biol Chem.* 2005;3:1025–1033;

   (b) Vik A, Hedner E, Charnock C, et al. Antimicrobial and cytotoxic activity of agelasine and agelasimine analogs. *Bioorg Med Chem.* 2007;15:4016–4037;

   (c) Proszenyák Á, Charnock C, Hedner E, Larsson R, Bohlin L, Gundersen L-L. Synthesis and antimicrobial and antineoplastic activities of agelasine and agelasimine analogs with a β-cyclocitral derived substituent. *Arch Pharm Chem Life Sci.* 2007;340:625–634.
6. (a) Utenova BT, Gundersen L-L. Synthesis of (+)-agelasine D from (+)-manool. *Tetrahedron Lett.* 2004;45:4233–4235;

   (b) Vik A, Hedner E, Charnock C, Samuelsen Ø, Larsson R, Gundersen L-L, Bohlin L. (+)-Agelasine D: improved synthesis and evaluation of antibacterial and cytotoxic activities. *J Nat Prod.* 2006;69:381–386;

   (c) Vik A, Gundersen L-L. Synthetic studies directed towards asmarines; construction of the tetrahydrodiazepinopurine moiety by ring closing metathesis. *Tetrahedron Lett.* 2007;48:1931–1934;

   (d) Roggen H, Gundersen L-L. Synthetic studies directed towards agelasine analogs. synthesis, tautomerism, and alkylation of 2-substituted N-methoxy-9-methyl-9H-purin-6-amines. *Eur J Org Chem.* 2008:5099–5106;

   (e) Proszenyák Á, Brændvang M, Charnock C, Gundersen L-L. The first synthesis of ent-Agelasine F. *Tetrahedron.* 2009;65:194–199;

   (f) Roggen H, Charnock C, Burman R, Felth J, Larsson R, Bohlin L, Gundersen L-L. Antimicrobial and antineoplastic activities of agelasine analogs modified in the purine 2-position. *Arch Pharm Chem Life Sci.* 2011;344:50–55;

   (g) Chamgordani EJ, Paulsen J, Gundersen L-L. Selective N-alkylation of 3-methyl-hypoxanthine; the first synthesis of malonganenone. *J Tetrahedron Lett.* 2016;57:4926–4929;

   (h) Hennum M, Odden HH, Gundersen L-L. Rearrangement reactions leading to optically active α, α-disubstituted primary allylamines. *Eur J Org Chem.* 2017:846–860
   (i) Wåhlander J, Amedjkouh M, Gundersen L-L. Synthesis directed towards trans-clerodanes employing an exo-selective Diels Alder reaction as a key-step, Monatsh Chem; In press. doi:10.1007/s00706-018-2277-9.
7. Giner-Sorolla A, O'Bryant S, Burchenal JH, Bendich A. The synthesis and properties of substituted 6-hydroxylaminopurines. *Biochemistry.* 1966;5:3057–3060.
8. NMR data matched those reported before: Ogawa K, Nishii M, Nohara F, Saito T, Itaya T, Fujii T, Purines LI. Synthesis and biological activity of hypoxanthine 7-N-oxide and related compounds. *Chem Pharm Bull.* 1992;40:612–616.
9. Vik A. *Synthetic Studies Directed towards Bioactive Purine-Containing Marine Natural Products and Analogs.* Dissertation for the degree of PhD University of Oslo; 2007.
10. Zhang W, Robins MJ. Removal of silyl protecting groups from hydroxyl functions with ammonium fluoride in methanol. *Tetrahedron Lett.* 1992;33:1177–1180.
11. (a) For some recent examples, see for instance: Yadav JS, Dutta P. Total synthesis of a diacetonide derivative of thuggacin A. *J Org Chem.* 2016;81:1786–1797;

    (b) Cui J, Watanabe T, Shibasaki M. Catalytic asymmetric synthesis of key intermediate for scytophycin C. *Tetrahedron Lett.* 2016;57:446–448;

    (c) Maity S, Kanikarapu S, Marumudi K, Kunwar AC, Yadav JS, Mohapatra DK. Asymmetric total tynthesis of the putative structure of diplopyrone. *J Org Chem.* 2017;82:4561–4568.
12. (a) For some recent examples, see for instance: Tatani K, Hiratochi M, Kikuchi N, Kuramochi Y, Watanabe S, Yamauchi Y, Itoh F, Isaji M, Shuto S. Identification of adenine and benzimidazole nucleosides as potent human concentrative nucleoside transporter 2 Inhibitors: potential treatment for hyperuricemia and gout. *J Med Chem.* 2016;59:3719–3731;

    (b) Barbie P, Kazmaier U. Total synthesis of cyclomarins A, C and D, marine cyclic peptides with interesting anti-tuberculosis and anti-malaria activities. *Org Biomol Chem.* 2016;14:6036–6054;

    (c) Line NJ, Burns AC, Butler SC, Casbohm J, Forsyth CJ. Total synthesis of (−)-salvinorin A. *Chem Eur J.* 2016;22:17983–17986;

    (d) Yang W, Ma H, Yang Q, Wang J, Liu Y, Yang Q, Wu J, Song C, Chang J. The first example of palladium-catalyzed cascade amidine arylation–intramolecular ester amidation for the synthesis of hypoxanthines: application to the synthesis of 8-aza-nebularine analogues. *Org Biomol Chem.* 2017;15:379–386;

    (e) Soeberdt M, Molenveld P, Storcken RPM, Bouzanne des Mazery R, Sterk GJ, Autar R, Bolster MG, Wagner C, Aerts SNH, van Holst FR, Wegert A, Tangherlini G, Frehland B, Schepmann D, Metze D, Lotts T, Knie U, Lin KY, Huang T-Y, Lai C-C, Staender S, Wuensch B, Abels C. Design and synthesis of enantiomerically pure decahydroquinoxalines as potent and selective κ-opioid receptor agonists with anti-inflammatory activity in vivo. *J Med Chem.* 2017;60:2526–2551;

    (f) Zgani I, Idriss H, Barbot C, Djedaïni-Pilard F, Petit S, Hubert-Roux M, Estour F, Gouhier GJ. Positive variation of the MRI signal via intramolecular inclusion complexation of a C-2 functionalized β-cyclodextrin. *Org Biomol Chem.* 2017;15:564–569;

    (g) Ejlersen M, Langkjær N, Wengel J. 3'-Pyrene-modified unlocked nucleic acids: synthesis, fluorescence properties and a surprising stabilization effect on duplexes and triplexes. *Org Biomol Chem.* 2017;15:2073–2085;

    (h) Sakamoto K, Hakamata A, Tsuda M, Fuwa H. Total Synthesis and Stereochemical Revision of Iriomoteolide-2a. *Angew Chem Int Ed.* 2018;57:3801–3805.
13. (a) Iio H, Asao K, Tokoroyama T. Syntheses of agelasin. *B and its analogues. Chem Commun.* 1985:774–775;

    (b) Piers E, Roberge JY. Total syntheses of the diterpenoids (−)-kolavenol and (−)-agelasine B. *Tetrahedron Lett.* 1992;33:6923–6926;

    (c) Piers E, Livain Breau M, Han Y, Plourde GL, Yeh W-L. Total synthesis of cis-clerodane diterpenoids: (−)-Agelasine A and (+)-(3R,4S,5R,8S,9R,10S)-3,4-epoxyclerod-13-en-15,16-olide. *J Chem Soc Perkin Trans.* 1995;1:963–966;

    (d) Marcos IS, García N, Sexmero MJ, Basabe P, Díez D, Urones JG. Synthesis of (+)-agelasine C. *Struct Rev Tetrahedron.* 2005;61:11672–11678.
14. Gundersen L-L, Görbitz CH, Neier L, Roggen H, Tamm T. X-ray structure and calculated tautomeric equilibria in 2-substituted N-methoxy-9-methyl-9H-purin-6-amines. *Theor Chem Acc.* 2011;129:349–358.
15. Capon RJ, Faulkner DJ. Antimicrobial metabolites from a Pasific sponge, Agelas sp. *J Am Chem Soc.* 1984;106:1819–1822.
16. (a) Cullen E, Devlin JP. Agelasine: A novel quarternary 9-methyladenine from the sponge Agelas dispar. *Can J Chem.* 1975;53:1690–1691;

    (b) Wu H, Nakamura H, Kobayashi J, Kobayashi M, Ohizumi Y, Hirata Y. Structures of agelasines, diterpenes having a 9-methyladeninium chromophore isolated from the Okinawan marine sponge Agelas nakamurai Hoshino. *Bull Chem Soc Jpn.* 1986;59:2495–2504;

    (c) Ishida K, Ishibashi M, Shigemori H, Sasaki T, Kobayashi J, Agelasine G. a new antileukemic alkaloid from the Okinawan marine sponge Agelas sp. *Chem Pharm Bull.* 1992;40:766–767.
17. Pettit GR, Tang Y, Zhang Q, et al. Isolation and structures of axistatins 1–3 from the Republic of Palau marine sponge Agelas axifera Hentschel. *J Nat Prod.* 2013;76:420–424.
18. Vik A, Proszenyák Á, Vermeersch M, Cos P, Maes L, Gundersen L-L. Screening of agelsine D and analogs for inhibitory activity against pathogenic protozoa; identification of hits for treatment of visceral leishmaniasis and Chagas disease. *Molecules.* 2009;14:279–288.
19. Nesse LL, Sekse C, Berg K, et al. Potentially pathogenic Escherichia coli can form a biofilm under conditions relevant to the food production chain. *Appl Environ Microbiol.* 2014;80:2042–2049.
20. Chhetri BK, Lavoie S, Sweeney-Jones AM, Kubanek J. Recent trends in the structural revision of natural products. *Nat Prod Rep.* 2018;35:514–531 and references therein.
21. Elion GB. Condensed pyrimidine systems. XXII. N-methylpurines. *J Org Chem.* 1958;27:2478–2491.
22. Cho S, Lee HS, Franzblau S. Microplate alamar blue assay (MABA) and low oxygen recovery assay (LORA) for mycobacterium tuberculosis. *Methods Mol Biol.* 2015;1285:281–292.
23. Stauber LA. Characterization of strains of Leishmania donovani. *Exp Paracitol.* 1966;18:1–11.
24. Buckner FS, Verlinde CL, La Flamme AC, Van Voorhis WC. Efficient technique for screening drugs for activity against Trypanosoma cruzi using parasites expressing beta-galactosidase. *Antimicrob Agents Chemother.* 1996;40:2592–2597.

Paper 2

The first synthesis of (–)-agelasine F; an antimycobacterial natural product found in marine sponges in the Agelas genus.

Paulsen, B. Gundersen, L-L. (In press)

The first synthesis of (–)-agelasine F; an antimycobacterial natural product found in marine sponges in the *Agelas* genus

Britt Paulsen,[a] and Lise-Lotte Gundersen*[a]

[a] Ms B. Paulsen, Prof. L.-L. Gundersen
Department of Chemistry, University of Oslo
P. O. Box 1033, Blindern, N-0315 Oslo, Norway
E-mail: l.l.gundersen@kjemi.uio.no

Supporting information for this article is given via a link at the end of the document.

Abstract: (–)-Agelasine F (also known as ageline A) is a diterpene-adenine hybrid natural product isolated from marine sponges (*Agelas* species) and this compound is known to display cytotoxic activity against a variety of cancer cell lines as well as microorganisms. We herein report the first total synthesis of (–)-agelasine F. The commercially available and inexpensive monoterpenoid (*S*)-carvone was found to be a highly suitable starting material for the construction of the terpenoid part of the desired agelasine and controlling the stereochemistry of the target compound. Two alternative strategies from (*S*)-carvone were evaluated. Key-intermediates in the (–)-agelasine F synthesis are believed also to be valuable starting materials for total syntheses of other bioactive marine sponge metabolites. The synthetic route to (–)-agelasine F described herein is more efficient than previously published syntheses of *racemic* or *ent*-agelasine F.

Introduction

Agelasines are bioactive purine-terpene hybrides isolated from marine sponges (*Agelas* sp.).[1] Agelasine F (also called ageline A) was reported isolated independently by two different research groups in 1984[2] and has been re-isolated on several occations.[1e,3] Agelasine F is found to display cytotoxicity against a variety of cancer cell lines[1e,3d] and microorganisms[1e,2a,3] including profound activity against *Mycobacterium tuberculosis*.[3b] A reverse docking study has revealed mycobacterial enoyl recuctase and 7,8-diaminopelargonic acid synthase as a possible enzyme target,[4] but generally the mechanism(s) of action for agelasines are poorly understood. Racemic agelasine F (**6**) was synthesized ca. 30 years ago[5] with the cyclization of aldehyde **2** to give the cyclohexanol **3**[6] as a key-step (Scheme 1).

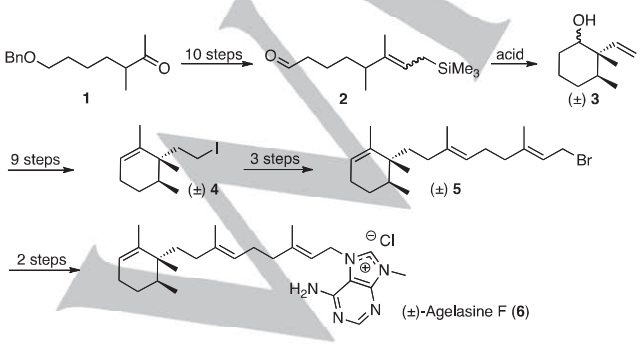

Scheme 1. Literature synthesis of (±)-agelasine F.[5,6]

It was clear to us that the synthetic strategy for racemic agelasine F could not readily be modified for synthesis of the (–)- or (+)-isomers. Previously we searched for readily available enatiopure monoterpenes as a starting point and we have synthesized *ent*-agelasine F [(+)-agelasine F] from commercially available (*R*)-pulegone (**7**).[7] Some steps in the synthesis of the desired enantiomer of the key-intermediate **5** are shown in Scheme 2. As a continuance of our work directed to synthesis of agelasines and analogs[7,8] and evaluation of their biological activities,[7-9] we herein present the first total synthesis of the naturally occurring (–)-agelasine F.

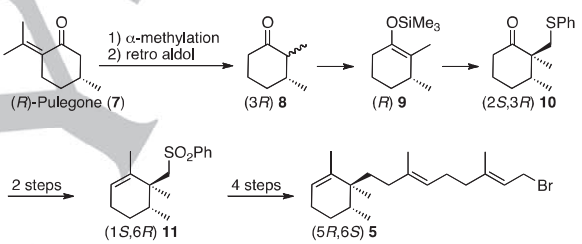

Scheme 2. Literature synthesis of the key compound **5** for the preparation of *ent*-agelasine F.[7].

Results and Discussion

Since (*S*)-pulegone is substantially more expensive compared to the *R*-enantiomer, we searched for a more convenient starting point for the preparation of (–)-agelasine F, and we herein report the first total synthesis of this natural product from (*S*)-(+)-carvone. Conjugate addition of Me_2CuLi to the enone **12** gave the ketone **13** with excellent diastereoselectivity, the minor isomer most probably *epi* at C-2,[10] and compound **13** was converted to the dimethylketone **8** by ozonolysis followed by catalytic hydrogenation (Scheme 3).[10] When the reduction was performed in Et_2O substantial epimerization at C-2 in ketone **8** was observed, but when the solvent was changed to pentane, the epimerization was minimized. In our hands, Pd/C was a superior catalyst compared to Rh/C. Ketone **8** was converted to the silyl enol ether **9** which was alkylated with $ClCH_2SPh$ as described for the enatiomer of **9** before.[7] At its best the silyl enol ether **9** was isolated in 92% yield containing 6% of the unwanted regioisomer **16**, but these results turned out to be not completely reproducible with respect to total yield and regioselectivity. Compound **11** was available in two steps from ketone **10** following the published procedures for synthesis of *ent*-**11**.[7]

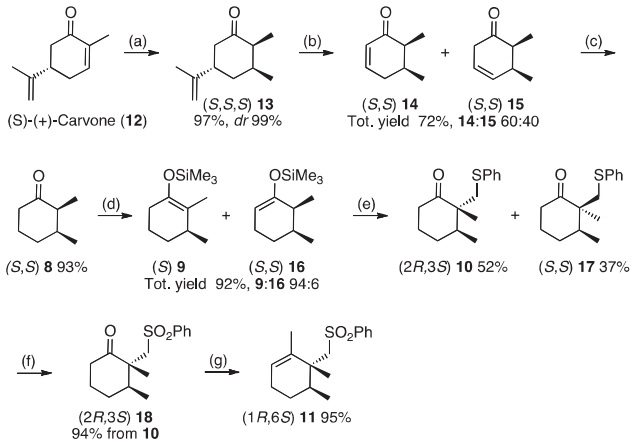

Scheme 3. (a) 1. MeLi, CuI, $CH_2(OEt)_2$, Et_2O, -78 °C → -30 °C, 2. Phenyl salicylate, -78 °C → r.t.; (b) 1. O_3, MeOH, -40 → -10 °C, 2. $Cu(OAc)_2$. -20 °C, 3. $FeSO_4•7H_2O$, -20 °C → r.t.; (c) H_2, Pd/C, pentane; (d) Et_3N, TMSCl, DMF, 130 °C; (e) $TiCl_4$, $PhSCH_2Cl$, CH_2Cl_2, -23 °C; (f) oxone, MeOH, H_2O, 0 °C → r.t.; (g) 1. MeMgBr, Et_2O, 0 °C → r.t, 2. HCO_2H, 80 °C.

As reported before,[7] $TiCl_4$ mediated alkylation of the silyl enol ether **9** gave only a modest selectivity for the desired isomer **10**. *Rac*- or (*R*)-enol ether **9** has previously been reacted with other electrophiles (activated alkenes, acetals) in the presence of a Lewis acid to give 2-substituted 2,3-dimethylcyclohexanones with high diastereoselectivity,[11] and this has been rationalized by attack of the electrophile on the least hindered side of the most stable conformer **B** of the silyl enol ether (Fig. 1).[11a] Thus, we were somewhat surprised and disappointed to find that alkylation of compound **9** with $ClCH_2SPh$ under standard conditions for reactions between silyl enol ethers and alkyl halides ($TiCl_4$, CH_2Cl_2)[12] took place with only a moderate selectivity (*dr* ca. 1.8:1). The isomeric ratio was virtually unaffected by temperature and changing the Lewis acid to zinc halides gave only a fair improvement (Table 1).

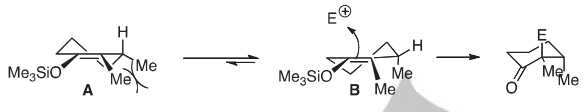

Figure 1. Attack of an electrophile on the least hindered side of the most stable conformer **B** of the silyl enol ether **9** (adapted from ref. 11a).

Due to difficulties in reproducing the synthesis of silyl enol ether **9** in high yields and the relatively poor stereoselectivity in the alkylation of this compound with $ClCH_2SPh$, we also evaluated an alternative synthesis of ketone **18** from (*S*)-carvone (**12**) (Scheme 4). The enolate generated from 1,4-addition of methyl cuprate to carvone was trapped directly with $ClCH_2SPh$. The ratio between the isomers **19** and (what is believed to be) **20** was ca. 3:1 which was an improvement compared the alkylation of silyl enol ether **9**, but the desired isomer **19** was, due to tedious chromatographic separation, only isolated in 54% which was comparable to the yield of sulfide **10** (Scheme 3). When sulfide **19** was oxidized to the corresponding sulfone **21** the yield was low, probably due to side reactions on the propenyl substituent, but compound **21** could be converted to the dimethylketone **18** by ozonolysis followed by catalytic hydrogenation. When the removal of the propenyl group was carried out before the S-oxidation, conversion of the sulfide to the corresponding sulfoxides **24** and **25** took place. As reported for other sulfides before,[13] the ozone mediated oxidation stopped at the sulfoxide level at the low temperature required for the removal of the propenyl group. The crude product was oxidized further to sulfones **22** and **23** by treatment with oxone.

Table 1. Table Caption. Alkylation of silyl enol ether **9**

Lewis acid	Solvent	Temp.]	Time	Ratio **10**:**17**[a]
$TiCl_4$	CH_2Cl_2	RT	30 min	1:0.55
$TiCl_4$	CH_2Cl_2	0 °C	1 h	1:0.56
$TiCl_4$	CH_2Cl_2	-23 °C	1 h	1:0.55
$TiCl_4$	CH_2Cl_2	-78 °C	1h 20 min	1:0.51
Et_2AlCl	CH_2Cl_2/toluene	0 °C	20 min	1:0.51
$ZnBr_2$	THF	RT	4 h	1:0.26
$ZnBr_2$	THF	-78 °C → RT	21 h	1:0.26
ZnI_2	THF	RT	3 h	1:0.28
$ZnCl_2$	THF	RT	3 h	1:0.30

[a] Determined by crude product ^{1}H NMR.

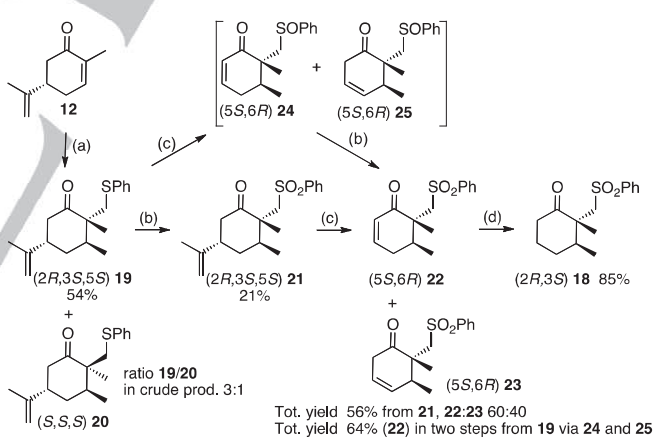

Scheme 4. (a) 1. MeMgI, CuI, LiCl, THF, -40 °C, 2. $ClCH_2SPh$, Δ; (b) oxone, MeOH, H_2O, 0 °C → r.t.; (c) 1. O_3, MeOH, -78 °C, 2. $Cu(OAc)_2$. -78 °C, 3. $FeSO_4•7H_2O$ -78 °C → r.t.; (d) H_2, Pd/C, Et_2O.

Having obtained an efficient synthesis of the sulfone (1*R*,6*S*) **11** (Schemes 3 and 4), we completed the synthesis of (–)-agelasine F (**6**) (Scheme 5). Sulfone (1*R*,6*S*) **11** was lithiated and reacted with the iodide **26** before the sulfone group in compound **27** was reductively removed. The iodide **26** was synthesized from the corresponding alcohol[14] by a modified literature[7] procedure. THP-ether **28** was converted to the corresponding bromide (5*S*,6*R*) **5** over two steps. Finally, N^6-*tert*-butoxy-9-methyl-9*H*-purin-6-amine[8c] was alkylated quite selectively on N-7 by treatment with the allyl bromide **5** under neutral conditions and the *tert*-butoxy directing group was removed under reductive conditions to give the target (–)-agelasine F (**6**).

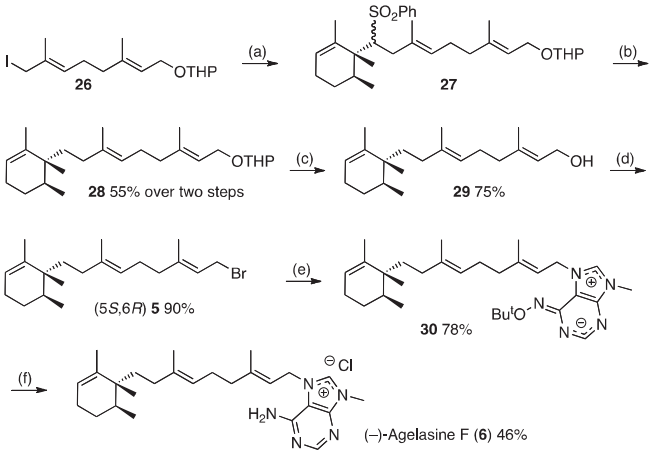

Scheme 5. (a) 1. *n*-BuLi, 2. comp. **11**, THF, 50 ºC; (b) Na, Na_2HPO_4, EtOH, THF; (c) PPTS, EtOH, 55 ºC; (d) PBr_3, Et_2O, 0 ºC; (e) N^6-*tert*-butoxy-9-methyl-9*H*-purin-6-amine, DMA, 50 ºC; (f) Zn, AcOH, MeOH, H_2O, 75 ºC.

Conclusion

We have performed the first synthesis of the bioactive marine natural product (–)-agelasine F. Commercially available and inexpensive (*S*)-carvone was found to be a highly suitable starting material for the construction of the terpenoid part of the target molecule. Two different routes from (*S*)-carvone to the key-intermediate **11** were evaluated. All though the total yields in both reactions sequences were almost identical, we consider the route depicted in Scheme 4 more robust since the method developed for generation of the desired silyl enol ether **9** (Scheme 3) was not completely reliable and ketones **8**, **14** and **15** were somewhat difficult to handle due to volatility. We depict that the chemistry described herein may also be applied in syntheses of other natural products, i.e. (–)-agelasidine C and D,[15] (–)-isoagelasidine B,[1g] (–)-axistatin 3[3d] and 10-hydro-9-hydroxyagelasine F[1e] (Fig. 2). These are all bioactive compounds isolated from marine sponges (*Agelas* sp.), but none of them have been prepared by chemical synthesis.

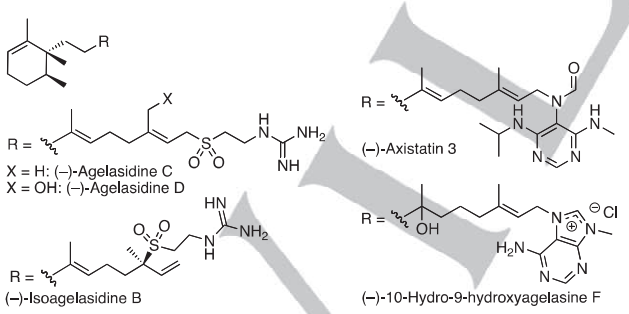

Figure 2. Natural products with structural resemblance to (–)-agelasine F.

Experimental Section

General remarks: ^{1}H NMR spectra were recorded at 800 MHz with a Bruker AVIII HD 800, at 600 MHz with a Bruker AVI 600 or Bruker AVII 600, or at 400 MHz with a Bruker AVIII HD 400 or Bruker AVII 400 instrument. The ^{13}C NMR spectra were recorded at 200, 150 or 100 MHz using the above-mentioned spectrometers. Mass spectrometry was performed using electrospray (ESI) with either a Bruker Maxis II ETD or a Micromass Q-TOF-2 instrument. Melting points were determined on a Büchi Melting Point B-545 apparatus. Optical rotations were determined on a Perkin Elmer Model 341 Polarimeter. Ozone was generated with a BOC MK II ozonizer. GC analyses were carried out with a GC 8000 Top gas chromatograph with H_2 as carrier gas. All reactions were performed in thoroughly dried glassware. CH_2Cl_2, Et_2O, MeCN and THF were collected from an MB-SPS 800 solvent purifying system. DMA was distilled over BaO and stored over 3 Å molecular sieves. MeOH and toluene were dried over 3 Å molecular sieves. TMSCl and Et_3N were distilled over CaH_2 before use. LiCl, $ZnCl_2$, $ZnBr_2$ and ZnI_2 were dried by heating with a heat gun under vacuum. All other reagents were commercially available and used as received. Compounds available by literature methods: (2*E*,6*E*)-2,6-Dimethyl-8-(tetrahydro-2*H*-pyran-2-yloxy)octa-2,6-dien-1-ol,[14] N^6-*tert*-butoxy-9-methyl-9*H*-purin-6-amine.[8c]

(*S,S,S*)-2,3-Dimethyl-5-(2-propen-2-yl)-cyclohexanone (13): MeLi (5.5 mL, 15 mmol, 3.0 M solution in diethoxymethane) was added dropwise at -20 ˚C to a stirring suspension of CuI (1.437 g, 7.545 mmol) in Et_2O (30 mL) under Ar. The resulting clear solution was stirred at -20 ˚C for 5 min and cooled to -78 ˚C before (*S*)-carvone (**12**) (0.78 mL, 5.0 mmol) in Et_2O (10 mL) was added dropwise. The mixture was warmed to -30 ˚C for 1 h, cooled to -78 ˚C and transferred *via* a cannula to a stirring solution of phenyl salicylate (4.285 g, 20.00 mmol) in Et_2O (30 mL) at -78 ˚C. The mixture was warmed to ambient temperature, and acetic acid (1.15 mL, 20.0 mmol) was added. The resulting mixture was filtered, washed with sat. aq. $NaHCO_3$ (30 mL), dried ($MgSO_4$) and evaporated in vacuo. The product was isolated by flash chromatography on silica gel eluting with CH_2Cl_2-pentane (1:1) to give **13** (803 mg, 97%) as a colorless liquid. The diastereomeric ratio was determined by GC to be 99%. $[\alpha]_D^{25} = +24$ (*c* 0.5, $CHCl_3$). ^{1}H NMR (400 MHz, $CDCl_3$): δ 0.83 (d, *J* = 7.2 Hz, 3 H, Me at C-3), 0.99 (d, *J* = 6.6 Hz, 3 H, Me at C-2), 1.74 (s, 3 H, Me in propenyl), 1.78-1.93 (m, 2 H, 4-H), 2.21-2.42 (m, 3 H, 6-H, 3-H), 2.55-2.65 (m, 2 H, 5-H, 2-H), 4.74 (s, 1 H, H_a in $=CH_2$), 4.77 (s, 1 H, H_b in $=CH_2$) ppm. ^{13}C NMR (100 MHz, $CDCl_3$): δ 12.1 (Me at C-2), 14.1 (Me at C-3), 20.7 (Me in propenyl), 36.4 (C-3), 37.9 (C-4), 41.2 (C-5), 46.8 (C-6), 48.6 (C-2), 109.9 (=CH_2), 147.8 (C=), 213.0 (CO) ppm. HRMS (ESI) found 189.1249, calcd. for $C_{11}H_{18}NaO^+$ 189.1250.

***(S,S)*-5,6-Dimethyl-2-cyclohexenone (14) and (*S,S*)-5,6-dimethyl-3-cyclohexenone (15)**: Ozone was passed through a solution of compound **13** (593 mg, 3.57 mmol) in dry MeOH (10 mL) for 1.5 h starting at -40 ˚C and gradually letting the temperature increase to -10 ˚C. The solution was then purged with O_2 for 10 min followed by N_2 for 15 min before $Cu(OAc)_2$ (1.600 g, 8.014 mmol) was added whilst stirring at -20 ˚C. After 15 min, $FeSO_4 \bullet 7H_2O$ (1.333 g, 4.795 mmol) was added, and the mixture was warmed slowly to ambient temperature. After stirring for 18 h, water (5 mL) was added and the mixture was extracted with Et_2O (5 × 7 mL). The combined organic phases were washed with sat. $NaHCO_3$ (5 mL) brine (5 mL) and water (5 mL), dried ($MgSO_4$) and evaporated in vacuo (on ice bath). The crude product was purified by flash chromatography on silica gel eluting with Et_2O-pentane (1:10) to give **14** and **15** in a ratio of 1:0.7 (320 mg, 72%) as a colorless liquid. HRMS (ESI) found 147.0780, calcd. for $C_8H_{12}ONa^+$ 147.0780. The isomers could be isolated in pure form, albeit in low yields, by further purification by flash chromatography on silica gel eluting with Et_2O-pentane (1:10).

***(S,S)*-5,6-Dimethyl-2-cyclohexenone (14):** ^{1}H NMR (400 MHz, $CDCl_3$): δ 0.96 (d, *J* = 7.0 Hz, 3 H, Me at C-5), 1.05 (d, *J* = 7.0 Hz, 3 H, Me at C-6), 2.08-2.56 (m, 4 H, 4-H, 5-H, 6-H), 5.95 (dt, *J* = 10.0, 2.0 Hz, 1 H, 2-H), 6.84 (dt, *J* = 10.0, 4.3 Hz, 1 H, 3-H) ppm. ^{13}C NMR (100 MHz, $CDCl_3$): δ 10.9 (Me at C-6), 15.9 (Me at C-5), 32.0 (C-4), 33.6 (C-5), 46.5 (C-6), 128.8 (C-2), 148.3 (C-3), 203.5 (CO) ppm.

***(S,S)*-5,6-Dimethyl-3-cyclohexenone (15):** ^{1}H NMR (400 MHz, $CDCl_3$): δ 0.87 (d, *J* = 6.9 Hz, 3 H, Me at C-5), 1.05 (d, *J* = 6.9 Hz, 3 H, Me at C-6), 2.64-2.94 (m, 4 H, 2-H, 5-H, 6-H), 5.67 (dt, *J* = 9.6, 3.5 Hz, 1 H, 3-H), 5.89-5.99 (m, 1 H, 4-H) ppm. ^{13}C NMR (100 MHz, $CDCl_3$): δ 11.2 (Me at

C-6), 15.7 (Me at C-5), 37.8 (C-5), 40.3 (C-2), 47.4 (C-6), 123.0 (C-3), 133.8 (C-4), 211.9 (CO) ppm.

(*S,S*)-2,3-Dimethylcyclohexanone (8): A stirring solution of compounds **14** and **15** (647 mg, 5.21 mmol) in pentane (30 mL) was treated with palladium on charcoal (100 mg, 10%) and H_2-gas at ambient pressure for 20 h. The catalyst was filtered off and the solvent was removed in vacuo (on ice bath) to give **8** (612 mg, 93%) as a colorless liquid. ^{1}H NMR indicated that ca. 6% of an isomer, probably *epi* at C-2, was present. $[\alpha]_D^{25} = +73.0$ (*c* 1.2, $CHCl_3$). ^{1}H NMR (400 MHz, $CDCl_3$): δ 0.84 (d, *J* = 7.1 Hz, 3 H, Me at C-3), 0.99 (d, *J* = 7.0 Hz, 3 H, Me at C-2), 1.62-1.68 (m, 1 H, 4-Ha), 1.80-1.94 (m, 3 H, 5-H, 4-Hb), 2.19-2.29 (m, 2 H, 3-H, 6-Ha), 2.31-2.39 (m, 1 H, 6-Hb), 2.55-2.61 (m, 1 H, 2-H) ppm. ^{13}C NMR (100 MHz, $CDCl_3$): δ 12.0 (Me at C-2), 14.7 (Me at C-3), 23.5 (C-5), 31.3 (C-4), 37.5 (C-3), 40.8 (C-6), 49.5 (C-2), 214.5 (CO) ppm. HRMS (ESI) found 149.0936, calcd. for $C_8H_{14}ONa^+$ 149.0937.

(*S*)-(2,3-Dimethylcyclohex-1-enyloxy)trimethylsilane (9): TMSCl (1.10 mL, 8.66 mmol) was added dropwise to a stirring solution of compound **8** (545 mg, 4.33 mmol) in dry Et_3N (1.21 mL, 8.66 mmol) and dry DMF (5 mL) under Ar. The mixture was heated to 130 °C and stirred for 16 h. After cooling, Et_2O (7 mL) was added and the mixture washed with cold sat. aq. $NaHCO_3$ (7 mL). The aqueous phase was extracted with cold Et_2O (3 × 7 mL) and the combined organic extracts were washed rapidly with cold 0.5 M aq. HCl (9 mL), cold sat. aq. $NaHCO_3$ (2 × 7 mL), and cold brine (7 mL). The organic layer was dried ($MgSO_4$) and evaporated in vacuo. The residue was purified by flash chromatography on silica gel eluting with EtOAc-hexane (1:100) to give **9** (785 mg, 92%) as a colorless oil containing ca. 6% of the isomer **16.** ^{1}H NMR (300 MHz, $CDCl_3$): δ 0.16 (s, 9 H, $SiMe_3$), 0.99 (d, *J* = 6.9 Hz, 3 H, Me at C-3), 1.25-1.30 (m, 1 H, 4-H_a), 1.52-1.58 (m, 4 H, Me at C-2, 5-H_a), 1.64-1.74 (m, 2 H, 4-H_b, 5-H_b) 1.98-2.01 (m, 2 H, H-6), 2.09-2.12 (m, 1 H, 3-H) ppm. ^{13}C NMR (150 MHz, $CDCl_3$): δ 0.8 ($SiMe_3$), 14.4 (Me at C-2), 20.1 (Me at C-3), 20.6 (C-5), 30.7 (C-6), 31.5 (C-4), 33.7 (C-3), 116.6 (C-2), 143.4 (C-1) ppm. HRMS (ESI) found 221.1332, calcd. for $C_{11}H_{22}OSiNa^+$ 221.1334.

(2*R*,3*S*)-2,3-Dimethyl-2-[(phenylthio)methyl]cyclohexan-1-one (10) and (2*S*,3*S*)-2,3-dimethyl-2-[(phenylthio)methyl]cyclohexan-1-one (17): A solution of $TiCl_4$ (4.0 mL, 1.0 M in CH_2Cl_2, 4.0 mmol) was added to a stirring solution of compound **9** (704 mg, 3.55 mmol) and chloromethyl phenyl sulfide (0.66 mL, 5.0 mmol) in CH_2Cl_2 (3.5 mL) at -23 °C under Ar. After 1 h, the resulting deep red solution was poured into sat. aq. $NaHCO_3$ (20 mL) and extracted with Et_2O (2 × 30 mL). The combined organic extracts were dried ($MgSO_4$) and evaporated in vacuo. The products were separated by flash chromatography on silica gel eluting with EtOAc-hexane (1:15) to give **10** (455 mg, 52%) and **17** (329 mg, 37%).

(2*R,3S*)-2,3-Dimethyl-2-[(phenylthio)methyl]cyclohexan-1-one (10): Colorless oil, $[\alpha]_D^{25} = +0.4$ (*c* 1.5, $CHCl_3$). ^{1}H NMR (600 MHz, $CDCl_3$): δ 0.86 (d, *J* = 6.8 Hz, 3 H, Me at C-3), 1.11 (s, 3 H, Me at C-2), 1.51-1.61 (m, 1 H, 4-H_a), 1.63-1.80 (m, 2 H, 4-H_b, 5-H_a), 1.90-2.00 (m, 1 H, 5-H_b), 2.21-2.31 (m, 1 H, 3-H), 2.32-2.48 (m, 2 H, 6-H), 2.98 (d, *J* = 12.5 Hz, 1 H, H_a in CH_2S), 3.39 (d, *J* = 12.5 Hz, 1 H, H_b in CH_2S), 7.14-7.19 (m, 1 H, Ph), 7.23-7.29 (m, 2 H, Ph), 7.38-7.42 (m, 2 H, Ph) ppm. ^{13}C NMR (150 MHz, $CDCl_3$): δ 15.7 (Me at C-3) 18.7 (Me at C-2), 24.4 (C-5), 29.3 (C-4), 37.8 (C-3), 38.2 (C-6), 41.2 (CH_2S), 53.9 (C-2), 126.2 (CH in Ph), 128.9 (2 × CH in Ph), 130.3 (2 × CH in Ph), 138.2 (C in Ph), 213.8 (CO) ppm. HRMS (EI) found 248.1235, calcd. for $C_{15}H_{20}OS^+$ 248.1235.

(2*S,3S*)-2,3-Dimethyl-2-[(phenylthio)methyl]cyclohexan-1-one (17): Colorless oil, $[\alpha]_D^{25} = +51.0$ (*c* 1.5, $CHCl_3$). ^{1}H NMR (600 MHz, $CDCl_3$): δ 0.97 (d, *J* = 6.9 Hz, 3 H, Me at C-3), 1.27 (s, 3 H, Me at C-2), 1.55-1.66 (m, 1 H, 4-H_a), 1.66-1.77 (m, 1 H, 5-H_a), 1.78-1.89 (m, 1 H, 4-H_b), 1.90-2.00 (m, 2 H, 5-H_b and 3-H), 2.30-2.46 (m, 2 H, 6-H), 3.10 (d, *J* = 12.0 Hz, 1 H, H_a in CH_2S), 3.26 (d, *J* = 12.0 Hz, 1 H, H_b in CH_2S), 7.13-7.19 (m, 1 H, Ph), 7.23-7.28 (m, 2 H, Ph), 7.32-7.36 (m, 2 H, Ph) ppm. ^{13}C NMR (150 MHz, $CDCl_3$): δ 15.8 (Me at C-3), 21.3 (Me at C-2), 24.9 (C-5), 29.1 (C-4), 38.4 (C-6), 39.0 (CH_2S), 42.3 (C-3), 52.9 (C-2), 126.3 (CH in Ph), 129.0 (2 × CH in Ph), 129.8 (2 × CH in Ph), 137.2 (C in Ph), 214.2 (CO) ppm. HRMS (EI) found 248.1234, calcd. for $C_{15}H_{20}OS^+$ 248.1235.

(2*R*,3*S*)-2,3-Dimethyl-2-(phenylsulfonylmethyl)-cyclohexanone (18). Method A: A solution of oxone (2.273 g, 3.700 mmol) in water (7 mL) was added to a stirring solution of sulfide **10** (459 mg, 1.85 mmol) in MeOH (7 mL) at 0 °C under Ar. The cooling bath was removed and the reaction mixture was stirred for 18 h, at ambient temperature before Et_2O (150 mL) was added and the resulting mixture was washed with water (40 mL) and brine (30 mL), dried ($MgSO_4$), and evaporated in vacuo. The residue was purified by flash chromatography on silica gel eluting with acetone-hexane (1:4) to give **18** (488 mg, 94%) as colorless crystals.

Method B: A 1:0.16 mixture of sulfones **22** and **23** (295 mg, 1.13 mmol) in Et_2O (25 mL) was treated with palladium on charcoal (68 mg, 10%) and hydrogenated at atmospheric pressure for 20 h. Additional catalyst (32 mg) was added after 16 h. The mixture was filtered and the solvent was removed in vacuo to give **18** (267 mg, 85%) as colorless crystals, m.p. 99-100 ºC. $[\alpha]_D^{25} = +89.1$ (*c* 1.1, $CHCl_3$). ^{1}H NMR (600 MHz, $CDCl_3$): δ 1.06 (s, 3 H, Me at C-2), 1.09 (d, *J* = 6.8 Hz, 3 H, Me at C-3), 1.55-1.64 (m, 1 H, 4-H_a), 1.76-1.83 (m, 1 H, 4-H_b), 1.85-1.99 (m, 2 H, 5-H), 2.39-2.58 (m, 2 H, 6-H), 2.69-2.78 (m, 1 H, 3-H), 3.25 (d, *J* = 14.0 Hz, 1 H, H_a in CH_2S), 3.96 (d, *J* = 14.0 Hz, 1 H, H_b in CH_2S), 7.54-7.58 (m, 2 H, Ph), 7.61-7.65 (m, 1 H, Ph), 7.96-7.98 (m, 2 H, Ph) ppm. ^{13}C NMR (150 MHz, $CDCl_3$): δ 16.3 (Me at C-3), 18.9 (Me at C-2), 23.5 (C-5), 29.4 (C-4), 36.7 (C-3), 37.8 (C-6), 52.5 (C-2), 61.0 (CH_2S), 127.8 (2 × CH in Ph), 129.3 (2 × CH in Ph), 133.5 (CH in Ph), 142.1 (C in Ph), 211.9 (CO) ppm. HRMS (ESI) found 303.1025, calcd. for $C_{15}H_{20}O_3SNa^+$ 303.1025.

1-{[(1*S*,6*S*)-1,2,6-Trimethylcyclohex-2-enyl]methylsulfonyl}benzene (11): To a stirring solution of ketone **18** (205 mg, 0.732 mmol) in dry Et_2O (13 mL) under Ar was added MeMgBr (0.34 mL, 2.4 M in Et_2O, 0.82 mmol) at 0 °C. The reaction mixture was stirred at 0 °C for 1 h and at ambient temperature for 16 h. After cooling to 0 °C, sat. aq. NH_4Cl (4 mL) was added. The mixture was diluted with Et_2O (5 mL) and the phases were separated. The aqueous phase was extracted with Et_2O (10 mL), the combined organic extracts were dried ($MgSO_4$), and concentrated in vacuo. The residue was stirred in conc. formic acid (2 mL) at 80 °C for 2 h before the mixture was concentrated in vacuo. The residue was purified by flash chromatography on silica gel eluting with acetone-hexane (1:5) to give **11** (190 mg, 94%) as a colorless oil, $[\alpha]_D^{25} = +31.4$ (*c* 1.2, $CHCl_3$). ^{1}H NMR (600 MHz, $CDCl_3$): δ 0.94 (d, *J* = 6.8 Hz, 3 H, Me at C-6), 1.07 (s, 3 H, Me at C-1), 1.38-1.48 (m, 1 H, 5-H_a), 1.57-1.65 (m, 1 H, 5-H_b), 1.66-1.69 (m, 3 H, Me at C-2), 1.94-2.08 (m, 2 H, 4-H), 2.57-2.65 (m, 1 H, 6-H), 3.21 (d, *J* = 14.6 Hz, 1 H, H_a in CH_2S), 3.33 (d, *J* = 14.6 Hz, 1 H, H_b in CH_2S), 5.42 (m, 1 H, 3-H), 7.52-7.56 (m, 2 H, Ph), 7.61-7.64 (m, 1 H, Ph), 7.90-7.93 (m, 2 H, Ph) ppm. ^{13}C NMR (150 MHz, $CDCl_3$): δ 15.9 (Me at C-6), 19.7 (Me at C-2), 21.5 (Me at C-1), 24.0 (C-4), 26.4 (C-5), 33.4 (C-6), 42.4 (C-1), 62.0 (CH_2S), 124.8 (C-3), 127.7 (2 × CH in Ph), 129.3 (2 × CH in Ph), 133.5 (CH in Ph), 136.4 (C-2), 142.2 (C in Ph) ppm. HRMS (ESI) found 303.1234, calcd. for $C_{16}H_{22}O_2SNa^+$ 303.1233.

(2*R*,3*S,5S*)-2,3-Dimethyl-2-[(phenylthio)methyl]-5-(prop-1-en-2-yl)cyclohexan-1-one (19): LiCl (33 mg, 0.79 mmol) and CuI (75 mg, 0.39 mmol) was dissolved in dry THF (24 mL) under Ar and stirred for 15 minutes at ambient temperature before cooling to -40 ºC. (*S*)-Carvone (**12**) (590 mg, 3.93 mmol) in dry THF (5.3 mL) was added and the resulting mixture was stirred for 10 min before a solution of MeMgI (1.9 mL, 2.5 M in Et_2O, 4.7 mmol) was added dropwise, and the resulting mixture was stirred for 1 h at -40 ºC. The reaction mixture was allowed to reach ambient temperature before chloromethyl phenyl sulfide (1.0 mL, 7.5 mmol) was added and the resulting mixture was heated at reflux for 18 h. After cooling to ambient temperature sat. aq. NH_4Cl (20 mL) was added and the mixture was extracted with Et_2O (3 × 25 mL). The combined organic layers were dried ($MgSO_4$) and concentrated in vacuo. ^{1}H NMR showed the isomers **19** and (what is presumed to be) **20** to be present in ca. 3:1 ratio. Further purification by flash chromatography on

silica gel twice eluting with EtOAc-hexane (1:30) gave **19** (598 mg, 54%) as a colorless oil, $[\alpha]_D^{25} = -82.9$ (*c* 1.1, $CHCl_3$). ^1H NMR (600 MHz, $CDCl_3$): δ 0.89 (d, *J* = 7.2 Hz, 3 H, Me at C-3), 1.12 (s, 3 H, Me at C-2), 1.64-1.69 (m, 1 H, 4-H_a), 1.72 (s, 3 H, Me in propenyl), 1.94 (m, 1 H, 4-H_b), 2.32 (m, 1 H, 3-H), 2.39 (ddd, *J* = 14.2, 5.2, 1.0 Hz, 1 H, 6-H_a), 2.47 (dd, *J* = 14.2, 9.8 Hz, 1 H, 6-H_b), 2.55-2.60 (m, 1 H, 5-H), 3.18 (d, *J* = 12.3 Hz, 1 H, H_a in CH_2S), 3.32 (d, *J* = 12.3 Hz, 1 H, H_b in CH_2S), 4.70 (s, 1 H, H_a in $=CH_2$), 4.82 (s, 1 H, H_b in $=CH_2$), 7.19 (m, 1 H, Ph), 7.26-7.28 (m, 2 H, Ph), 7.37-7.39 (m, 2 H, Ph) ppm. ^{13}C NMR (150 MHz, $CDCl_3$): δ 16.0 (Me at C-3), 19.2 (Me at C-2), 21.2 (Me in propenyl), 32.8 (C-4), 36.1 (C-3), 40.5 (C-5), 42.8 (C-6), 42.8 (CH_2S), 53.1 (C-2), 110.9 ($=CH_2$), 126.5 (CH in Ph), 129.1 (2 × CH in Ph), 130.5 (2 × CH in Ph), 137.3 (C in Ph), 147.2 (C=), 213.5 (CO) ppm. HRMS (ESI) found 311.1440, calcd. for $C_{18}H_{24}OSNa^+$ 311.1440.

(2*R*,3*S*,5*S*)-2,3-Dimethyl-2-[(phenylsulfonyl)methyl]-5-(prop-1-en-2-yl)cyclohexan-1-one (21): A solution of oxone (894 mg, 1.46 mmol) in water (4 mL) was added to a stirring solution of sulfide **19** (200 mg, 0.728 mmol) in MeOH (4 mL) at 0 ºC under Ar. The cooling bath was removed and the reaction mixture was stirred for 2.5 h at ambient temperature before Et_2O (40 mL) was added. The resulting mixture was washed with water (10 mL) and brine (5 mL), dried ($MgSO_4$) and evaporated in vacuo. The residue was purified by flash chromatography on silica gel eluting with acetone-hexane (1:5) to give **21** (48 mg, 21%) as a colorless oil, $[\alpha]_D^{25} = +2.8$ (*c* 1.5, $CHCl_3$). ^1H NMR (400 MHz, $CDCl_3$): δ 1.04 (d, *J* = 6.9 Hz, 3 H, Me at C-3), 1.11 (s, 3 H, Me at C-2), 1.70-1.78 (m, 1 H, 4-H_a), 1.76 (s, 3 H, Me in propenyl), 1.89 (ddd, *J* = 13.4, 8.0, 5.3 Hz, 1 H, 4-H_b), 2.48 (dd, *J* = 14.5, 4.6 Hz, 1 H, 6-H_a), 2.55-2.63 (m, 1 H, 5-H), 2.71 (ddd, *J* = 9.0, 6.9, 5.3 Hz, 1 H, 3-H), 2.82 (dd, *J* = 14.5, 10.6 Hz, 1 H, 6-H_b), 3.36 (d, *J* = 14.2 Hz, 1 H, H_a in CH_2S), 3.73 (d, *J* = 14.2 Hz, 1 H, H_b in CH_2S), 4.76 (s, 1 H, H_a in $=CH_2$), 4.83 (s, 1 H, H_b in $=CH_2$), 7.54-7.58 (m, 2 H, Ph), 7.62-7.66 (m, 1 H, Ph), 7.90-7.93 (m, 2 H, Ph) ppm. ^{13}C NMR (100 MHz, $CDCl_3$): δ 15.8 (Me at C-3), 19.0 (Me at C-2), 20.8 (Me in propenyl), 32.8 (C-4), 34.0 (C-3), 39.2 (C-5), 42.2 (C-6), 51.1 (C-2), 62.3 (CH_2S), 111.0 ($=CH_2$), 127.8 (2 × CH in Ph), 129.4 (2 × CH in Ph), 133.7 (CH in Ph), 141.6 (C in Ph), 146.9 (C=), 212.5 (CO) ppm. HRMS (ESI) found 343.1338, calcd. for $C_{18}H_{24}O_3SNa^+$ 343.1338.

(5*S*,6*R*)-5,6-Dimethyl-6-[(phenylsulfonyl)methyl]cyclohex-2-en-1-one (22) and (5*S*,6*R*)-5,6-dimethyl-6-[(phenylsulfonyl)methyl]cyclohex-3-en-1-one (23): Ozone was passed through a solution of sulfone **21** (40 mg, 0.13 mmol) in dry MeOH (15 mL) for 1.3 h whilst cooling at -78 ˚C. The solution was purged with O_2 for 10 min followed by Ar for 10 min before $Cu(OAc)_2$ (54 mg, 0.27 mmol) was added to the stirring mixture. After 15 min, $FeSO_4 \bullet 7H_2O$ (45 mg, 0.16 mmol) was added, and the mixture was warmed slowly to ambient temperature. After stirring for 18 h, the solution was concentrated to approx. ¼ of its volume, and water (5 mL) was added. The mixture was extracted with Et_2O (5 × 10 mL). The combined organic phases were washed with sat. aq. $NaHCO_3$ (5 mL), water (5 mL) and brine (5 mL), dried ($MgSO_4$) and evaporated in vacuo. The crude product was purified by flash chromatography on silica gel eluting with acetone-hexane (1:5) to give **22** and **23** in a ratio of 1:0.7 (21 mg, 56%). The isomers could be isolated in pure form, albeit in low yields, by further purification by flash chromatography on silica gel eluting with acetone-hexane (1:5).

***(5S,6R)*-5,6-Dimethyl-6-[(phenylsulfonyl)methyl]cyclohex-2-en-1-one (22):** Colorless oil, $[\alpha]_D^{25} = +36.3$ (*c* 2.34, $CHCl_3$). ^1H NMR (600 MHz, $CDCl_3$): δ 0.99 (s, 3 H, Me at C-6), 1.19 (d, *J* = 6.8 Hz, 3 H, Me at C-5), 2.18-2.24 (m, 1 H, 4-H_a), 2.42-2.47 (m, 1 H, 4-H_b), 3.09-3.14 (m, 1 H, 5-H), 3.20 (d, *J* = 14.0 Hz, 1 H, H_a in CH_2S), 4.09 (d, *J* = 14.0 Hz, 1 H, H_b in CH_2S), 6.10 (dd, *J* = 10.0, 2.3 Hz, 1 H, 2-H), 6.95 (ddd, *J* = 10.0, 5.9, 2.3 Hz, 1 H, 3-H), 7.53-7.57 (m, 2 H, Ph), 7.62-7.66 (m, 1 H, Ph), 7.95-7.96 (m, 2 H, Ph) ppm. ^{13}C NMR (150 MHz, $CDCl_3$): δ 15.7 (Me at C-5), 17.7 (Me at C-6), 31.5 (C-4), 33.3 (C-5), 49.6 (C-6), 60.1 (CH_2S), 127.8 (2 × CH in Ph), 128.1 (C-2), 129.3 (2 × CH in Ph), 133.6 (CH in Ph), 141.8 (C in Ph), 148.8 (C-3), 200.1 (CO) ppm. HRMS (ESI) found 301.0869, calcd. for $C_{15}H_{18}O_3SNa^+$ 301.0869.

***(5S,6R)*-5,6-Dimethyl-6-[(phenylsulfonyl)methyl]cyclohex-3-en-1-one (23):** Colorless oil, $[\alpha]_D^{25} = +22.2$ (*c* 1.9, $CHCl_3$). ^1H NMR (600 MHz, $CDCl_3$): δ 1.09 (d, *J* = 7.2 Hz, 3 H, Me at C-5), 1.15 (s, 3 H, Me at C-6), 2.97-3.00 (m, 1 H, 2-H_a), 3.09-3.18 (m, 2 H, 2-H_b and 5-H), 3.49 (d, *J* = 14.3 Hz, 1 H, H_a in CH_2S), 3.72 (d, *J* = 14.3 Hz, 1 H, H_b in CH_2S), 5.66-5.68 (m, 1 H, 4-H), 5.75-5.78 (m, 1 H, 3-H), 7.55-7.58 (m, 2 H, Ph), 7.63-7.66 (m, 1 H, Ph), 7.92-7.94 (m, 2 H, Ph) ppm. ^{13}C NMR (150 MHz, $CDCl_3$): δ 15.4 (Me at C-5), 18.4 (Me at C-6), 38.5 (C-5), 38.6 (C-2), 50.6 (C-6), 61.5 (CH_2S), 122.9 (C-3), 127.8 (2 × CH in Ph), 129.4 (2 × CH in Ph), 132.3 (C-4), 133.7 (CH in Ph), 141.6 (C in Ph), 209.9 (CO) ppm. HRMS (ESI) found 301.0867, calcd. for $C_{15}H_{18}O_3SNa^+$ 301.0869.

(5*S*,6*R*)-5,6-Dimethyl-6-[(phenylsulfonyl)methyl]cyclohex-2-en-1-one (22): Ozone was passed through a solution of sulfide **19** (564 mg, 1.96 mmol) in dry MeOH (100 mL) for 1.5 h at -78 ˚C. The solution was then purged with O_2 for 10 min followed by Ar for 10 min before $Cu(OAc)_2$ (781 mg, 3.91 mmol) was added whilst stirring. After 15 min, $FeSO_4 \bullet 7H_2O$ (652 mg, 2.35 mmol) was added, and the mixture was warmed slowly to ambient temperature. After stirring for 18 h, water (40 mL) was added, before the mixture was concentrated to approx. ¼ of its volume. The mixture was extracted with Et_2O (3 × 100 mL), the combined organic phases were washed with sat. $NaHCO_3$ (30 mL), water (30 mL) and brine (30 mL), dried ($MgSO_4$) and evaporated in vacuo. The crude product contained a mixture of the sulfoxides **24** and **25** (356 mg). HRMS (ESI) found 285.0919, calcd. for $C_{15}H_{18}OSNa^+$ 285.0920. Parts of this mixture was used directly in the next step: A solution of oxone (1.404 g, 2.287 mmol) in water (5.4 mL) was added to a stirring solution of sulfoxides **24** and **25** (300 mg, 1.14 mmol) in MeOH (5.4 mL) at 0 ºC under Ar. The reaction mixture was stirred at 0 ºC for 3.5 h before heating to ambient temperature. Et_2O (70 mL) was added and the resulting mixture was washed with water (15 mL) and brine (10 mL), dried ($MgSO_4$) and evaporated in vacuo. The product was purified by flash chromatography eluting with acetone-hexane (1:5) to give **22** (295 mg, 64% from compound **19**) as a colorless oil. Data, see above.

2-{[(2*E*,6*E*)-8-Iodo-3,7-dimethylocta-2,6-dien-1-yl]oxy}tetrahydro-2*H*-pyran (26): To a stirring solution of (2*E*,6*E*)-2,6-dimethyl-8-(tetrahydro-2*H*-pyran-2-yloxy)octa-2,6-dien-1-ol[14] (200 mg, 0.786 mmol), Ph_3P (310 mg, 1.18 mmol), and imidazole (72 mg, 1.2 mmol) in a mixture of MeCN (1 mL) and Et_2O (2 mL) under Ar was added I_2 (298 mg, 1.18 mmol) portion wise at 0 ºC over 10 min. The reaction mixture was stirred for another 20 min, diluted with Et_2O (17 mL), washed with sat. aq. $Na_2S_2O_3$ (4 mL), water (4 mL), and brine (4 mL), dried ($MgSO_4$), and evaporated in vacuo. Et_2O (1.5 mL) was added to the residue, the mixture was and filtered and the filtrate was evaporated in vacuo to give **26** (228 mg, ca. 80%, cont. ca. 8% $POPh_3$) as a pale yellow liquid used immediately in the next step. ^1H NMR (800 MHz, $CDCl_3$): δ 1.49-1.62 (m, 4 H, CH_2 in THP), 1.67 (s, 3 H, Me at C-6), 1.69-1.75 (m, 1 H, CH_2 in THP), 1.77 (s, 3 H, Me at C-2), 1.80-1.87 (m, 1 H, CH_2 in THP), 2.05-2.12 (m, 4 H, H-4 and H-5), 3.50-3.53 (m, 1 H, CH_2 in THP), 3.88-3.91 (m, 1 H, CH_2 in THP), 3.93 (s, 2 H, 1-H), 4.01-4.04 (dd, *J* = 12.0, 7.0 Hz, 1 H, H-8$_a$), 4.23-4.25 (dd, *J* = 12.0, 7.0 Hz, 1 H, H-8$_b$), 4.62 (t, *J* = 3.7 Hz, 1 H, CH in THP), 5.36 (t, *J* = 7.0 Hz, 1 H, H-7), 5.66 (t, *J* = 7.0 Hz, 1 H, H-3) ppm. ^{13}C NMR (200 MHz, $CDCl_3$): δ 15.6 (Me at C-2), 16.5 (Me at C-6), 16.8 (C-1), 19.8 (CH_2 in THP), 25.7 (CH_2 in THP), 27.0 (C-4), 30.9 (CH_2 in THP), 38.6 (C-5), 62.5 (CH_2 in THP), 63.8 (C-8), 98.1 (CH in THP), 121.4 (C-7), 129.4 (C-3), 133.3 (C-2), 139.4 (C-6) ppm. The spectral data were in good agreement with those reported before.[7]

2-{(2*E*,6*E*)-3,7-Dimethyl-9-[(1*R*,6*S*)-1,2,6-trimethylcyclohex-2-en-1-yl]nona-2,6-dien-1-yloxy}tetrahydro-2*H*-pyran (28): *n*-BuLi (0.9 mL, 2.2 M in hexanes, 2 mmol) was added dropwise to a stirring solution of sulfone **11** (250 mg, 0.898 mmol) in dry THF (4.2 mL) at 0 ºC under Ar and the resulting mixture was stirred at 50 ºC for 40 min before a solution of iodide **26** (741 mg, 2.04 mmol) in THF (4.2 mL) was added. The mixture was stirred for further 3 h at 50 ºC. Et_2O (24 mL) was added and the mixture was washed with sat. aq. NH_4Cl (10 mL), water (3 × 10 mL) and brine (10 mL), and evaporated in vacuo. The crude product was

partially purified by flash chromatography eluting with acetone-hexane (1:11) to give **27** (450 mg) as a pale yellow oil. A mixture of compound **27** (450 mg), Na_2HPO_4 (3.80 g, 26.8 mmol), Na (860 mg, 37.4 mmol), and abs. EtOH (3.2 mL) in THF (66 mL) was stirred at ambient temperature for 17 h under Ar, before the mixture was filtered and the filtrate was diluted with Et_2O (80 mL). The resulting mixture was washed with water (60 mL), sat. aq. NH_4Cl (45 mL) and brine (45 mL), dried ($MgSO_4$), and evaporated in vacuo. The product was purified by flash chromatography eluting with EtOAc-hexane (1:23) to give **28** (186 mg, 55% from compound **11**) as a pale yellow oil. ^{1}H NMR (600 MHz, $CDCl_3$): δ 0.85 (s, 3 H, Me at C-1'), 0.86 (d, *J* = 6.7 Hz, 3 H, Me at C-6'), 1.40-1.55 (m, 6 H, 1 H in THP, 3 H in cyclohexene, 9-H), 1.57-1.64 (m, 8 H, Me at C-7, Me at C-2', 8-H_a, 1 H in THP), 1.67 (s, 3 H, Me at C-3), 1.69-1.74 (m, 2 H, 1 H in THP, 6'-H), 1.80-2.02 (m, 4 H, 3 H in THP, 8-H_b), 2.02-2.05 (m, 2 H, 4-H), 2.08-2.12 (m, 2 H, 5-H), 3.49-3.53 (m, 1 H, H_a in OCH_2 in THP), 3.87-3.91 (m, 1 H, H_b in OCH_2 in THP), 4.02 (dd, *J* = 11.8, 7.5 Hz, 1 H, 1-H_a), 4.22 (dd, *J* = 11.8, 6.5 Hz, 1 H, 1-H_b), 4.62 (t, *J* = 3.8 Hz, 1 H, CH in THP), 5.09 (t, *J* = 6.8 Hz, 1 H, 6-H), 5.33-5.38 (m, 1 H, 2-H), 5.41 (br s, 1 H, 3'-H) ppm. ^{13}C NMR (150 MHz, $CDCl_3$): δ 16.0 (Me at C-6'), 16.4 (Me at C-7), 16.6 (Me at C-3), 19.4 (Me at C-2'), 19.8 (CH_2 in THP), 21.2 (Me at C-1'), 25.7 (C-4'), 25.7 (CH_2 in THP), 26.4 (C-5), 27.2 (C-5'), 33.3 (C-6'), 34.4 (C-8), 35.3 (C-9), 39.8 (C-4), 40.5 (C-1'), 62.2 (OCH_2 in THP), 63.8 (C-1), 97.9 (CH in THP), 120.7 (C-2), 123.4 (C-6), 124.2 (C-3'), 136.4 (C-7), 139.9 (C-2'), 140.4 (C-3) ppm. HRMS (ESI) found 397.3077, calcd. for $C_{25}H_{42}O_2Na^+$ 397.3077.

(2*E*,6*E*)-3,7-Dimethyl-9-[(1*R*,6*S*)-1,2,6-trimethylcyclohex-2-en-1-yl]nona-2,6-dien-1-ol (29): Compound **28** (173 mg, 0.462 mmol) was dissolved in abs. EtOH (6 mL) before pyridinium *p*-toluenesulfonate (28 mg, 0.11 mmol) was added and the resulting mixture was stirred at 55 ºC for 17 h under Ar. The mixture was evaporated in vacuo and the residue was purified by flash chromatography eluting with acetone-hexane (1:15) to give **29** (105 mg, 75%) as a transparent oil, $[\alpha]_D^{25} = -19.8$ (*c* 1.3, $CHCl_3$). ^{1}H NMR (800 MHz, $CDCl_3$): δ 0.85 (s, 3 H, Me at C-1'), 0.86 (d, *J* = 6.8 Hz, 3 H, Me at C-6'), 1.41-1.50 (m, 4 H, 9-H, 5'-H), 1.60 (s, 6 H, Me at C-7, Me at C-2'), 1.60-1.64 (m, 1 H, 8-H_a), 1.68 (s, 3 H, Me at C-3), 1.70-1.74 (m, 1 H, 6'-H), 1.88-1.94 (m, 2 H, 8-H_b, 4'-H_a), 1.94-2.01 (m, 1 H, 4'-H_b), 2.03-2.05 (m, 2 H, 4-H), 2.09-2.12 (m, 2 H, 5-H), 4.14 (d, *J* = 6.8 Hz, 2 H, 1-H), 5.09 (t, *J* = 6.8 Hz, 1 H, 6-H), 5.40-5.41 (m, 2 H, 2-H and 3'-H) ppm. ^{13}C NMR (200 MHz, $CDCl_3$): δ 16.0 (Me at C-6'), 16.38 (Me at C-3), 16.43 (Me at C-7), 19.3 (Me at C-2'), 21.2 (Me at C-1'), 25.7 (C-4'), 26.5 (C-5), 27.2 (C-5'), 33.4 (C-6'), 34.4 (C-8), 35.4 (C-9), 39.7 (C-4), 40.6 (C-1'), 59.6 (C-1), 123.3 (C-6), 123.5 (C-2), 124.2 (C-3'), 136.6 (C-7), 139.9 (C-2'), 140.0 (C-3) ppm. HRMS (ESI) found 313.2501, calcd. for $C_{20}H_{34}ONa^+$ 313.2502.

(5*S*,6*R*)-6-[(3*E*,7*E*)-9-Bromo-3,7-dimethylnona-3,7-dien-1-yl]-1,5,6-trimethylcyclohex-1-ene (5): The alcohol **29** (99 mg, 0.34 mmol) was dissolved in dry Et_2O (1.25 mL) at 0 ºC under Ar. PBr_3 (0.027 mL, 0.34 mmol) was added and the mixture was stirred at 0 ºC for 3 h. The mixture was diluted with Et_2O (8 mL) and washed with 10% aq. $NaHCO_3$ (2 mL). The aqueous phase was extracted with Et_2O (3 mL) and the combined organic extracts were dried ($MgSO_4$), and evaporated in vacuo to give **5** (108 mg, 90%) as a pale yellow oil, which was used directly in the next step without further purification. ^{1}H NMR (400 MHz, $CDCl_3$): δ 0.85 (s, 3 H, Me), 0.86 (d, *J* = 6.8 Hz, 3 H, Me), 1.39-1.52 (m, 4 H), 1.58-1.64 (m, 7 H), 1.69-1.75 (m, 5 H), 1.86-1.99 (m, 4 H), 2.05-2.12 (m, 4 H), 4.02 (d, *J* = 7.9 Hz, 2 H), 5.05-5.09 (m, 1 H), 5.41 (br s, 1 H), 5.52 (t, *J* = 8.1 Hz, 1 H) ppm. ^{13}C NMR (100 MHz, $CDCl_3$): δ 16.0 (Me), 16.1 (Me), 16.5 (Me), 19.4 (Me), 21.2 (Me), 25.7 (CH_2), 26.2 (CH_2), 27.2 (CH_2), 29.9 (C-1), 33.3 (CH), 34.3 (CH_2), 35.3 (CH_2), 39.7 (CH_2), 40.5 (C-1'), 120.7 (C-2), 122.8 (CH=), 124.2 (CH=), 136.8 (C=), 139.9 (C-1'), 143.8 (C-3) ppm. HRMS (ESI) found 375.1658, calcd. for $C_{20}H_{33}{}^{79}BrNa^+$ 375.1658.

7-{(2'*E*,6'*E*)-3,7-Dimethyl-9-[(1*R*,6*S*)-1,2,6-trimethylcyclohex-2-enyl]nona-2,6-dienyl}-6-*tert*-butoxyamino-9-methyl-7*H*-purinum (30): A mixture of N^6-*tert*-butoxy-9-methyl-9*H*-purin-6-amine[8c] (57 mg, 0.26 mmol) and bromide **5** (108 mg, 0.306 mmol) in dry DMA (2.5 mL) was stirred at 50 ºC for 21 h under Ar and evaporated in vacuo. The residue was purified by flash chromatography eluting with CH_2Cl_2-MeOH saturated with NH_3 (12:1 followed by 9:1) to give **30** (99 mg, 78%) as yellow crystals, m.p. 134-136 ºC, $[\alpha]_D^{25} = -5.6$ (*c* 1.0, $CHCl_3$). ^{1}H NMR (800 MHz, $CDCl_3$): δ 0.85 (s, 3 H, Me at C-1'), 0.86 (d, *J* = 6.8 Hz, 3 H, Me at C-6'), 1.33 (s, 9 H, *t*-Bu), 1.41-1.47 (m, 4 H, 8-H_a or 9-H, 5'-H), 1.59 (s, 6 H, Me at C-7, Me at C-2') 1.60-1.64 (m, 1 H, 8-H_a or 9-H), 1.69-1.72 (m, 1 H, 6'-H), 1.84 (s, 3 H, Me at C-3), 1.88-1.96 (m, 3 H, 8-H_b, 4'-H), 2.11-2.14 (m, 4 H, 4-H, 5-H), 3.90 (s, 3 H, NMe) 5.06 (br s, 1 H, 6-H), 5.10 (d, *J* = 7.6 Hz, 2 H, 1-H), 5.41 (br s, 1 H, 3'-H), 5.47 (t, *J* = 7.6 Hz, 1 H, 2-H), 7.84 (s, 1 H, H-2 in purine), 9.20 (s, 1 H, H-8 in purine) ppm. ^{13}C NMR (200 MHz, $CDCl_3$): δ 16.0 (Me at C-6'), 16.4 (Me at C-7), 17.2 (Me at C-3), 19.3 (Me at C-2'), 21.2 (Me at C-1'), 25.7 (C-4'), 26.3 (C-5), 27.2 (C-5'), 27.8 (3 × Me in *t*-Bu) 31.8 (NMe), 33.4 (C-6'), 34.5 (C-8), 35.4 (C-9), 39.7 (C-4), 40.6 (C-1'), 48.1 (C-1), 78.6 (C in *t*-Bu), 111.2 (C-5 in purine), 116.0 (C-2), 122.8 (C-6), 124.3 (C-3'), 133.0 (C-8 in purine), 137.1 (C-7), 139.8 (C-2'), 140.8 (C-6 in purine), 143.2 (C-4 in purine), 145.9 (C-3), 153.0 (C-2 in purine) ppm. HRMS (ESI) found 494.3853, calcd. for $C_{30}H_{48}O^+$ 494.3853.

(–)-Agelasine F (6): A mixture of compound **30** (83 mg, 0.17 mmol), Zn (142 mg, 2.10 mmol), and AcOH (0.17 mL) in MeOH (9 mL) and water (0.9 mL) was stirred vigorously at 75 ºC for 20 h under Ar. The mixture was filtered and the solid washed with MeOH (9 mL). Brine (5 mL) and water (5 mL) were added to the MeOH solution, and the mixture was stirred for 1 h at ambient temperature and evaporated in vacuo. The residue was transferred to a separatory funnel using brine (20 mL) and $CHCl_3$ (20 mL). The phases were separated and the aqueous phase was extracted with $CHCl_3$ (150 mL). The combined organic layers were dried ($MgSO_4$) and evaporated in vacuo. The residue was purified by flash chromatography eluting with MeOH-CH_2Cl_2 (1:9→1:6). The residue was dissolved in $CHCl_3$ and filtered, before evaporation in vacuo to give **6** (38 mg, 46%) as a colorless waxy solid, $[\alpha]_D^{25} = -9.0$ (*c* 1.3, $CHCl_3$) [lit.[2a] $[\alpha]_D^{25} = -8.4$ (*c* 3.0, $CHCl_3$)]. ^{1}H NMR (800 MHz, $CDCl_3$): δ 0.83 (s, 3 H, Me at C-1'), 0.84 (d, *J* = 6.8 Hz, 3 H, Me at C-6'), 1.35-1.45 (m, 4 H, 8-H_a or 9-H, 5'-H), 1.55 (s, 3 H, Me at C-7), 1.57 (s, 3 H, Me at C-2'), 1.53-1.58 (m, 1 H, 8-H_a or 9-H), 1.66-1.70 (m, 1 H, 6'-H), 1.83 (s, 3 H, Me at C-3), 1.80-1.85 (m, 1 H, 8-H_b), 1.88-1.99 (m, 2 H, 4'-H), 2.03-2.07 (m, 4 H, 4-H, 5-H), 4.08 (s, 3 H, NMe), 5.01 (br s, 1 H, 6-H), 5.40 (br s, 1 H, 3'-H), 5.47 (t, *J* = 6.8 Hz, 1 H, 2-H), 5.62 (d, *J* = 6.8 Hz, 2 H, 1-H), 6.91 (br s, 2 H, NH_2), 8.45 (s, 1 H, H-2 in purine), 10.34 (s, 1 H, H-8 in purine) ppm. ^{13}C NMR (200 MHz, $CDCl_3$): δ 16.0 (Me at C-6'), 16.4 (Me at C-7), 17.6 (Me at C-3), 19.3 (Me at C-2'), 21.2 (Me at C-1'), 25.7 (C-4'), 26.5 (C-5), 27.2 (C-5'), 32.3 (NMe), 33.4 (C-6'), 34.4 (C-8), 35.4 (C-9), 39.7 (C-4), 40.6 (C-1'), 48.9 (C-1), 110.0 (C-5 in purine), 116.2 (C-2), 122.6 (C-6), 124.3 (C-3'), 137.2 (C-7), 139.7 (C-2'), 141.9 (C-8 in purine), 146.7 (C-3), 149.7 (C-4 in purine), 152.4 (C-6 in purine), 156.1 (C-2 in purine) ppm. HRMS (ESI) found 422.3278, calcd. for $C_{26}H_{40}N_5^+$ 422.3278.

Acknowledgements

The Research Council of Norway is gratefully acknowledged for financial support (Grant No. 209330) to BP. This work was also partly supported by the Research Council of Norway through the Norwegian NMR Package in 1994 and the Norwegian NMR Platform, NNP (Grant No. 226244/F50). Additional support by the Department of Chemistry and the Faculty of Mathematics and Natural Sciences at University of Oslo is also acknowledged.

Keywords: Chiral pool • Heterocycles • Natural products • Terpenoids • Total synthesis

[1] a) L.-L. Gundersen, *Phytochem. Rev.* **2013**, *12*, 467–486, and references therein; b) F. Yang, M. T. Hamann, Y. Zou, M.-Y. Zhang, X.-B. Gong, J.-R. Xiao, W.-S. Chen, H.-W. Lin, *J. Nat. Prod. 75*, **2012**,

774–778; c) E. P. Stout, L. C. Yu, T. F. Molinski, *Eur. J. Org. Chem.* **2012**, 5131–5135; d) T. Kubota, T. Iwai, A. Takahashi-Nakaguchi, J. Fromont, T. Gonoi, J. Kobayashi, *Tetrahedron* **2012**, *68*, 9738–9744; e) D. B. Abdjul, H. Yamazaki, S.-i. Kanno, O. Takahashi, R. Kirikoshi, K. Ukai, M. Namikoshi, *J. Nat. Prod.* **2015**, *78*, 1428–1433; f) L.-L. Hong, J. B. Sun, F. Yang, M. Liu, J. Tang, F. Sun, W.-H. Jiao, S.-P. Wang, W. Zhang, H.-W. Lin, *RCS Adv.* **2017**, *7*, 23970–23976; g) M.-J. Chu, X.-L. Tang, G.-F. Qin, Y.-T. Sun, L. Li, N. J. de Voogd, P.-L. Li, G.-Q. Li, *Chem. Biodiversity* **2017**, *14*, e1600446.

[2] a) R. J. Capon, D. J. Faulkner, *J. Am. Chem. Soc*. **1984**, *106*, 1819–1822; b) H. Wu, H. Nakamura, J. Kobayashi, Y. Ohizumi, *Tetrahedron Lett.* **1984**, *25*, 3719–3722.

[3] a) X. Fu, F. J. Schmidtz, R. S. Tanner, M. Kelly-Borges, *J. Nat. Prod.* **1998**, *61*, 548–550; b) G. C. Mangalindan, M. T. Talaue, L. J. Cruz, S. G. Franzblau, L. B. Adams, A. D. Richardson, C. M. Ireland, G. P. Concepcion, *Planta Med.* **2000**, *66*, 364–365; c) L. Calcul, K. Tenney, J. Ratnam, J. H. McKerrow, *Aust. J. Chem.* **2010**, *63*, 915–921; d) G. R. Pettit, Y. Tang, Q. Zhang, G. Y. Bourne, C. A. Arm, J. E. Leet, J. C. Knight, R. K. Pettit, J.-C. Chapuis, D. L. Doubek, F. J. Ward, C. Weber, J. N. A. Hooper, *J. Nat. Prod.* **2013**, *76*, 420–424.

[4] J. B. Billones, *Orient. J. Chem.* **2016**, *32*, 851–858.

[5] K. Asao, H. Iio, T. Tokoroyama, *Tetrahedron Lett.* **1989**, *30*, 6401–6404.

[6] K. Asao, H. Iio, T. Tokoroyama, *Tetrahedron Lett.* **1989**, *30*, 6397–6400.

[7] Á. Proszenyák, M. Brændvang, C. Charnock, L.-L. Gundersen, *Tetrahedron* **2009**, *65*, 194–199.

[8] a) B. T. Utenova, L.-L. Gundersen, *Tetrahedron Lett.* **2004**, *45*, 4233–4235; b) A. K. Bakkestuen, L.-L. Gundersen, D. Petersen, B. T. Utenova, A. Vik, *Org. Biol. Chem.* **2005**, *3*, 1025–1033; c) A. Vik, E. Hedner, C. Charnock, Ø. Samuelsen, R. Larsson, L.-L. Gundersen, L. Bohlin, *J. Nat. Prod.* **2006**, *69*, 381–386; d) A. Vik, E. Hedner, C. Charnock, L. W. Tangen, Ø. Samuelsen, R. Larsson, L. Bohlin, L.-L. Gundersen, *Bioorg. Med. Chem.* **2007**, *15*, 4016–4037; e) Á. Proszenyák, C. Charnock, E. Hedner, R. Larsson, L. Bohlin, L.-L. Gundersen, *Arch. Pharm. Chem. Life Sci.* **2007**, *340*, 625–634; f) H. Roggen, L.-L. Gundersen, *Eur. J. Org. Chem.* **2008**, 5099–5106; g) H. Roggen, C. Charnock, R. Burman, J. Felth, R. Larsson, L. Bohlin, L.-L. Gundersen, *Arch. Pharm. Chem. Life Sci.* **2011**, *344*, 50–55; h) B. Paulsen, K. A. Fredriksen, D. Petersen, L. Maes, A. Matheeussen, A.-O. Naemi, A. Aa. Scheie, R. Simm, R. Ma, B. Wan, S. G. Franzblau, L.-L. Gundersen, *Bioorg. Med. Chem.* **2019**, *27*, 620–629.

[9] a) M. Sjögren, M. Dahlström, E. Hedner, P. R. Jonsson, A. Vik, L.-L. Gundersen, L. Bohlin, *Biofouling* **2008**, *24*, 251–258; b) A. Vik, Á. Proszenyák, M. Vermeersch, P. Cos, L. Maes, L.-L. Gundersen, *Molecules*, **2009**, *14*, 279–288; c) M. Jacubec, Ø. Totland, F. Rise, E. J. Chamgordani, B. Paulsen, L. Maes, L.-L. Gundersen, Ø. Halskau, *Mar. Drugs* (accepted, marinedrugs-699896).

[10] S. Ebert, N. Krause, *Eur. J. Org. Chem.* **2001**, 3831–3835.

[11] a) P. Duhamel, G. Dujardin, L. Hennequin, J.-M. Poirier, *J. Chem. Soc. Perkin Trans. 1* **1992**, 387–396; b) P. Dagneau, P. Cannone, *Tetrahedron Asymm.* **1996**, *7*, 2817–2820; c) T. Taishi, S. Takechi, S. Mori, *Tetraheron Lett.* **1998**, *39*, 4347–4350; d) Z. Meng, B. Liu, *Org. Biomol. Chem.* **2018**, *16*, 957–962.

[12] E. W. Colvin, *Silicon in Organic Synthesis*. Krieger Publishing Comp., Malabar, Florida, **1985**, pp 221–223.

[13] A. Maggiolo, E. A. Blair, Ozone oxidation of sulfides and sulfoxides. In *Advances in Chemistry*, American Chemical Society, Washington DC, **1959**; *21*, 200–201, and references therein.

[14] J. J. Morales, A. D. Rodriguez, *J. Nat. Prod.* **1992**, *55*, 389–394.

[15] A. K. Bakkestuen, L.-L. Gundersen, *Tetrahedron* **2003**, *59*, 115–121.

Entry for the Table of Contents

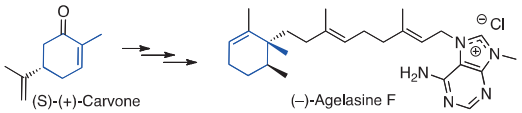

The first total synthesis of the bioactive marine natural product (–)-agelasine F has been performed. The synthetic sequence starts with readily available (*S*)-(+)- carvone which controls the stereochemistry in the target compound.